UNIVERSITY OF LIVERPOOL

Polyoxometalate catalysis for oxidative desulfurization

Thesis submitted in accordance with the requirements of the University of Liverpool for the degree of Doctor in Philosophy

by

Rana Omar H. Yahya

November 2015

Declaration

I hereby declare that except where specific reference is made to the work of others, the contents of this dissertation are original and have not been submitted in whole or in part for consideration for any other degree or qualification in this, or any other university. This dissertation is my own work and contains nothing which is the outcome of work done in collaboration with others except as specified in the text.

Rana Yahya

November 2015

Abstract

Polyoxometalate catalysis for oxidative desulfurization

PhD thesis by Rana Omar Yahya

Oxidative desulfurization removes sulfur-containing molecules from petroleum feedstocks to upgrade the quality of fuels. It is driven by environmental legislation demanding very low sulfur levels in fuels. The oxidative desulfurization technology usually involves oxidation of sulfur-containing molecules with an appropriate oxidant, e.g. hydrogen peroxide, organic peroxide, etc., followed by extraction of oxidation products from the petroleum feedstock.

In this study, new efficient catalysts have been developed for the oxidation of benzothiophenes commonly found in diesel fuel, such as benzothiophene, dibenzothiophene and 4,6-dimethyldibenzothiophene, to the corresponding sulfones with hydrogen peroxide in two-phase system including immiscible aqueous and organic phases. These catalysts are based on polyoxometalates comprising Keggin type heteropolyanions $[XM_{12}O_{40}]^{m-}$ {X= P^{v} (m = 3) and S^{iv} (m = 4) and phase transfer agents such as aminocyclotriphosphozenes or terminally functionalized polyisobutylene (PIB) oligomers. In this system, Keggin polyanions are transformed by excess H_2O_2 in aqueous phase to active peroxo polyoxometalate species which are transferred to the organic phase by the phase transfer agent where the oxidation of sulfur-containing molecules takes place.

Organoaminocyclotriphosphazene-POM aggregates, (RPN)-POM, where R = iPr, iBu and Bz, were studied as catalysts in toluene-H_2O and 1,2-dichloroethane-H_2O biphasic systems. These aggregates form directly in the reaction system and contain mono and dications $RPNH^{+}$ and $RPNH_2^{2}$. The catalytic activity of POM has been found to decrease in the order: $PMo_{12}O_{40}^{3-} \geq PW_{12}O_{40}^{3-} >> SiW_{12}O_{40}^{4-}$, which is in agreement with the increasing stability of POM to degradation in solution in this series. The activity RPN increases with the size of group R in line with increasing phase-transfer efficiency of RPN: iPr < iBu < Bz. The oxidation of dibenzothiophene (DBT) in the presence of BzPN-$PMo_{12}O_{40}^{3-}$ occurs with 100% DBT

conversion and >99% efficiency of H_2O_2 utilization at 60 ^oC in 0.5 h. The catalyst can be recycled and reused without significant decrease in activity.

As well as RPN, terminally functionalized polyisobutylene (PIB) compounds have also been found to be effective peroxo POM carriers between the phases. PIB derivatives are readily soluble in nonpolar solvents like heptane and have been demonstrated to have the potential to improve the recovery and recycling of homogeneous catalysts. These derivatives can be synthesized by functionalization of vinyl terminated PIB oligomers with a molecular weight of 1000-2300 Da, which are commercially available. This work has focused on the use of amine terminated PIB oligomer as a highly efficient hydrocarbon solubilizing agent for Keggin POM catalysts in the oxidation of DBT with hydrogen peroxide. It has been demonstrated that the PIB oligomer-bound Keggin polyoxometalates are active and recyclable catalysts for environmentally benign biphasic oxidation of DBT to DBT sulfone with hydrogen peroxide in a heptane-water two-phase system. These catalysts self-assemble in situ by mixing commercial Keggin POMs and amine terminated PIB oligomer. The oxidation occurs through facile phase transfer of peroxo POM intermediates into the heptane phase facilitated by the amine terminated heptane phase selectively soluble PIB oligomer.

Publications and presentations

The following papers have been published and presented on conferences in the United Kingdom and France as poster presentations.

Paper publications

1. M. Craven, **R. Yahya**, E. Kozhevnikova, R. Boomishankar, C. Robertson, A.Steiner and I. Kozhevnikov, *Novel polyoxometalate–phosphazene aggregates and their use as catalysts for biphasic oxidations with hydrogen peroxide*, Chem. Commun. **49** (2013) 349.
2. **R. Yahya**, M. Craven, E. F. Kozhevnikova, A. Steiner, P. Samunual, I. V. Kozhevnikov, D. E. Bergbreiter, *Polyisobutylene oligomer-bound polyoxometalates as efficient and recyclable catalysts for biphasic oxidations with hydrogen peroxide*, Catal. Sci. Technol. **5** (2015) 818.
3. M. Craven, **R. Yahya**, E. F. Kozhevnikova, C. M. Robertson, A. Steiner, I. V. Kozhevnikov, *Alkylaminophosphazenes as efficient and tuneable phase transfer agents for polyoxometalate catalyzed biphasic oxidation with hydrogen peroxide,* ChemCatChem **8 (**2016) 200.

Poster presentations

1. R. Yahya, E. Kozhevnikova and I. Kozhevnikov, *Postgraduate research, online poster day*, University of Liverpool, Liverpool, UK, 8-27th April, 2012.
2. R. Yahya, E. Kozhevnikova and I. Kozhevnikov, *XIth European Congress on Catalysis (EuropaCat)*, Lyon, France, 1-6th September, 2013.
3. R. Yahya, E. Kozhevnikova and I. Kozhevnikov, *7th Saudi Students Conference SSC)*, Edinburgh University, Edinburgh, UK, 1-2nd February, 2014.
   R. Yahya, M. Craven, E. Kozhevnikova and I. Kozhevnikov, *4th Northern Sustainable Chemistry (4th NORSC)*, Huddersfield University, Huddersfield, 23rd October, 2014.

Acknowledgements

First of all, I would like to thank Almighty God, who has blessed and guided me so that I am able to accomplish this thesis as a partial fulfillment of the requirements for the degree.

In this very special occasion I would like to express my deep gratitude and appreciation to **Prof. Ivan Kozhevnikov** and his wonderful wife **Dr. Elena Kozhevnikova**, who have given me their valuable time, advice, criticism and correction to this thesis from the beginning up to the end of writing. I also want to thank the entire Ivan's group that have taught and helped me during the years of my study at Chemistry Department, Liverpool University.

In this very special moment, I would like to express my deep thanks to my beloved parents, **Omar Yahya** and **Samia Alabasi** for their love, encouragement and support both financially and mentally that made it possible for me to finish my study. I also thank my sisters **Reham** and **Rawan** and my brothers **Mohammed**, **Ahmed** and **Ammar** for their support and encouragement.

Rana Yahya

Abbreviations

AC	Activated Carbon
BDS	Biodesulfurization
BT	Benzothiophene
BZP	Benzophenone
BzPN	Benzyl Phosphazene
CARB	California Air Resource Board
CPC	Cetyl Pyridinium Chloride
DBT	Dibenzothiophene
DMDBT	4,6-Dimethyldibenzothiophene
DMF	Dimethylformamide
DMSO	Dimethyl Sulfoxide
DRIFTS	Diffuse Reflectance Infrared Fourier Transform Spectroscopy
DSC	Differential Scanning Calorimetry
DTA	Differential Thermal Analysis
DTG	Derivative Thermogravimetric Analysis
1,2- DCE	1,2- Dichloroethane
EDS	Extractive Desulfurization
EPA	Environmental Protection Agency
FID	Flame Ionisation Detector
FTIR	Fourier Transform Infrared Spectroscopy
GC	Gas Chromatography
GC-MS	Gas Chromatography-Mass Spectrometry
HDS	Hydrodesulfursation
HPA	Heteropoly Acid
SiW	Silicotungstic Acid
iBuPN	Isobutyl Phosphazene

Il	Ionic Liquid
iPrPN	Isopropyl Phosphazene
IR	Infrared
LSD	Low Sulfur Diesel
M	Transition Metal Addenda Atom
MPcS	Metal-Sulfophthalocyanines
NMR	Nuclear Magnetic Resonance
Nox	Nitric Oxides
NP	Naphthalene
NRLMs	Non-Road Diesel Fuels
ODS	Oxidative Desulfurization
OSCs	Organic Sulfur Compounds
PIB	Terminally Functionalized Polyisobutylene
PM	Particulate Matter
PMo	Phosphomolybdic Acid
POM	Polyoxometalate
PTC	Phase Transfer Catalyst
PW	Phosphotungstic Acid
RPN	Aminocyclophosphazene
Sox	Sulfur Oxides
TH	Thiophene
TGA	Thermal Gravimetric Analysis
TPA	Tungstophosphoric Acid
UAOD	Ultrasound Assisted ODS
ULSD	Ultra-Low Sulfur Diesel
UV-Vis	Ultraviolet–Visible Spectroscopy

Contents

List of figures

List of tables

Chapter 1. Introduction

1.1 Environmental background

The two main transportation fuels used today are diesel and gasoline. They are derived from a common source, crude oil, and are typically extracted *via* fractional distillation. They share similarities in physical properties and chemical composition; both are composed of mixtures of aliphatic hydrocarbon chains of variable lengths and both may contain small amounts of aromatic hydrocarbons and trace elements such as sulfur. Emission gasses produced from both natural and anthropogenic sources can strongly influence atmospheric chemistry [1-3]. Primarily carbon dioxide, sulfur dioxide, and nitrogen oxides react in contact with water in the atmosphere or on the ground; under such conditions they can be chemically converted to acidic substances that cause environmental pollution. Sulfur and nitrogen oxides, in particular, react with atmospheric water vapor to make strong acids (sulfuric and nitric acids) in the form of harmful acid rain [1-6].

Compared to the industrial revolution, levels of sulfur and nitrogen oxides are on the rise. The increasing level of emissions of these harmful gasses can be attributed to the burning of fossil fuels in industry, energy-generating facilities and the transportation sector [5]. Once released into the atmosphere, the gasses may be carried hundreds of miles before they are converted to acids and deposited as acid rain. The problem with acid rain, therefore, does not only have the amount produced increased with population and industrial growth, but it has also become more widespread [3-7].

In the last few decades, environmental regulations have focused attention on reducing emissions from the transport sector with the purpose of improving air quality and welfare [5]. The Directive of the European Union declared that gasoline and diesel fuels in Europe should not exceed 10 ppm of total sulfur content starting from 2010 [6]. US regulations established a maximum of 15 ppm for diesel starting from 2006 and 30 ppm for gasoline starting from 2005 [7-9].

1.2 The overview of fuel

1.2.1 General overview

A modern refinery is a highly integrated industrial plant, the main enterprise of which is to produce efficiently large yields of valuable products from a crude oil feed of variable composition [8]. Diesel fuel and gasoline are the two main transportation fuels used today. They are derived from crude oil *via* distillation and share similarities in physical properties and chemical composition. The environmental consequences of sulfur and nitrogen containing compounds in gasoline initiated the groundbreaking environmental regulations collectively known as the various "clean air acts" of the late 20th century. The focus today is to achieve similar goals for diesel fuels. This introduction will describe the physical and chemical composition of diesel fuels, emphasizing proposed environmental regulations regarding the sulfur-containing constituents and the current technologies employed to meet these goals [6,7,8].

1.2.2 Diesel fuel

Diesel fuel is produced from petroleum. The density of diesel fuel is between 820 to 950 grams per liter, somewhat heavier than the density of gasoline which is between 710 to 740 grams per liter [12]. The average empirical formula for diesel fuel lies in the range of $C_{10}H_{22}$ to $C_{15}H_{32}$ [9]. Diesel fuel is predominantly a mixture of 75% aliphatic hydrocarbons and 25% aromatic hydrocarbons [12,13]. Aliphatic hydrocarbons include paraffin (alkanes) and naphthenes (cycloalkanes), and aromatic hydrocarbons include alkylbenzenes and aryl olefins [12,13].

Recently, a great deal of attention has been focused on diesel engines with respect to fuel availability and fuel economy [7,8]. The major drawback of diesel engines is that they emit large amounts of harmful particulate matter (PM) and nitric oxides (NOx) into their surroundings which are a cause for environmental concern. Fig. 1.1 shows that the NOx non-road diesel emissions have been dramatically reduced over the past two decades. Due to the associated environmental and health issues, increasingly restrictive legislation has been applied [11-15].

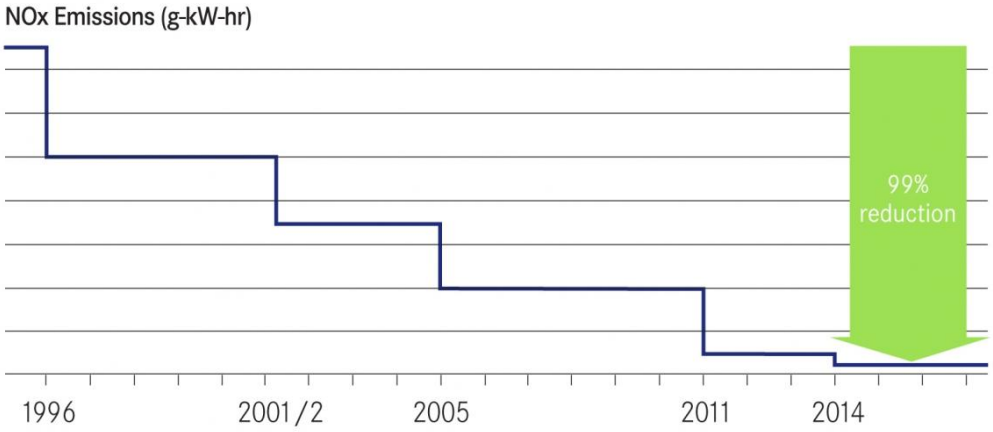

Fig. 1.1 Mobile off-highway emissions reduction achievements [15].

One of the major factors that contribute to the emission of particulate matter and sulfur oxides (Sox) is organic sulfur. Sulfur emissions, particularly in large quantities, can contribute significantly to health issues and environmental effects; for instance, sulfur oxides can react with water vapour in the atmosphere to produce acid rain with its well-known environmental consequences such as building corrosion and damage to forest and crops. Within the diesel engine itself, sulfur can also damage the catalytic converter, acidify the lubricating oil, and reduce the fuel economy [11-20].

Besides elemental sulfur, thiols, sulfides and thiophenes are also classified as organic sulfur compounds (OSCs). There are three major types of OSCs: thiophene (T), benzothiophene (BT) and dibenzothiophene (DBT). Table 1 shows the chemical structures of major types of sulfur compounds in diesel. DBT and its derivatives have higher molecular weights due to the inclusion of two “benzene” rings within their structures [21].

1.2.2.1 Highway diesel fuels

Sulfur content regulation for highway diesel fuels was 500 parts per million (ppm) by the end of 1993; diesel fuels meeting these regulations were termed “Low Sulfur Diesels” (LSDs). In 2001, the Environmental Protection Agency (EPA) established new regulations for highway diesel fuels with a maximum sulfur content of 15 ppm. This resulted in the production of Ultra-low Sulfur Diesels (ULSDs) [22]. Since 2006, all highway diesel fuel produced by

refineries must meet these standards. As of 2007, all light and heavy duty diesel engines should only use ULSD fuels instead of LSD fuel [22].

Table 1.1 Major types of OSCs in diesel fuel.

Compound	**Structure**
Thiols	R-SH
Sulfides	R-S-R
Cyclic Sulfide	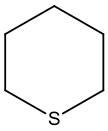
Thiophene	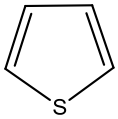
Benzothiophene	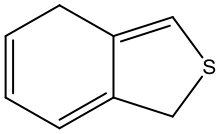
Dibenzothiophene	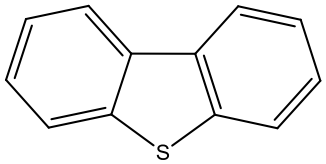
4,6-Dimethyldibenzothiophene	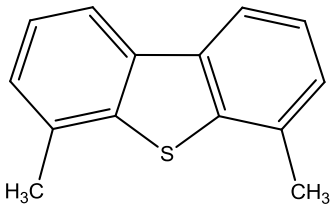

1.2.2.2 Non-road diesel fuels

Non-road diesel fuels (NRLMs) are land-based, non-road, locomotive and marine fuels. Between 1993 and 2000, the legislation for non-road diesel fuels stipulated a maximum sulfur content of 5000 ppm. In 2007, the sulfur content of non-road diesel fuels was limited to 500 ppm (LDS standard). In 2010, this was further reduced to a 15 ppm ULSD fuels standard as per EPA regulations. As of 2012, locomotive and marine diesel fuels must also meet the 15 ppm ULSD fuels standard [22].

1.2.3 Sulfur regulations

In 2006, The EPA and the California Air Resource Board (CARB) approved new standards requiring the petroleum industry to produce Ultra Low Sulfur Diesel (ULSD) fuel containing only 15 ppm of sulfur. The new regulations were designed to not only improve air quality and public health, but also vehicle performance. ULSD fuels enhance the efficiency and durability of engines, and allow the use of more advanced emission control devices, thus assuring dramatic reductions in PM and NOx emissions. Table 1.2 summarizes the sulfur standard for both highway diesel fuels and non-road diesel fuels [18-22].

Table 1.2 U.S.A. EPA diesel fuel sulfur standards [22].

Diesel type	**Implementation date**	**Maximum sulfur level (PPM)**
Highway	1993	500
Highway	2006	15
Land-base non-road	1993	500
Land-base non-road	2007	500
Land-base non-road	2010	15
Non-road (locomotive & marine)	2012	15

1.3 Classification of desulfurization technologies

Desulfurization processes can be categorized by the destination of the organosulfur compounds during desulfurization, the role of hydrogen within the system, or the nature of the process used (chemical and/or physical) [23]. The processes can be divided into three groups depending on the way in which the organosulfur compounds are transformed: whether the sulfur compounds are decomposed separated from refinery stream without decomposition or both separated and then decomposed (Fig. 1.2) [23]. Typically, as the organosulfur compounds decompose, gaseous or solid sulfur products are formed as a result of processing and the hydrocarbon component of the initial organosulfur compound is recovered and remains in the refinery streams. Hydrodesulfurization (HDS) is the most typical example of this type of process [23]. In other processes, the organosulfur compounds are simply separated from the refinery streams [23]. In combined processes, organosulfur compounds are separated from the streams and simultaneously decomposed in a single reactor unit rather than in a series of reaction and separation vessels [23]. These combined processes, which provide the basis for many technologies currently proposed for industrial application, may prove very promising for producing ultra-low sulfur fuels [23].

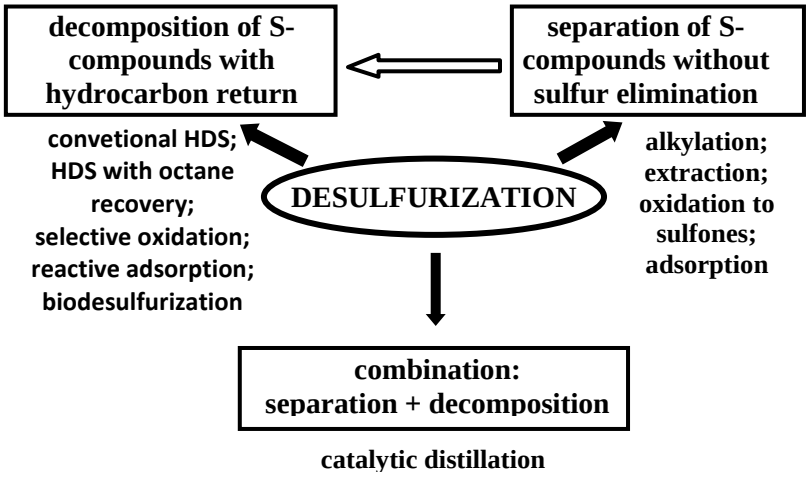

Fig. 1.2 Classification of desulfurization processes based on organosulfur compound transformation [23].

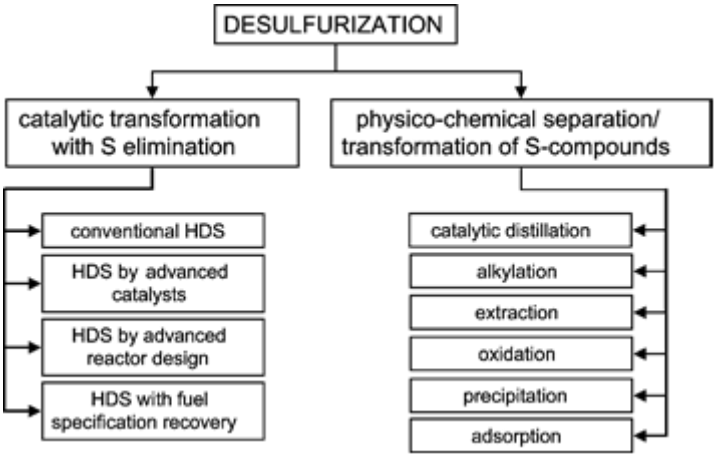

Fig. 1.3 Desulfurization technologies classified by nature of a key process to remove sulfur [23].

Desulfurization processes can be categorised into two groups, 'HDS based' and 'non-HDS based', depending on the role of hydrogen in removing sulfur. Non-HDS based processes do not require hydrogen to operate, while HDS processes use hydrogen to decompose organosulfur compounds and eliminate sulfur from refinery streams [23]. Different combinations of refinery streams pre- or post-distilling treatments with hydrotreating to maintain desired fuel specifications can also be assigned as HDS based processes since HDS treatment is one of the key steps [23]. The two process classifications overlap to some extent. Most sulfur elimination processes are HDS based with the exception of selective oxidation. [23]. The separation processes of organosulfur compounds are usually non-HDS based since they do not require hydrogen if concentrated sulfur-rich streams are not subsequently hydrotreated [23].

The different nature of physio-chemical processes that are used for sulfur removal is presented in Fig. 1.3 [23]. The most developed and commercialized technologies are those which catalytically convert organosulfur compounds with sulfur elimination. Such catalytic conversion technologies include conventional hydrotreating, hydrotreating with advanced catalysts and/or reactor design, and a combination of hydrotreating with some additional chemical processes to maintain fuel specifications [23]. The main characteristic of the technologies of the second type is the application of physio-chemical processes different in nature from catalytic HDS to separate and/or to transform organosulfur compounds from

refinery streams. Such technologies include alkylation, oxidation, extraction, adsorption or combination of these processes as a key step distillation [23].

1.3.1 Hydrodesulfurization

Since the 1950s, hydrodesulfurization (HDS) has been one of the most common desulfurization methods used in refinery processes. It is traditionally applied to a process to reduce the sulfur content in fuels [24-26]. Interest in HDS was initially stimulated by the availability of hydrogen from catalytic reformers. Typically, the HDS process involves catalytic treatment with hydrogen to convert the various sulfur compounds to H_2S and sulfur-free organic compounds at high temperature and partial pressure of hydrogen. Conventional catalytic HDS methods for reducing sulfur content require severe conditions of operation. In refineries, the H_2S resulting from the HDS reaction is eventually converted to elemental sulfur by a modified version of the Claus process [24-35].

HDS takes place in a fixed bed reactor. The mixture of sulfur-bearing hydrocarbon feed and hydrogen gas enters the reactor at a pressure ranging from 13 to 130 atmospheres. The higher pressure feed will join with hydrogen gas and then pass through a heat exchanger to heat up the gas/liquid mixture to temperatures ranging from 300 to 400^{o}C. The catalyst - containing cobalt and molybdenum supported on alumina ($CoMo/Al_2O_3$) - is used to speed up the reaction that results in a conversion of OSCs to hydrogen sulfide. Figure 1.4 shows the reaction for HDS of various OSCs under catalytic reaction [23].

The resulting gas/liquid mixture of hydrogen sulfide, hydrogen gas and liquid fuel is separated by a gas separator vessel; the remaining hydrogen gas is recycled and passed through an amine tower for purification to give sulfur-free hydrogen gas. The hydrogen sulfide is oxidized to sulfur dioxide by air and sulfur is formed. This process is called the Claus process. The overall reaction is shown below [22-35].

$$2H_2S + SO_2 \rightarrow 3S(s) + 2H_2O$$

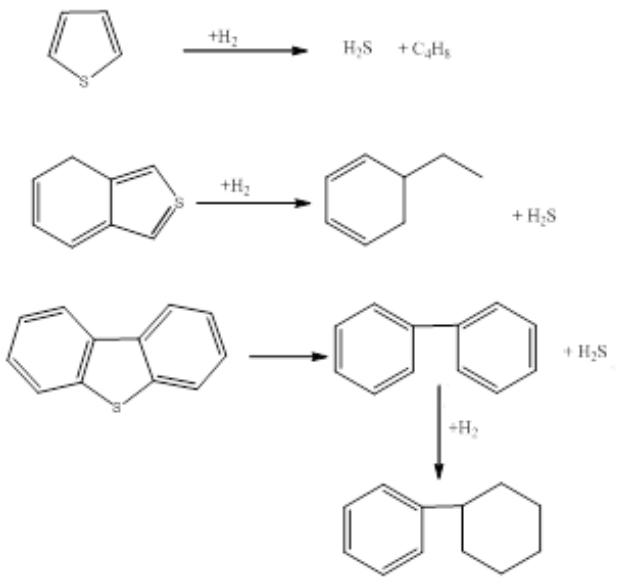

Fig. 1.4 HDS of OSCs [23].

The fuel separated from the gas separator vessel is passed through a stripper distillation tower in the final stage of HDS. Inside the distillation tower, sour gas (hydrogen sulfide, methane, ethane and some volatile organic compounds) is removed from liquid fuel. Some of the sour gas can be reused for a further purpose such as a refinery fuel gas. Figure 1.5 gives a process flow chart of typical HDS unit in a refinery [22-30].

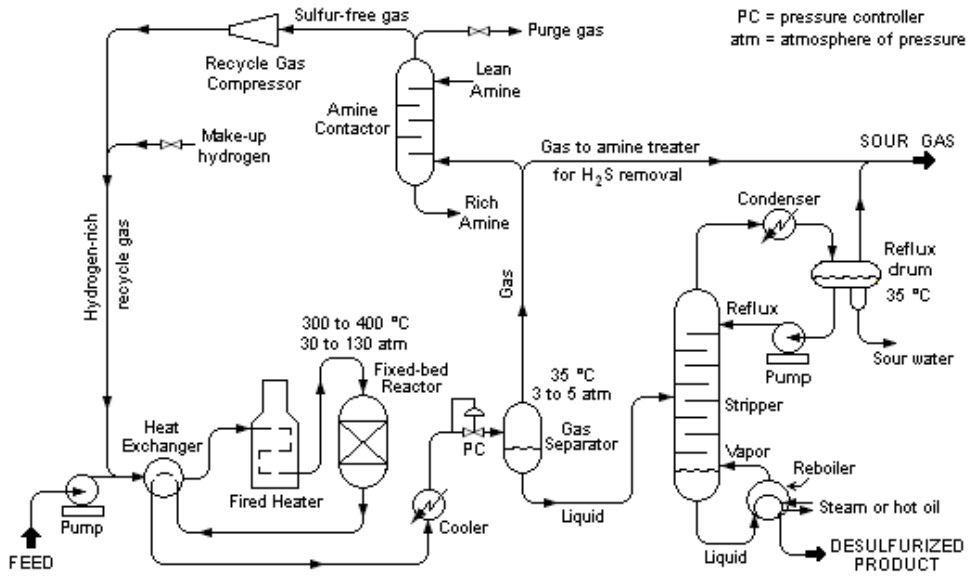

Fig. 1.5 HDS unit [39].

Deep desulfurization of refinery streams becomes possible when the severity of the HDS process conditions is increased [17,18]. Unfortunately, there are several disadvantages of HDS. Firstly, HDS requires high operating temperatures and pressures, which results in higher costs. Secondly, some of the gas and heat from the waste gas stream cannot be reused, resulting in poor energy efficiency and creating new environmental concerns. Lastly, the capital costs to build a reactor, pipelines and land usage are high.

The reactivity of sulfur compounds in HDS decrease in the order: thiophenes >benzothiophenes > dibenzothiophenes > alkylated DBT with alkyl substituents at the 4 and 6 positions [36,40]. Deep desulfurization of the fuels implies that more and more of the least reactive sulfur compounds must be converted [22-46]. Fig. 1.6 presents a qualitative relationship between the type and size of sulfur molecules in various distillate fuel fractions and their relative reactivities [22,47].

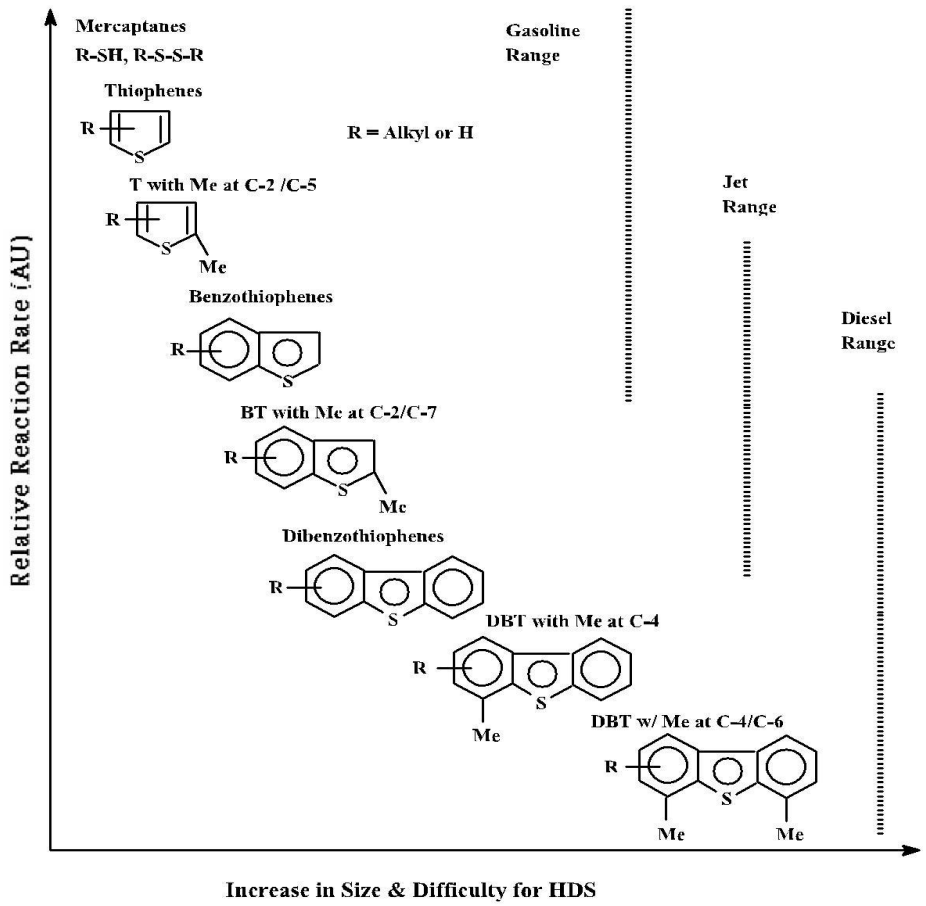

Fig. 1.6 Reactivity of various organic sulfur compounds in HDS versus their ring sizes and positions of alkyl substitutions on the ring [39].

To meet regulations, deeper HDS is required which can be achieved by increasing the catalyst to fuel ratio, modification of the catalysts, increasing hydrogen usage and/or by using a new reactor configuration. Studies show that doubling the amount of catalyst used will only reduce the sulfur content by 100 ppm with LSD fuel by current HDS unit. In other words, adding six or seven times more catalyst for HDS is required to meet the new sulfur standard [30-41].

1.3.2 Biodesulfurization

Biodesulfurization (BDS) has attracted wide attention recently because of its green processing of fossil fuels for removal of sulfur compounds using a series of enzyme-catalyzed reactions [47]. During initial research, many bacterial species that had the ability to consume DBTs as their energy source were isolated from their natural habitats. However, these isolated microbial species could not specifically remove sulfur from DBTs. Some of the isolated microorganisms used thiophenic compounds as carbon and sulfur sources. Other species used metabolized DBTs as a carbon source and, in a series of oxidizing steps, converted them into several water-soluble compounds. The accumulation of these water-soluble end products significantly inhibited microbial growth and DBT oxidation [47-52]. Other microbial biocatalysts have been identified that can biotransform sulfur compounds found in fuels, including ones that selectively remove sulfur from dibenzothiophene heterocyclic compounds [47]. The discovery of these biocatalysts coupled with a better understanding of the mechanism of biodesulfurization could eventually lead to commercial applications of biodesulfurizaton. A further improvement would be required to enhance biocatalyst stability; achieve faster kinetics; improve mass transfer limitations, temperature and solvent tolerance, as well as broader substrate specificity to attack a greater range of heterocyclic compounds. Indeed, assuming that these specifications can be met, biocatalysis may become a cost-effective approach to achieve low sulfur fuels [47-55].

There are two primary pathways for BDS of alkyl-DBTs. One pathway involves initial catalysis directed at the sulfur center (the 4S pathway) (Fig. 1.7) whereas in the other pathway the initial attack is directed towards one of the carbon atoms (the Kodama pathway) (Fig. 1.8) [58].

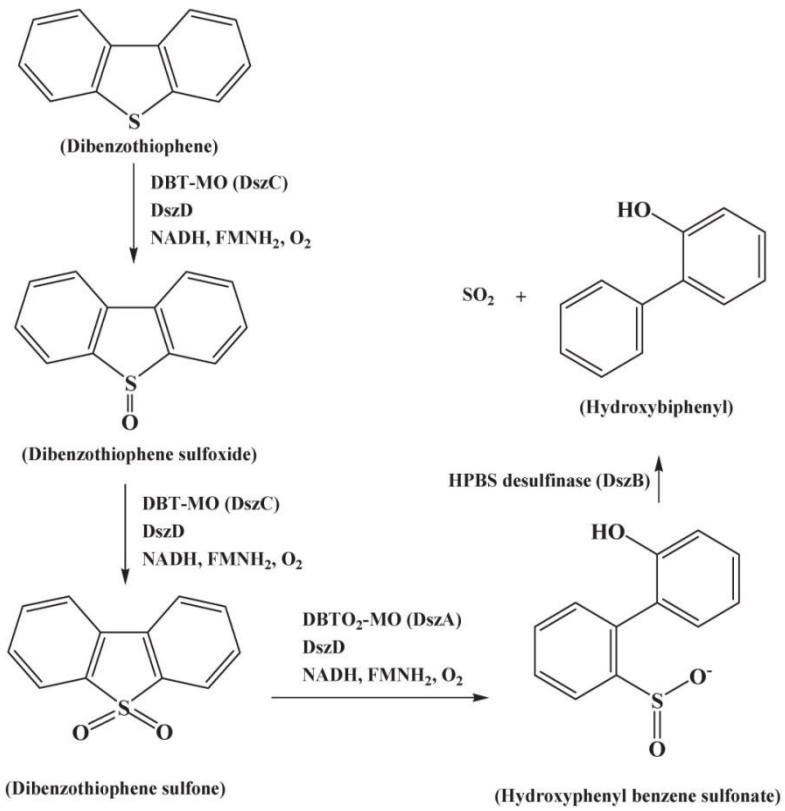

Fig. 1.7 BDS of DBT by multi-enzyme pathway (DBT mono-oxygenase (DszC or DBT-MO (a tetramer encoded by the desulfurization-c gene)) and DBT-sulfone mono-oxygenase (DszA or DBTO2-MO (a dimer encoded by the desulfurization-a gene)) are first two of these enzymes that require a third enzyme (the flavin reductase DszD) for their activity. The fourth enzyme, HPBS desulfinase (DszB), completes the reaction sequence) [58].

Naturally occurring bacteria are used to act as biocatalysts to remove OSCs within diesel fuel. During this process, oil feedstock is mixed with a water phase that contains biocatalysts. The oil/water mixture is operated inside a bioreactor under ambient temperature and pressure. During desulfurization, air or oxygen is pumped into reactor to consume sulfur. OSCs such as DBT or alkyl-DBTs are oxidized through a multi-stage enzymatic reaction [58].

Some biocatalysts have high enzymatic activities and selectivity's with regards to oxidizing OSCs without degrading the fuel value of the hydrocarbon matrix; therefore, BDS can be viewed as a potential form of alternative desulfurization technology. This however, would require further improvement in several aspects such as production of active resting cells (biocatalysts) with a high specific activity, preparation of a biphasic system containing oil fraction, aqueous phase and biocatalyst, biodesulfurization of a wide range of organic sulfur

compounds at a suitable rate, separation of desulfurized oil fraction, recovery of the biocatalyst and its return to the bioreactor, and efficient wastewater treatment [57].

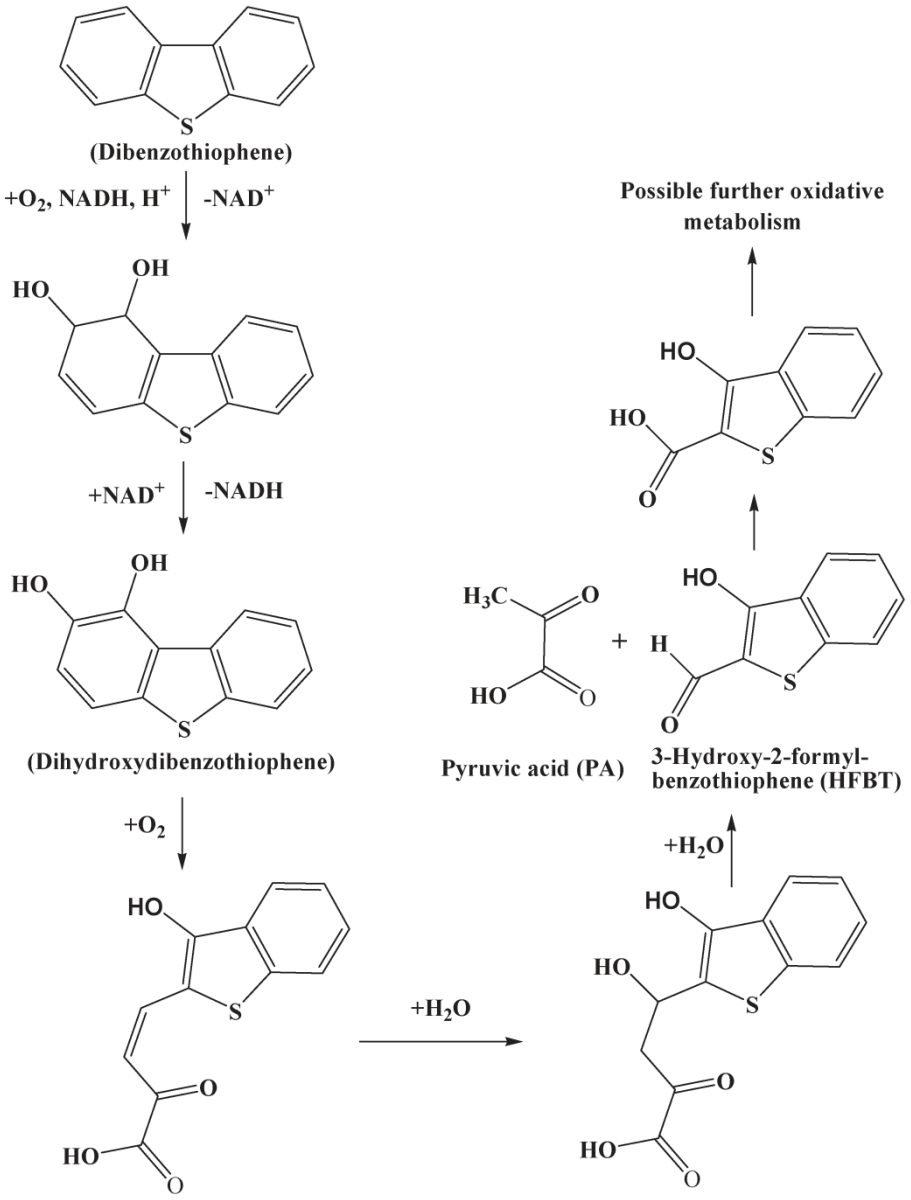

Fig. 1.8 Kodama enzymatic pathway for BDS of dibenzothiophene [58].

1.3.3 Adsorption desulfurization

This technology is based on the ability of a solid sorbent to selectively adsorb organosulfur compounds from refinery streams. Adsorption has been applied variously for removal of sulfur compounds from liquid hydrocarbon fuels. It has been studied over zeolites, aluminosilicates, activated carbon (AC), alumina and zinc oxide as adsorbents for removal of

DBT and other sulfur compounds. However, only a few adsorbents have shown high selectivity for difficult-to-hydrotreat sulfur compounds such as 4,6-dimethyl DBT [58-62].

In this technique, the active adsorbent is placed on a porous, non-reactive substrate that provides a high surface area for the adsorption of sulfur compounds. Adsorption occurs when the sulfur molecules attach to the adsorbent and remain there separate from the fuel. A lot of investigation has utilized this technique for the removal of sulfur from various types of fuels and model oils by various types of adsorbents [59].

Alumina, in particular has attracted attention as it has a good adsorptive property and has been used for the removal of organic compounds from aqueous solutions and surfactants like sodium dodecyl and octyl phenol from single and multi-surfactant aqueous solutions. It has been utilised by various research groups for the adsorptive removal of metal phosphates such as Co(II), Ni(II), Cu(II), Cr(II) and Zn(II) and dibenzothiophene sulfone [65-67].

Desulfurization by adsorption faces the challenge of developing an easily remunerable adsorbent with a high adsorption capacity. Adsorbents developed must have a high selectivity for the adsorption of refractory aromatic sulfur compounds [59].

1.3.4 Oxidative desulfurization

Oxidative desulfurization (ODS) is one of the most promising technologies for the removal of sulfur at low temperature (~50 ^{o}C) and atmospheric pressure. In ODS, heavy sulfides are oxidised by adding one or two oxygen atoms to the sulfur using appropriate oxidants without breaking any carbon–sulfur bonds, yielding the sulfoxide and sulfone (Eqn. 1.1), respectively. Then, the oxidized compounds are extracted or adsorbed from the light oil due to their increased relative polarity. ODS is a two stage process including oxidation, followed by liquid extraction [58-68].

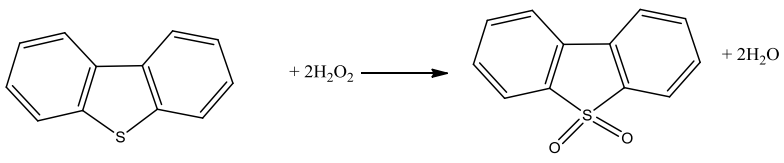

(1.1)

The oxidation occurs at ambient pressure. It continues until oxidized sulfur-containing compounds (e.g. sulfone) are formed and the reaction is stopped before the oxidant attacks hydrocarbons in fuel [58]. The unused oxidant is then regenerated or recycled by washing, extracting and chemical post-treatment.

Sulfone can be extracted from the diesel fuel by contacting with a non-miscible solvent. This is possible due to the high polarity of sulfone. Sulfone can be removed from diesel fuel by various methods; liquid-liquid (L/L) extraction with solvent followed by centrifugation is one method. Alternatively sulfone can be removed by absorption using silica gel and aluminum oxide. In liquid/liquid extraction, the extraction solvent is separated from the mixture of solvent and sulfone by a simple distillation and cleansed solvent can be re-used in subsequent reactions [58-68].

Many oxidants have been considered for ODS that include organic and inorganic peroxy acids, hydroperoxides, peroxy salts, NO_2, tert-butyl-hydroperoxide and O_3. ODS using nitrogen dioxide as an oxidant, followed by extraction with methanol was employed to remove both sulfur and nitrogen compounds from petroleum stocks [58]. Few researchers have used an oxidizing gas containing nitrogen oxides for purifying hydrocarbon aqueous oils containing both sulfur and nitrogen compounds. Nonetheless, this technology yields many undesirable byproducts because of initiation of very non-selective reactions by nitrogen oxides in the presence of oxygen. Also, there is always a safety problem due to the possibility of a rapid and explosive reaction [58,68-76].

Several peroxy organic acids (formic, acetic, propionic, pertrifluoro acetic acid, etc.) and Caro's acid (peroxysulfuric acid) have been used at 35–52^{o}C near atmospheric pressure for selective oxidation of organosulfur compounds. Many investigations were carried out on the oxidation of model sulfur compounds and diesel oil by K_2FeO_4 in a water phase, in organic acids and in the presence of phase-transfer catalysts [58]. The results indicated that the oxidation activity of BT and DBT was low in the water phase, even after adding phase transfer catalyst to the system. This was because K_2FeO_4 reacted rapidly with water to form brown $Fe(OH)_3$ which resulted in a loss of oxidation ability. The oxidation activity of the BT and DBT increased markedly in acetic acid. Furthermore, the addition of a solid catalyst to

the acetic acid medium promoted oxidation of organic sulfur compounds. Conversions of the BT and DBT were 98% and 70%, respectively [58,77-80].

Nehlsen reported the oxidation and extraction of organo-sulfur compounds, including thiophene (TH) and alkyl sulfides, with concentrated sulfuric acid [58]. Sulfuric acid is not typically regarded as an oxidizing agent because of the stability of the sulfate ion. However, in the presence of sulfur atoms with lower oxidation states, such as those in sulfides, sulfate can be reduced. The reaction between H_2S and concentrated sulfuric acid is fast and yields elemental sulfur, water and SO_2 as reaction products [58,81].

H_2O_2 is regarded as one of the best oxidising agents and is commonly used due its perceived environmental friendliness, producing only water as a by-product. Various catalytic systems such as HCOOH, CCl_3COOH, polyoxometalate, CF_3COOH, methyltrioxorhenium(VII), titanosilicates, and solid bases have been studied in the oxidation of sulfur compounds with H_2O_2 [58,70,82-88].

Sulfur and nitrogen removal from light oils using hydrogen peroxide and acetic acid was reported by Shiraishi [58,83]. Lanju et al. investigated the ODS of simulated gasoline consisting of model sulfur compounds of TH and 3-methythiophene dissolved in n-heptane in hydrogen peroxide and formic acid oxidative system over metal oxide loaded molecular sieve [58]. The sulfur removal rate of simulated gasoline was higher in H_2O_2/organic acid systems than in H_2O_2/inorganic acid systems. The cerium oxide-loaded molecular sieve was found to be a very active catalyst for oxidation of simulated gasoline in this system. When phase transfer catalyst (PTC) was added, the sulfur removal rates of C_4H_4S and 3-MeC_4H_3S were enhanced. On the other hand, with the addition of cyclohexene and xylene into the solvent n-heptane, the sulfur removal rate of simulated gasoline was reduced [58,89].

Al-Shahrani employed a catalytic system composed of Na_2WO_4, 30% H_2O_2 and CH_3COOH for the deep removal of sulfur in diesel [58]. The system showed 100% conversion of the THs to sulfones at 70 ^oC in less than 1 h in a system of model solutions of octane containing DBT and 4,6-dimethyl DBT. The catalytic system was effective for removing most of the last few hundred ppm of HDS-persistent organic sulfur-containing compounds in diesel at modest temperatures and under atmospheric pressure [58,90].

Various transition metal based catalysts, particularly methyltrioxorhenium mixed molybdenum/tungsten oxides and tungstophosphoric acid (TPA), have been used in conjunction with hydrogen peroxide as oxidants [58, 91].

D'Alessandro reported a catalytic system consisting of metal-sulfophthalocyanines (MPcS) and monopersulfate or hydrogen peroxide as oxidants for DBT oxidation [58]. Among the various MPcS catalysts examined (M=Fe, Co and Ru), the ruthenium derivative showed the best performance [58,93]. Gutierrez developed and evaluated a system which contains Mo/Al_2O_3 catalysts for the ODS of diesel fuel also using H_2O_2 as the oxidizing reagent [58]. The results indicated that the activity for sulfur elimination in this system depended mainly on the presence of hepta- and octamolybdate species in the catalyst support and the use of a polar aprotic solvent [58,94]. In addition, the presence of phosphate markedly increased the amount of sulfur eliminated. Sulfur levels in diesel fuel from about 320 to less than 10 parts per million by weight were reduced by using this catalyst at 333 K and atmospheric pressure.

Caero investigated ODS activities of DBTs in hexadecane for a series of V_2O_5 catalysts supported on alumina, titania, ceria, niobia and silica [58]. It was discovered that the sulfone yield was not related to textural properties or V content. Total removal of sulfur was close to 99% using vanadia on titania as the catalyst, and this decreased according to the support used in the order: alumina > titania > niobia > Al–Ti mixed oxide > SBA-15. It was shown that the catalytic activity of V catalyst supported on niobia or alumina was higher than that for all other supports (niobia > alumina > SBA-15 > titania > ceria > Al–Ti mixed oxide). However, in the presence of an N-compound such as indole the best catalytic performance was achieved with titania-supported catalysts [58,95].

Yang reported the oxidation of DBT to sulfone using polyoxometalates with a Keggin structure such as $H_3PM_{12}O_{40}$. $H_3PW_{12}O_{40}$ (HPW) supported on mesoporous molecular sieves in SBA-15 exhibited both catalytic oxidation ability and adsorption ability [58]. Polar DBT sulfones that were easily absorbed on HPW/SBA-15 were produced from non-polar DBT [58,71].

1.3.5 Oxidative desulfurization by other methods

1.3.5.1 Radiation assisted oxidation

Radiation assisted oxidation is a technique that can be applied to remove sulfur-containing compounds from a mixture using radiation-induced hydrogenation reactions. These reactions produce hydrogen as a product of hydrocarbon destruction. This technique was enhanced by radiation methods developed for H_2S extraction from gaseous mixes [58]. The method for irradiation of desulfurization includes two steps: The first one is radiation processing, and the second is the extraction of highly oxidized sulfuric compounds [58,98]. Radiation processing can be efficiently used for conversion of mercaptans and other light sulfuric species to sulfones, sulfur oxides and acids [58].

Nadirov and Zaykin studied the processing of heavy fuel oil by two irradiation methods under two different modes with the purpose of producing light oil fractions from the feedstock [58]. In the temperature range of 300–400 ^{o}C, the feedstock was irradiated by 2 MeV electrons using different values of other operational parameters (dose rate, P; dose, D). Mode 1 (P = 6 kGy/s, D = 30 kGy) used severe irradiation conditions and resulted in high yields of motor fuels. Mode 2 (P = 2 kGy/s, D = 70 kGy) was milder and caused lesser changes in hydrocarbon contents and appeared to be more favorable for conversion of sulfur compounds. 80% mercaptan conversion was reached in this milder mode and more than 90% of the total sulfur was concentrated in the heavy liquid fraction with boiling temperature higher than 350 ^{o}C. Furthermore, sulfur was transformed into harmless and easily extractable forms. [58,99,100].

1.3.5.2 Ultrasound assisted ODS

Ultrasound is used to improve the liquid–liquid interfacial area of viscous films containing gas-filled bubbles and cavitation bubbles through emulsification. Very fine ultra-emulsions formed with the help of ultrasonic waves greatly improve the interfacial area available for reaction, thus increasing the effective local concentration of reactive species, and enhancing the mass transfer in the interfacial region. Consequently, ultrasound increases the reaction rate and efficiency under phase transfer conditions [58,101-103].

The ODS process under phase transfer conditions and ultrasonication are termed "Ultrasound Assisted ODS" (UAOD). It relies on shock waves to agitate sulfur molecules and allows for their extraction from oil as sulfones [58,104].

The conceptual model of the oxidation step in the UAOD process may be depicted as a catalytic cycle. First, the metal precursor (simply represented as $W(O)_n$) is peroxidized and disaggregated to form anionic peroxometal complexs such as $W(O_2)_n$ in the presence of excess H_2O_2 and phosphotungstic acid; second, quaternary ammonium salts such as $(C_8H_{17})_4N^+Br^-$ with a large lipophilic cation function as phase transfer agent (PTA) to transfer the peroxometal anion into the organic phase; third, organic sulfur compounds such as DBT are oxidized by the peroxometal complex with high efficiency and high selectivity; lastly, the reduced oxo species, which dissociate with PTA, returns to aqueous phase and restores the catalytic cycle [58,73].

Ultrasonication followed by solvent extraction has been used for diesel fuels containing various levels of sulfur content and showed removal efficiency of sulfur-bearing compounds exceeding 99% in a short contact time at ambient temperature and atmospheric pressure [58,73,105-108].

1.3.5.3 Photooxidation

Photo-decomposition with UV light in the organic phase has also been studied, with a removal of resulting sulfur compounds into water or acetonitrile phase. Hirai studied photodecomposition of DBTs dissolved in tetradecane using a high-pressure mercury lamp (λ > 280 nm) [58]. The decomposed products were removed into the water phase as SO_4^{2-} at room temperature and atmospheric pressure. The reactivity order for the DBTs was 4,6-DMDBT > 4-MDBT > DBT which was the opposite to results found when the HDS method was used [58]. The yield of commercial light oil was only 22% following 30 h of irradiation due to the depression of photoreaction of the DBT by the presence of aromatic compounds such as naphthalene and its derivatives in the light oil. It was also discovered that light oil was able to utilize light in the visible region (λ > 400 nm) most efficiently. [58,106-112].

Hirai established that the addition of benzophenone (BZP), a triplet photosensitizer, enhanced the removal of DBT from tetradecane. However, this reaction did not proceed in the presence

of naphthalene (NP) because of triplet energy transfer from photoexcited DBT or BZP to ground-state NP. The addition of H_2O_2 enhanced the desulfurization of commercial light oil as well as the removal of DBT from tetradecane. This was probably due to H_2O_2 acting as a weak oxidizing agent for photoexcited DBT and interrupted the energy transfer from excited DBT to NP to some extent. The yield of desulfurization with the use of 30% H_2O_2 solution was 75% following 24 h of photo-irradiation and the sulfur content in the light oil was reduced from 0.2 wt% to less than 0.05 wt% [58,106-113].

Although early research shows the process to be successful, there are a number of problems that need to be solved to make extractive photo-oxidation desulfurization practically and economically feasible. Better solvents and better recovery of solvents are required, and the combination of a solvent and a photosensitizer has to be optimized to increase the rate of the organosulfur compounds photo-transformation [58].

1.3.5.4 Electrochemical catalytic oxidation

Wang developed a process for gasoline desulfurization using electrochemical catalytic oxidation within an electrochemical fluidized bed reactor with a particle group anode [58]. The particle group anode was activated carbon-supported cerium dioxide (CeO_2/C), the electrolyte was aqueous cerium nitrate solution, and a copper pillar was used as a cathode in electrochemical reactions. The CeO_2/C particle group anode accelerated the electrochemical reaction rate and promoted the electrochemical catalysis performance for the electrochemical desulfurisation reaction. The theoretical decomposition voltage ranged from 0.1–0.5 V in pure acid electrolyte system, however, desulfurization reactions could not be carried out spontaneously. The reaction became spontaneous after the use of aqueous cerium nitrate solution as an electrolyte. Cell voltage, a concentration of the Ce^{3+} ions, feed volume flow rate and the CeO_2 loading were established at the optimal desulfurization conditions [58,115,116].

1.3.5.5 Plasma ODS

Liu investigated plasma ODS of mixed organic sulfides in the liquid phase [58]. At a temperature of 285 ^{o}C and a pressure of 120 Pa, the organic sulfides namely mercaptan, thioether and TH were oxidized. The desulfurization was not complete, and the process was not economical [58,115].

1.3.5.6 Extraction in oxidative desulfurization

The sulfoxides and sulfones produced after ODS are preferentially extracted from light oil using a non-miscible solvent. A solvent's polarity is the key for extraction efficiency. However, the polarity is not the only criteria for the selection of suitable solvents. Other properties such as boiling point, freezing point, and surface tension need to be considered carefully to evaluate the potential for separation and recovery of the solvent for recycling and reuse [58,117,118].

The oxidized compounds and solvent are separated from the light oil by gravity or by centrifugation. The light oil is washed with water to recover any traces of dissolved extraction solvent and unused oxidant. It is then purified using other methods such as adsorption using silica gel and aluminum oxide. The solvent is separated from the oxidized compounds by simple distillation for recycling and re-use [58].

Dimethyl sulfoxide (DMSO), dimethylformamide (DMF) and acetonitrile are common water-soluble polar solvents. The former two solvents have a high extractability for sulfones but also have a high boiling point (573 K). This is close to the boiling point of the sulfones, thus creates difficulty in separation by distillation and reuse for further extraction [58].

Organic salts - composed of organic cations and organic/inorganic anions - with melting points below 100 ^{o}C can be used as ionic liquids (ILs). Nonvolatility, solubility for organic/inorganic compounds, good thermal/chemical stability, nonflammability, recyclability, and environmental friendliness are attractive properties of ILs and make ILs suitable extractants for sulfur compounds. ILs have been used for direct extraction of S-compounds (extractive desulfurization, EDS) or for extraction of oxidized S-compounds

obtained from ODS. Studies have been performed using ILs composed of anions such as BF_4^-, PF_6^-, $AlCl_4^-$, and $EtSO_4^-$ and cations such as imidazolium and pyridinium [58,119-143].

The first application of ILs for desulfurization was reported in 2001. They found that multi-step extraction using $AlCl_3$ ILs reduced the sulfur concentration from 500 mg down to 235 mg. Eber introduced industrial equipment designed for deep desulfurization of oil refinery streams by extraction with ILs. Imidazolium-based ILs with PF_6^- and BF_4^- anions; and N-alkyl-3-methylimidazoliumbis(trifluoromethylsulfonyl)imide ILs have also been used by several investigators [58,144,145].

Imidazolium based phosphoric ILs were also tested which showed encouraging results. Several extraction experiments with alkyl- and alkylmethyl-pyridinium-based ILs with ethanoate and thiocyanate anions as an alternative to the perfluorinated and tetrafluoborate ones gave good extraction performance. Instability and regeneration of the Ils, corrosion problem, negative effects on fuel quality and high total costs of deep fuel desulfurization make the use of Ils a challenging task for researchers [58,145-151].

1.4 Polyoxometalates

1.4.1 Introduction

The oxoanions of transition metal addenda atoms (M), such as Mo(VI), W(VI), V(V), Nb(V), Ta(V), and Ti(IV) form extensive series of *isopoly* and *heteropoly* anions. Both are built up by oxygen-sharing MO_x polyhedra. Isopoly anions, which contain only metal addenda atoms and oxygen, have stoichiometries such as, e.g. $Nb_6O_{19}^{8-}$ or $Mo_7O_{24}^{6-}$. In heteropoly anions an additional metal or non-metal atom located at structurally well-defined sites is present, for example, phosphorus in $PW_{12}O_{40}^{3-}$ [152,153].

Polyoxometalates can be produced in a variety of different forms with diverse functionalities. Indeed, the different types of polyoxometalates can be categorised and named depending on their compositions and substituent elements. Acid forms can be referred to as polyacids = polyoxoacids, including heteropoly acids (e.g. $H_3PW_{12}O_{40}$) and isopolyacids (e.g. $H_2Mo_6O_{19}$); and for oxoanions, polyanions = polyoxoanions = polyoxometalates, including heteropoly anions (e.g. $PW_{12}O_{40}^{3-}$). Non-oxygen elements in the inner part of polyanions

(usually P, Si, As, Ge, etc.) are called *heteroatoms* (in some cases, *central* atoms) and those in peripheral part (usually Mo, W, V, Nb, etc.) are called *addenda atoms* or *polyatoms*. A systematic nomenclature of polyoxometalates is too complicated and practically never used for a routine purpose. In catalytic applications, a simplified nomenclature is used, where the heteroatom is considered as the central atom of a complex, and the addenda as a ligand, for example, $H_3PW_{12}O_{40}$ is called 12-tungstophosphoric acid. For simplicity, while writing the formulas of heteropoly acids, the countercations, the charge of polyanion and even the oxygen atoms may be omitted; e.g. $H_3PMo_{12}O_{40}$ may be abbreviated as HPMo or PMo [153-156].

Catalysis by heteropoly acids (HPAs) and related heteropoly oxometalates or metal-oxygen cluster compounds is a field of increasing importance. Their catalytic properties have drawn wide attention in the preceding three decades owing to the versatility and tunability of these compounds and their compatibility with environmentally and economically attractive conditions, which has been demonstrated both by successful large-scale applications and by promising laboratory results [152-165].

1.4.2 Historical background

The first heteropoly compound can be traced to the work of Berzelius who in 1826 prepared ammonium 12-molybdophosphate as a yellow precipitate from the addition of ammonium molybdate to phosphoric acid. Later on in 1848, Svanberg and Struve introduced this compound in analytical chemistry as the basis for the determination of phosphorus that has been widely used since. In 1862, Marignac prepared 12-tungstosilicic acid and provided analytical compositions [166,167].

Although hundreds of polyoxometalates were synthesised during the next half-century, little progress was made in understanding their structures. It was Keggin who in 1933 solved the structure of the most important 12:1 type of heteropoly anions by a powder X-ray diffraction study of $H_3PW_{12}O_{40}\cdot 5H_2O$. This structure, now named after its discoverer, contained 12 WO_6 octahedra linked by edge and corner sharing oxygens, with the heteroatom occupying a tetrahedral hole in the centre. In 1948, Evans determined the structure of another widespread type – the Anderson's heteropoly anion (6:1 series) – by single-crystal X-ray analysis of

$Te^{6+}Mo_6O_{24}^{6-}$ salts; this structure is now often referred to as the Anderson-Evans structure. In 1953, Dawson reported the next new structure (now frequently referred to as the Wells-Dawson structure) of an 18:2 heteropoly anion $P_2W_{18}O_{62}^{6-}$. This structure was shown to be closely related to the Keggin structure. By the early 1970s, the chemistry of polyoxometalates had been greatly expanded. This period is associated with extensive work of many groups and especially those of Souchay (France), Ripan (Romania), Spitsyn (USSR) and Baker (USA) [169-171].

In the 1980-90s, the number of groups involved in the field increased enormously in parallel with expanding applications of polyoxometalates. Baker and Glick reviewed the history of polyoxometalate chemistry and contributions of various groups to date. The application of modern characterisation techniques had led to a much better understanding of the structural principles of polyoxometalates and their properties. However, many fundamental questions regarding the structural principles, mechanisms of synthesis and reactivity of polyoxometalates remain unanswered [155,172].

First attempts to use polyoxometalates as catalysts can be traced back to the beginning of the 20^{th} century. A systematic investigation began in the early 1970s when the great potential of these compounds for catalytic applications became apparent. Most of the pioneering work at that time was carried out in Japan (Izumi, Misono, Ono, Otake, Yoneda and co-workers) and Russia (Matveev and co-workers). Successful industrial applications of polyoxometalate catalysts in the 1970-80s stimulated further innovative research in this field, which has continued to date and is likely to go on in the future [153,155].

Heteropoly compounds have several advantages as catalysts, the most important being their multifunctionality and structural mobility. On the one hand, they (heteropoly acids) have a very strong Brønsted acidity; on the other, they are efficient oxidants, exhibiting fast reversible multielectron redox transformations under mild conditions. Their acid-base and redox properties can be varied over a wide range by changing the chemical composition. Solid heteropoly compounds possess a discrete ionic structure, comprising fairly mobile structural units – heteropoly anions and countercations - unlike the network structure of, e.g., zeolites and metal oxides. The structure is frequently preserved upon substitution or oxidation/reduction. Heteropoly compounds exhibit extremely high proton mobility and a

"pseudoliquid phase"; many of them have a very high solubility in polar solvents and fairly high thermal stability in the solid state [153,155,156].

1.4.3 Structural types of heteropoly compounds

1.4.3.1 Primary, secondary and higher structures of heteropoly compounds

Misono advanced a special structural classification that recognises the importance of structural flexibility of solid heteropoly compounds. This classification, which is now widely adopted in heterogeneous catalysis by polyoxometalates, distinguishes the primary structure (polyoxoanion structure), the secondary structure (crystal structure and packing), and the tertiary structure (texture of solids, i.e. particle size, porosity, surface area, distribution of protons, etc.) [156,163]. This structural hierarchy is schematically illustrated in Fig. 1.9.

Heteropoly anions are polymeric oxoanions. The structure of a heteropoly anion itself is called a *"primary structure"*. Dozens of structural types and stoichiometries of heteropoly anions are known to date. According to Pope and Müller, it is convenient to discuss the variety of heteropoly anion structures starting from a few highly symmetrical "parent" polyanions; then many other heteropoly anion structures may be considered as their "derivatives". There are four "parent" structures: the Keggin structure, the Wells-Dawson structure, the Anderson-Evans structure and the Dexter-Silverton structure. Some of these structures will be briefly discussed below [173].

In aqueous solution, heteropoly anions are usually present as free units of primary structure (Fig. 1.9a). These anions are weakly solvated and may be protonated. Most heteropoly anions tend to hydrolyse readily at high pH (> 2.0) [2]. Protonation and hydrolysis of the primary structure may be a major structural concern for catalysis in solution.

Typically, heteropoly compounds in the solid state are ionic crystals consisting of large polyanions, cations, water of crystallisation, and other molecules. This three-dimensional arrangement is called the *"secondary structure"* (Fig. 1.9 b, c). Solid HPAs form ionic crystals composed of heteropoly anions, countercations (H^+, H_3O^+, $H_5O_2^+$, etc.) and hydration water. The crystal structure of HPAs depends on the amount of hydration water. This water can be easily removed by heating, whereby the acid strength is increased due to the

dehydration of protons. This is a reversible process accompanied by changing the volume of the crystal cell. Unlike the rigid network structure of zeolites, in HPA crystal the Keggin anions are quite mobile. Not only water but also a variety of polar organic molecules can enter and leave HPA crystals. Such structural flexibility is important when using HPA as a heterogeneous catalyst [155].

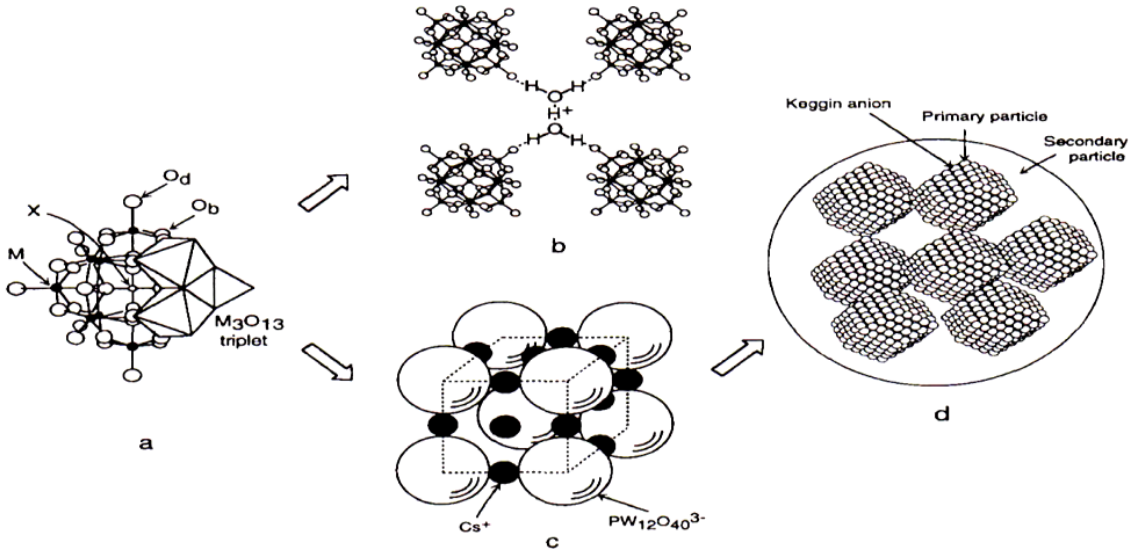

Fig. 1.9 Primary, secondary and tertiary structures of heteropoly compounds: (a) primary structure (Keggin structure, $XM_{12}O_{40}$); (b) secondary structure ($H_3PW_{12}O_{40}\cdot 6H_2O$); (c) secondary structure ($Cs_3PW_{12}O_{40}$ unit cell); (d) tertiary structure of bulk $Cs_{2.}5H_{0.5}PW_{12}O_{40}$ [156].

The anionic charge of the big heteropoly units is delocalised over a large number of oxygen atoms, thus greatly diminishing electrostatic attractions. Protons of crystalline $H_3PW_{12}O_{40}\cdot 6H_2O$ are present as hydrated species, $H_5O_2^+$, each of which links four neighbouring heteropoly anions by hydrogen bonding to the terminal $W–O_d$ oxygen atoms (Fig. 1.9b). The loss of water brings changes in the anion packing of $H_3PW_{12}O_{40}\cdot nH_2O$: n = 29 (cubic diamond-like), n = 21 (orthorhombic), n = 6 (cubic). $Cs_3PW_{12}O_{40}$, in which the Cs^+ ions occupy the sites of $H_5O_2^+$ ions of $H_3PW_{12}O_{40}$ hexahydrate, has a dense secondary structure and is anhydrous (Fig. 1.9c) [156].

In addition to the primary and the secondary structure, *"tertiary"* and higher-order structures are suggested to influence the catalytic function. The tertiary structure is the structure of solid heteropoly compounds as assembled (Fig. 1.9d). The sizes of the primary and secondary particles, pore structure, distribution of protons and cations, etc. are the elements of the tertiary structure [156].

Counter-cations greatly influence the tertiary structure of a heteropoly compound. The salts of small ions such as Na^+ (classified into group A salts [5]) behave similarly to the acid form in several respects. The group A salts are highly soluble in water and other polar organic solvents. The surface areas of group A salts are usually low. On the other hand, the salts of large cations such as NH_4^+ and Cs^+ (classified as group B) are insoluble in water and exhibit low absorptive capacity for polar molecules. The surface areas of group B salts are usually high due to the smaller sizes of the primary particles, giving favourable properties for heterogeneous catalysis. The thermal stability of most group B salts is relatively high, which is also important in heterogeneous catalysis [156].

1.4.3.2 The Keggin structure

This is the first characterised and the best known structure that is adopted by many polyoxometalates. Among a wide variety of heteropoly compounds, the Keggin's are the most stable and more easily available. These, together with some of their derivatives, are the most important for catalysis [169,155].

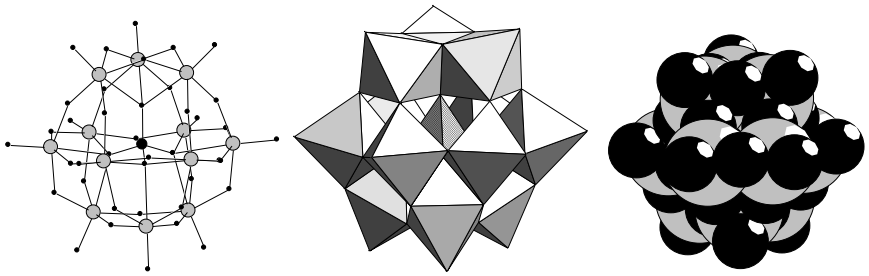

Fig. 1.10 The Kegin structure of the $XM_{12}O_{40}^{x-8}$ anion (α-isomer): (a) bond, (b) polyhedral and (c) space-filling representations [155].

The Keggin heteropoly anions are typically represented by the formula $XM_{12}O_{40}^{x-8}$, where **X** is the heteroatom (central atom, e.g. P^{5+}, Si^{4+}, etc.), ***x*** is its oxidation state, and **M** is the addenda atom (metal ion, typically W^{6+} or Mo^{6+}). The addenda atoms can be partially substituted by many other metal ions, e.g., V^{5+}, Co^{2+}, Zn^{2+}, etc. The Keggin anion (Fig. 1.10) has a diameter of ca. 1.2 nm and is composed of a central tetrahedron XO_4 surrounded by 12 edge- and corner-sharing metal - oxygen octahedra MO_6 [1,18]. The octahedra are arranged in four M_3O_{13} groups. Each group is formed by three octahedra sharing edges and having a common oxygen atom, which is also shared with the central tetrahedron XO_4. The total assemblage contains 40 close-packed oxygen atoms.

The oxygens in the structure are of four types: twelve terminal M=O, twelve edge-bridging angular M-O-M shared by the octahedra within a M_3O_{13} group, twelve corner-bridging quasi-linear M-O-M connecting two different M_3O_{13} groups, and four internal X-O-M. These oxygens can be discriminated by ^{17}O NMR [1]. The corresponding bonds exhibit characteristic infrared bands in the range of 500-1100 cm^{-1} [152].

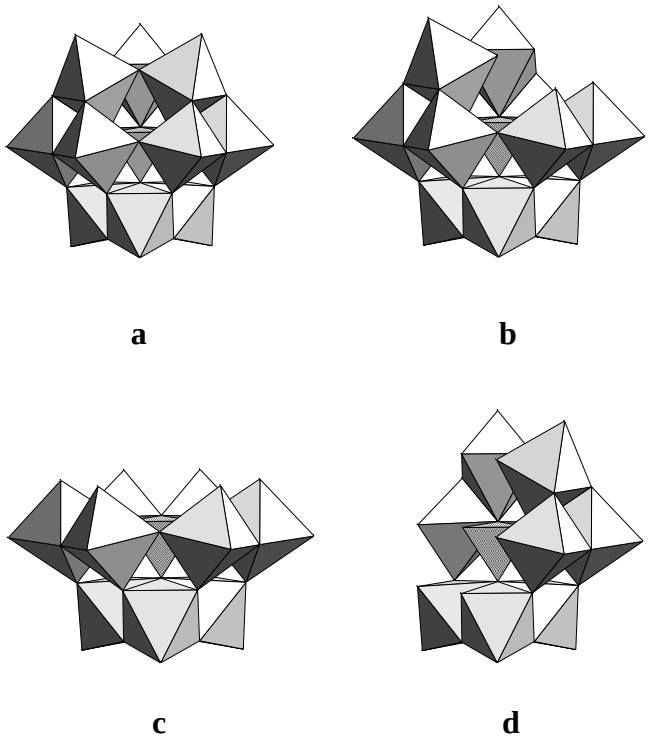

Fig. 1.11 The Kegin structures of the $XM_{12}O_{40}^{x-8}$ anion and its lacunary derivatives: (a) α-Keggin anion; (b) monovacant; (c) trivacant A-{XM_9} and (d) trivacant B-{XM_9} [155].

Each of the M_3O_{13} groups can be rotated 60° about its 3-fold axis, which leads to geometrical isomers. The most common is the α-isomer shown in Fig. 1.10. Rotation of one M_3O_{13} group produces the β-isomer. In some cases, these isomers can be separated, e.g., by fractional crystallisation. Rotation of two, three or all four M_3O_{13} groups produces the γ, δ, and ε isomer, respectively [152].

Lacunary derivatives of the Keggin anion result from the removal of one or more **M** atoms. Examples of three lacunary derivatives (one monovacant and two trivacant) of the α-Keggin anion are shown in Figure 1.11. Such species can assemble into larger polyoxometalate structures, either directly or with incorporation of metal ion linkers [152,155].

1.4.3.3 The Wells-Dawson structure

One of these derivatives is the Wells-Dawson dimeric heteropoly anion $X_2M_{18}O_{62}^{2x-16}$ (**M** = Mo^{6+} or W^{6+}, **X** = P^{5+}or As^{5+}) [4,5,20]. Its structure (α isomer) is shown in Figure 1.12. The primary structure can be described as two half units ($PW_9O_{31}^{3-}$ lacunary Keggin anions) linked together through 6 oxygen atoms, which are equally shared by the two halves.

1.4.3.4 The Anderson-Evans structure

The Anderson-Evans structure is adopted by 6-heteropoly anions (e.g. $Te^{6+}Mo_6O_{24}^{6-}$) [4,5,19]. It consists of six MO_6 octahedra arranged in a closed ring sharing edges. The heteroatom occupies the octahedral pocket in the centre of the ring (Figure 1.13) [155,156,170].

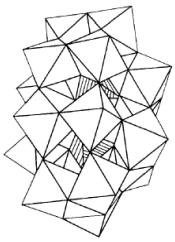

Fig. 1.12 The Dawson structure

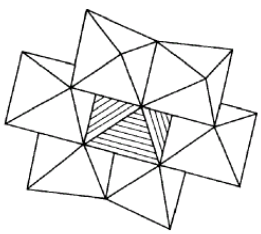

Fig. 1.13 The Anderson-Evans structure

of α- $P_2W_{18}O_{62}^{6-}$ anion [152]. of the $Te^{6+}Mo_6O_{24}^{6-}$ anion [152].

1.4.4 Proton structure of heteropoly acids

HPAs are strong Brønsted acids. Two types of protons have been found in crystalline HPAs, non-localised hydrated protons and non-hydrated protons localised at the oxygen atoms of the polyanion. The hydrated protons possess a high mobility; these are responsible for the extremely high proton conductivity of crystalline heteropoly acid hydrates. The non-hydrated protons are much less mobile; these are suggested to localise on the peripheral oxygens of the polyanion [4]. As the water content decreases, the protons become localised to a large extent. Thus, the water plays a crucial role in the formation of proton structure and, hence, catalytic features of HPA catalysts. Control of water content is important for reproducibility of catalyst preparation and their properties, in particular their acidity. The amount of water in HPA catalysts can be controlled by thermal pretreatment [155,156].

Structural characterisation of the HPA proton sites is an important step towards understanding the catalytic activity. Keggin anions have three types of outer oxygen atoms as potential protonation centres: terminal oxygens M=O and two types of bridging oxygens M-O-M, edge sharing and corner sharing (Fig. 1.10) [153-163].

In heteropoly acids in the solid state, protons play an essential role in the structure of the crystal, by linking the neighbouring heteropoly anions. The state of protons and their mobility strongly depends on the amount of hydration water in HPA. From single-crystal X-ray and neutron diffraction data [25], the crystal structure of HPW hexahydrate is formed by packing heteropoly anions into a body-centered cubic structure. In this structure, each proton is doubly hydrated, $H_5O_2^+$, and shared by four terminal oxygens, belonging to four different heteropoly anions (Fig. 1.14a). Interestingly, the same structure was suggested [25] for the structurally similar HPA salts, e.g., $Cs_3PW_{12}O_{40}$, in which the Cs^+ ions each have four equivalent terminal oxygens as the closest neighbours [155,174].

Evidence of the predominant protonation of the terminal oxygens in solid HPW and HSiW has been obtained by ^{17}O NMR by comparison of solution and solid-state spectra for these HPAs. Upon dehydration, the structure of HPW is suggested to transform to one shown in

Fig. 1.14b. Raman and IR spectroscopy have also been applied to provide further information on the structural arrangement and proton species [153,155,175-178].

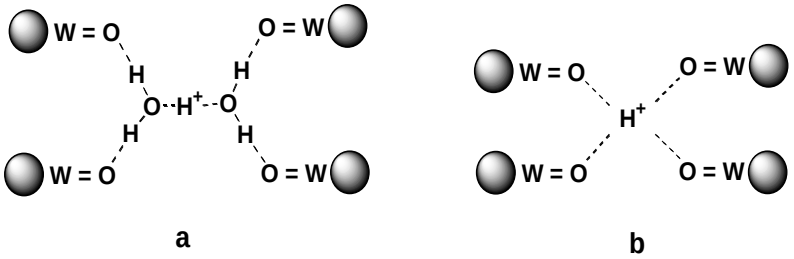

Fig. 1.14 Schematic structure of bulk proton sites in (a) $H_3PW_{12}O_{40}\cdot 6H_2O$ and (b) dehydrated $H_3PW_{12}O_{40}$ [152]. The protons are hydrogen-bonded to the terminal oxygens and link four neighbouring Keggin anions.

1.4.5 Stability of heteropoly acids

1.4.5.1 Stability of heteropoly acids in solution

Particular attention should be paid to both the hydrolytic stability in solution and the thermal stability. Each heteropoly anion is stable only at pH values lower than the corresponding solid line in Fig 1.15 [155,156].

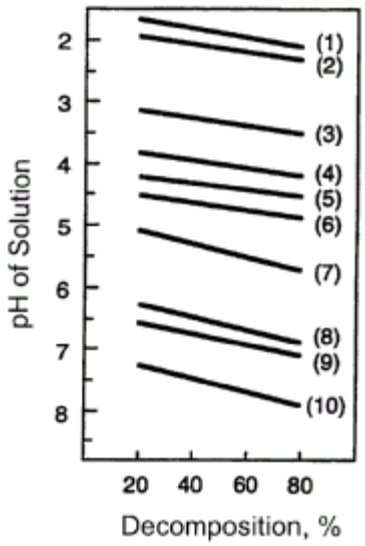

Fig. 1.15 pH range of existence of heteropoly acids [31]: (1) $PMo_{12}O_{40}^{3-}$, (2) $PW_{12}O_{40}^{3-}$, (3)

$GeMo_{12}O_{40}^{4-}$, (4) $GeW_{12}O_{40}^{4-}$, (5) $P_2W_{18}O_{62}^{6-}$, (6) $SiW_{12}O_{40}^{4-}$, (7) $PMo_{11}O_{39}^{7-}$, (8) $P_2Mo_5O_{23}^{6}$, (9) $H_2W_{12}O_{40}^{6-}$, (10) $PW_{11}O_{39}^{7-}$ [155].

Generally the stability of 12-heteropoly anions towards hydrolysis in aqueous solution decreases in the order of addenda atoms [179]:

$$W(VI) > Mo(VI) > V(V).$$

With respect to the stability of heteropoly compounds, it can be said that the nature of the central atom (heteroatom) is also critical for the stabilisation of the primary structure. Generally, the stability decreases in the following series of central atoms [179]:

$$Si^{4+} > Ti^{4+}, Zr^{4+} > Ge^{4+} > P^{5+} > As^{5+}.$$

1.4.5.2 Thermal stability of solid heteropoly acids

The thermal stability of heteropoly compounds is of great importance for their use in heterogeneous catalysis. Some compounds are fairly stable and can be applied as catalysts at moderately high temperatures, up to 300-350^{o}C. The thermal stability, however, may not be sufficient for catalyst regeneration, for example, for burning coke that may form on the catalyst surface [155].

Thermal decomposition of polyoxometalates (to eventually form a mixture of oxides) is a complex multistage process. The catalyst activity may be irreversibly lost at an early stage of decomposition. For example, solid acid catalysts based on tungsten heteropoly acids (e.g. $H_3PW_{12}O_{40}$) probably lose activity at the onset of thermal decomposition of the Keggin structure, when the acid protons are lost, i.e. well before the formation of WO_3 and P_2O_5 is complete [153].

The thermal stability is usually determined by thermal analytical methods (thermal gravimetric analysis (TGA), differential thermal analysis (DTA) and differential scanning calorimetry (DSC)) frequently in combination with other techniques, such as X-ray

diffraction, infrared spectroscopy, solid state NMR, etc. Tsigdinos introduced a simple method that allows estimation of the thermal stability of heteropoly compounds. This method includes heat treatment followed by a solubility test. If, after heating, the compound is soluble in water its structure is deemed to remain intact; otherwise the structure has decomposed [180].

A great deal of caution should be taken when comparing the thermal stabilities from different sources. The decomposition temperatures are subject to many parameters such as the heating rate, the amount of sample, the shape of the crucible, the purity of the sample, the atmosphere, etc. On top of that, the decomposition on the surface of the sample may occur at a lower temperature than in the bulk [155].

Generally, Keggin-type heteropoly compounds are the most stable among various polyoxometalates. The decomposition temperature (^{o}C) for the most typical Keggin heteropoly acids, as estimated from TGA, decreases in the following series [181]:

$H_3PW_{12}O_{40}$ >	$H_4SiW_{12}O_{40}$ >	$H_3PMo_{12}O_{40}$ >	$H_4SiMo_{12}O_{40}$
465	445	375	350

1.4.6 Acid properties of heteropoly acids in solution

Typical heteropoly acids with the Keggin structure, such as $H_3PW_{12}O_{40}$, $H_4SiW_{12}O_{40}$ and $H_3PMo_{12}O_{40}$, are strong acids; protons are dissociated completely from the structures in aqueous solution. Heteropoly acids are much stronger acids than H_2SO_4, HBr, HCl, HNO_3, and $HClO_4$ [155.156].

The greater acid strength of heteropoly acids is explained as follows. Since in heteropoly anions the negative charge of similar value is spread over much larger anions than those formed from mineral acids, the electrostatic interaction between a proton and anion is much weaker for heteropoly acids than for mineral acids. An additional important factor is the possibility of dynamic delocalisation of the charge or electron. The change in the charge caused by deprotonation may be spread over the entire polyanion unit [156,160].

As for the acid strength of heteropoly acids, the following order has been reported for the acetone solution [156]:

$$H_3PW_{12}O_{40} > H_4SiW_{12}O_{40} \approx H_3PMo_{12}O_{40} > H_4PMo_{11}VO_{40}.$$

The acid strength decreases when Mo or V replaces W and when the central P atom is replaced by Si (the acid strength increases in the order Co < B < Si, Ge < P). Tungsten acids are stronger than molybdenum ones. The strongest acid in the Keggin series is $H_3PW_{12}O_{40}$. This order agrees with the electrostatic theory, since the acid strength increases with a decrease in the negative charge of the heteropoly anion, or an increase in the valence of the central atom [162].

1.5 Polyoxometalates as catalysts for biphasic oxidation with H_2O_2

1.5.1 Phase transfer catalysis

The foundations of phase transfer catalysis (PTC) were laid in the late 1960s and early 1970s by the studies of Makosza (1975), Starks (1971) and Brandstrom (1977). Starks is considered to have coined the phrase *phase transfer catalysis.* Although some would tend to disagree with calling the PT cycle a catalytic process in the true sense of the word catalysis, this terminology has been widely adopted [183-187].

Many desirable reactions cannot be brought about because the reactants are inaccessible to each other. The problem of bringing together a water soluble nucleophilic reagent and an organic water insoluble electrophilic reagent has been solved by addition of a solvent that is both water-like and organic-like (such as ethanol, which derives its hydrophilic nature from its hydroxyl group and its lipophilicity from the ethyl group) [183]. However, rate acceleration is minimal due to excessive solvation of the nucleophile. Alternatively, dipolar aprotic solvents such as dimethyl formamide (DMF) or dimethyl sulfoxide (DMSO) can be used but they suffer from being difficult and expensive to separate from the reaction mixture during post-reaction recovery [183].

An achievable and industrially successful method developed over the last quarter century is the use of phase-transfer agents, employed in catalytic amounts, which transfer reactive

anions from the aqueous or solid phase into the organic phase, where reaction occurs. A very important means of transcending phase barriers in heterogeneous systems has been proved by using PTC. This is environmentally friendly and economically profitable method of synthesizing a wide variety of organic chemicals and it is extensively used in the fine chemicals industry [183].

1.5.2 Epoxidation of alkenes in two-phase systems catalysed by POM

The development of catalysts for selective and environmentally friendly oxidation of organic compounds is an important research goal. Catalytic epoxidation of alkenes has attracted much attention both in an industry and in organic synthesis because epoxides are among the most useful synthetic intermediates. The formation of epoxides *via* metal-catalyzed oxidation of alkenes represents the most elegant and green route for the production of this class of compounds. Epoxides are key raw materials for a wide variety of products and much effort has been applied to the development of new active and selective epoxidation catalysts for processes that avoid the formation of large amounts of by-products [191,192].

Polyoxometalates (POMs), large transition metal oxygen cluster anions, have been largely used as catalysts as consequence of their unusual versatility and compatibility with ecosustainable conditions. Transition metal substituted polyoxometalates are attractive as oxidation catalysts since they contain reactive low valence transition metal centres complexed by inorganic oxometalate ligands which may have high capacity as oxygen transfer agents [188-190].

Highly efficient POM-catalysed alkene epoxidation in two-phase water/organic systems has been developed in the past two decades. Much attention has been attracted to tungsten-based epoxidation systems with hydrogen peroxide because of their high reactivities compared with molybdenum analogues and inherent poor activity for decomposition of hydrogen peroxide. Ishii et al. reported effective H_2O_2-based epoxidation of terminal olefins catalyzed by $H_3PW_{12}O_{40}$ combined with cetyl pyridinium chloride (CPC) as a phase transfer agent [193] (eqn. 1.2). Other polyoxometalates such as $H_3PMo_{12}O_{40}$, $H_4SiW_{12}O_{40}$, and $H_3PMo_6W_6O_{40}$ were much less active than $H_3PW_{12}O_{40}$ [194].

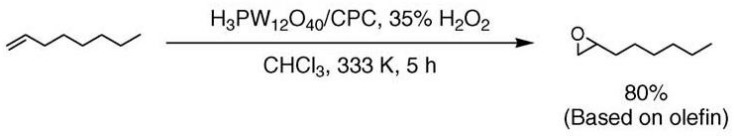

(1.2)

The $[PO_4\{WO(O_2)_2\}_4]^{3-}$ peroxotungstate was isolated and characterized crystallographically by Venturello et al. [195]. The anion consists of the PO_4^{3-} anion and two $[W_2O_2(O_2)_4]$ peroxo species (Fig. 1.16). The Venturello complex was postulated to be a catalytically active species for the $H_3PW_{12}O_{40}/H_2O_2$ system because $[PO_4\{WO(O_2)_2\}_4]^{3-}$ exhibited a very similar catalytic reactivity to that of the Ishii system [195]. The spectroscopic and kinetic investigations by Bregeault et al. [196], Griffith [197], Thouvenot [198], and Hill [199] showed that $[PO_4\{WO(O_2)_2\}_4]^{3-}$ is a catalytically important species among various peroxotungstates generated by the reaction of $H_3PW_{12}O_{40}$ with excess hydrogen peroxide (eqn. 1.3) [194].

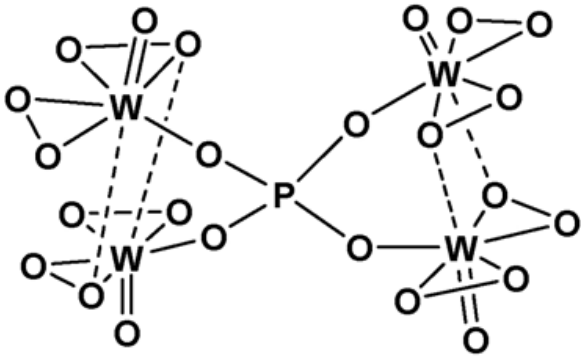

Fig. 1.16 Molecular structure of $[PO_4\{WO(O_2)_2\}_4]^{3-}$[194].

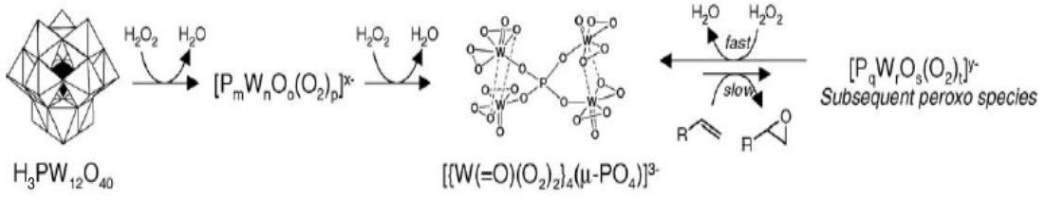

(1.3)

Biphasic epoxidation catalyzed by lanthanide-containing polyoxometalates with H_2O_2-based, $[LnW_{10}O_{36}]^{n-}$ and $[Ln\{PW_{11}O_{39}\}_2]^{m-}$ (Ln =Y, La, Ce, Pr, Sm, Eu, Gd, Dy, Er, Lu, etc.), was reported by Griffith [194,200-205]. Lanthanide itself plays no role in the catalysis and indeed in some cases even works as an inhibitor. The Raman and ^{31}P NMR spectroscopy show that

peroxotungstates such as $[PO_4\{WO(O_2)_2\}_4]^{3-}$ and $[W_2O_3(O_2)_4(H_2O)_2]^{2-}$ are active species in the same manner of the Ishii–Venturello system [194, 200–202].

1.5.3 Oxidative desulfurisation catalysed by POM in two-phase systems

The oil industry faces huge pressure to remove organic sulfur compounds from transportation fuels. To meet the growing demand for clean fuels, the implications are complex, as regards the need for a highly active desulfurization catalyst. The greatest advantage of oxidative desulfurization (ODS) as compared with other conventional processes is that it can be carried out in liquid phase under very mild conditions at near room temperature and under atmospheric pressure. In ODS reactions, the divalent sulfur can be oxidized by the electrophilic addition reaction of oxygen atoms to form the hexavalent sulfur of sulfones. The chemical and physical properties of sulfones are significantly different from those of hydrocarbons in fuel oil. Therefore, they can easily be removed by separation operations such as distillation, solvent extraction, adsorption and decomposition [203].

It has been reported that tungsten catalysts are very effective for the oxidation of thioethers into sulfoxides and sulfoxides into sulfones using H_2O_2 as the oxidant in a two liquid–liquid (L–L) phase system with a phase transfer catalyst (PTC). Such a biphasic oxidation reaction follows the cycle illustrated in Fig. 1.17, where phenylphosphonic acid acts as an accelerator. In the polar phase, the catalyst precursor H_2WO_4 is rapidly peroxidised by H_2O_2 according to the equation $H_2WO_4 + 2\ H_2O_2 \rightarrow H_2[WO(O_2)_2(OH)_2] + H_2O$. The resulting bisperoxotungstate compound is transferred to the apolar phase by ion exchange with the phase transfer agent (Q^+). The bisperoxotungstate compound in the apolar phase oxidizes thioethers into sulfones and can then be regenerated at the L–L interface with H_2O_2 or transferred to the polar phase where it reacts with hydrogen peroxide. The obtained sulfones are transferred to the polar phase due to the solubility of sulfones in a polar solution, yielding a sulfur free apolar phase [203,204].

It was reported that a $[(C_{18}H_{37})_2N(CH_3)_2]_3[PW_{12}O_{40}]$ catalyst, assembled in an emulsion in diesel, could selectively oxidize DBT and its derivatives into their corresponding sulfones using H_2O_2 as an oxidant under mild conditions. The sulfones can be readily separated from

the diesel using an extractant, and ultra-deep desulfurisation of diesel can be achieved [205]. However, the oxidative activity of this system is not high enough to efficiently oxidize benzothiophene (BT) and its derivatives, which are present largely in non-hydrotreated diesel, and achieving ultra-deep desulfurization of various actual diesels is difficult with this system [206].

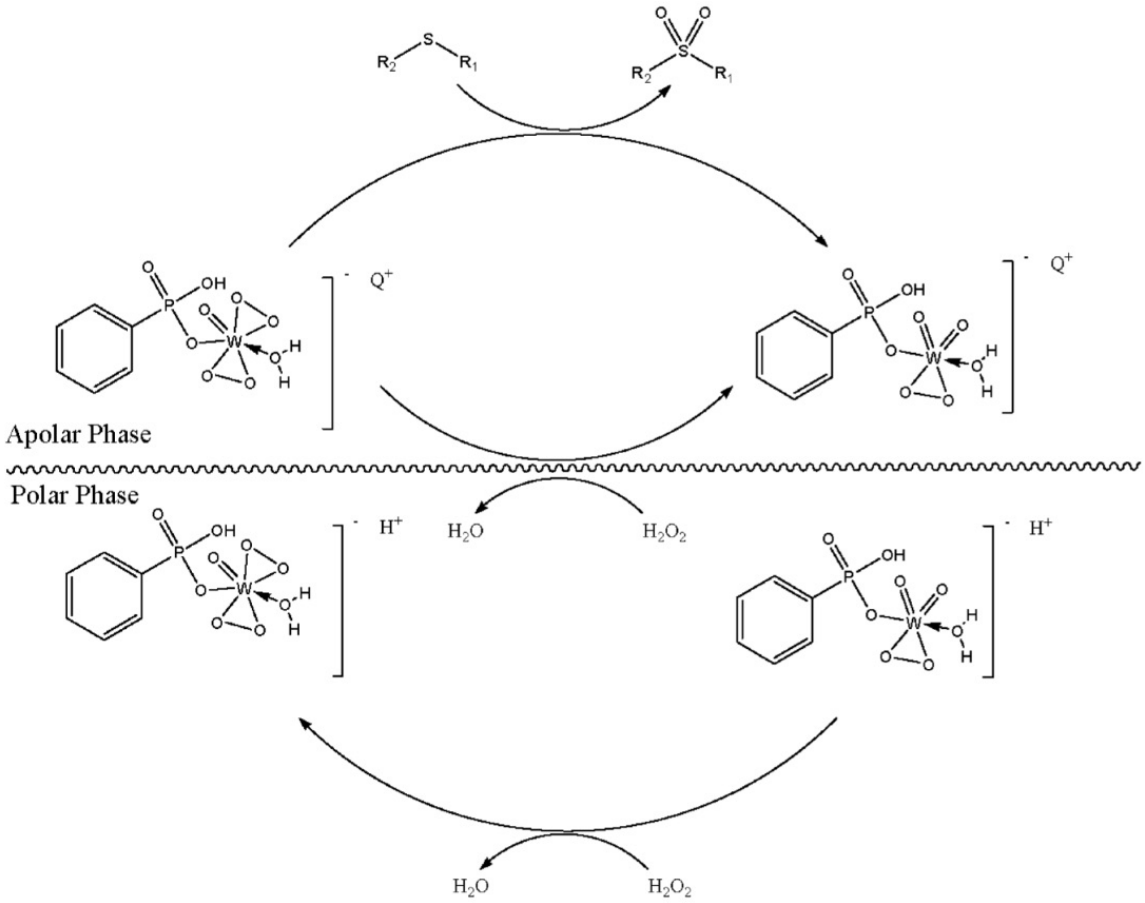

Fig. 1.17 Catalytic cycle of sulfur compounds oxidation ($Q^+ = CH_3(n\text{-}C_8H_{17})_3N^+$) [203].

Li et al. have reported several kinds of amphiphilic catalysts, such as $[(C_{18}H_{37})_2N(CH_3)_2]_3[PW_{12}O_{40}]$ [206, 208], $[C_{18}H_{37}N(CH_3)_3]_4[H_2NaPW_{10}O_{36}]$ [208, 209] and $Q[W(O)(O_2)_2(C_5H_4NCO_2)]$ (Q = $(C_4H_9)_4N$, $[(CH_3)_3N(C_{18}H_{37})]$ and $[(C_{18}H_{37})_2N(CH_3)_2]$) leading to the formation of emulsion droplets in their desulfurization research [29, 207]. Quaternary ammonium salts were used in preparation of catalysts to act as phase-transfer agents in new reaction systems, which achieved high reaction activity. The new desulfurization catalysts can be further improved by using longer chain quaternary ammonium surfactants.

Jiang et al. reported decatungstate $[W_{10}O_{32}]^{4-}$ bound to a quaternary ammonium salt with single long carbon chain as highly active desulfurization catalyst with H_2O_2 as the oxidant. The quaternary ammonium cation acted as phase-transfer agent. DBT in the model oil could be effectively oxidized into its corresponding sulfone to obtain oil with low sulfur content [207].

1.6 Phosphazenes

1.6.1 Background

Polyphosphazenes (Fig. 1.18) are a broad class of chemical compounds with a backbone of alternating phosphorus atoms covalently linked to a nitrogen atom by a double bond and to three other atoms or radicals by single bonds [210].

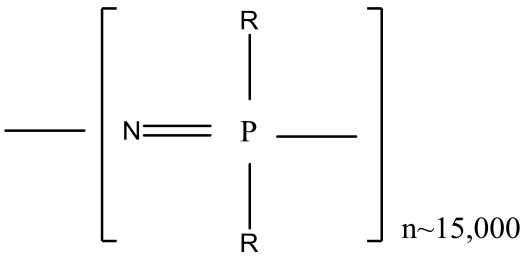

Fig. 1.18 The structure of phosphazene [210].

The skeletal architecture may be linear, branched, star, or dendritic, or it may be part of a di- or tri-block copolymer in conjunction with organic macromolecules or poly(organosiloxanes) (silicones). However, it is in the wide variety of side groups that this system differs from many other polymer platforms. More than 250 different organic, organometallic, or inorganic side groups have been utilized in single-substituent arrays or in di-, tri-, or higher mixed-substituent patterns. Thus, hundreds of different polyphosphazenes are known with a corresponding diversity of properties and potential uses. [210] These can be divided into different families of polymers such as inert biomaterials, bioerodible polymers, optical materials, membranes, ionic conductors, and so on.

In the 1950s, growing demand for materials with new and unusual properties led to an enormous increase in the research on substitution and polymerization reactions of phosphazenes [211]. In the 1960-70s van de Grampel and co-workers introduced a series of

mixed ring systems with one or more of the PC_{l2} centres replaced by a SOR group (Fig. 1.19) [212, 213]. These structures are known as cyclothiaphosphazenes.

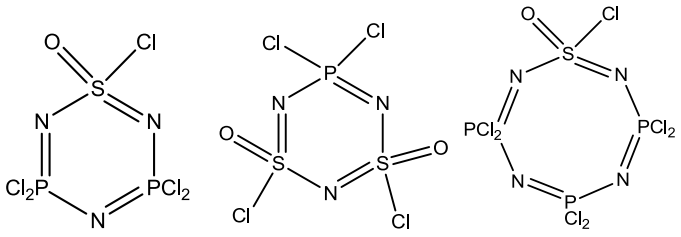

Fig.1.19 Structures of some cyclothiaphosphazenes.

1.6.2 Structure of phosphazenes

A considerable amount of research has been directed toward the elucidation of phosphazene structures using X-ray diffraction and spectroscopic techniques. NMR spectroscopy has been used extensively in phosphazene chemistry as a structural identification technique and as a means for probing bonding patterns. The investigations have included ^{1}H, ^{31}P and ^{19}F studies.

1.6.2.1 X-ray diffraction

Approximately 30 cyclo- and polyphosphazenes have been investigated by X-ray diffraction techniques. The results of single crystal studies confirm that those compounds which have the formula $(NPR_2)_{3\text{-}8}$ are cyclic, while fiber diagram work indicates that the rubbery materials of the formula $(NPR_z)_n$ are long-chain polymers. Cyclic phosphazenes are found with both planar and puckered phosphorus-nitrogen rings. Unlike organic aromatic species, moderate puckering of the ring appears to have little or no influence on molecular stability [214].

The majority of tetramers and higher cyclic species examined to date are non-planar. The exceptions are $(NPF_2)_4$, which forms a regular planar ring, and the cyclic pentamer, $(NPC1_2)_5$, which achieves near-planarity by indentation and loss of a regular cyclic shape (Fig. 1.20)**.** Octachlorocyclotetraphosphazene, $(NPC1_2)_4$, exists in two crystallographic modifications. The stable T form contains chair-shaped rings, and the metastable K form

contains molecules in a tub conformation. The bromophosphazene, $(NPBr_2)_4$ occupies a similar conformation to that of the K form of $(NPC1_2)_4$. An unusual conformation is found for $[NP(OMe)_2]_8$, in which the cyclic octameric ring consists of two planar sections. (Fig. 1.21) [214-219].

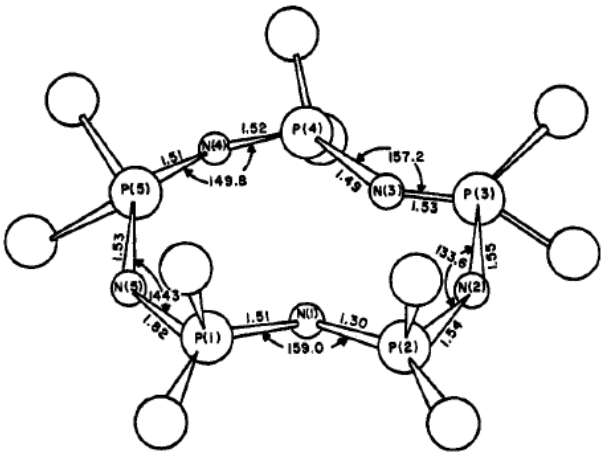

Fig. 1.20 Molecular structure of $(NPC1_2)_5$ [214].

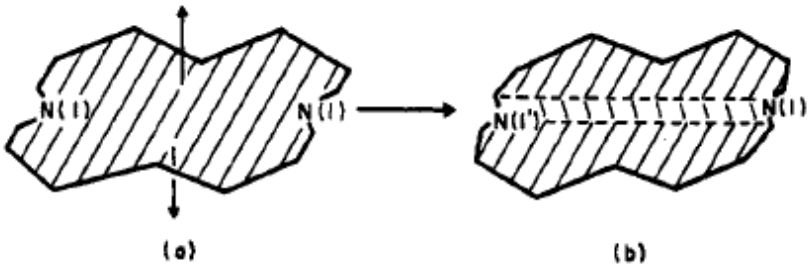

Fig. 1.21. Idealized molecular shape of phosphazene ring in $[NP\text{-}(OMe)_2]_8$ [214].

The conformation of one high polymer, $(NPF_2)_n$ has been solved by structure factor methods. At temperatures below -56^oC the stretched polymer occupies a cis-trans planar conformation (eqn 1.4), although at higher temperatures a non-planar arrangement predominates. Optical transform analysis of X-ray fiber patterns from $(NPC1_2)_n$ indicated the presence of a slightly distorted cis-trans planar arrangement [214, 220, 221].

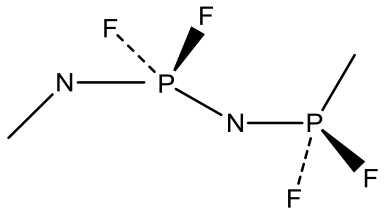

(1.4)

It seems clear that the high polymer conformations are more a response to intra- and intermolecular nonbonding forces than to the restricting effects of phosphorus-nitrogen bonding. For cyclic phosphazenes, the planarity or nonplanarity of the ring depends on the need for the molecule to avoid skeletal angular strain [214].

1.6.2.2 Phosphorus-Nitrogen bond lengths

A phosphorus-nitrogen single bond length is usually assumed to be in the region of 1.77-1.78 Å. The bond lengths in cyclo- and polyphosphazenes are in the range of 1.47-1.62 Å, and this represents an appreciable contraction. The shortest skeletal bonds are associated with highly electronegative substituents, and this bond contraction is ascribed to skeletal π-bond influences. A marginal trend also exists toward shorter skeletal bond lengths in cyclophosphazenes as the ring size increases for the smallest rings, although this trend does not continue to the high polymers [214,222-224].

Of particular importance is the fact that, if the substituents are symmetrically disposed around the ring, all the phosphorus-nitrogen bond lengths are equal. No separation into alternating long and short, σ and σ-π bonds is observed in the neutral system. This provides a sharp contrast with the situation encountered in cyclooctatetraene and in boronnitrogen and thiazyl fluoride heterocycles, where a separation into alternating long and short bonds occurs in the cyclic tetramer. However, the protonated phosphazenium cation in $[(NPMe_2)_4H]_2^+CoC1_4^{2-}$ shows some evidence of bond length alternation. It should be noted that asymmetric ligand arrangements lead to the presence of unequal bond lengths around the ring because of the ligand electronegativity influence [214,225-228].

1.6.2.3 Nuclear magnetic resonance

The chemical shift of a proton located in a substituent group will be influenced by: the other nuclei within that same group; by the other group attached to the same phosphorus atom; by the substituent groups attached to nearby phosphorus atoms, and often by the size of the phosphazene ring. However, in general, the proton chemical shifts are comparable to those found in related organic compounds, as illustrated by the following examples (chemical shift to TMS in parentheses): NMe_2 (7.27-7.79), OCH_3 (6.29-6.46), OPh (2.8-3.2) and Ph (2.2-2.7). Spin-spin coupling effects are also usually present. Thus, proton NMR spectra can be used for "fingerprint" identification and for the structure determination of unknown compounds [214,229,230].

^{31}P NMR spectroscopy is a valuable tool for structural identification, it cannot be used reliably for direct chemical identification by "group shift" methods. Cyclic trimers generally yield ^{31}P shifts in the range of 0 to -46 ppm. However, the large positive shift of the PBr_z unit (+37 to +45 ppm) is characteristic. Furthermore, apart from bromophosphazene trimers, positive shifts appear to be characteristic of cyclic tetramers, pentamers, hexamers, heptamers, octamers, and linear high polymers. Cyclic tetrameric and higher ring systems resemble the high polymers in providing more opportunities for conformational changes than do the rather rigid cyclic trimers [214].

Fluorine atoms bound directly to the phosphazene ring show ^{19}F NMR spectra which indicate an influence by the supporting phosphorus atom and by nearby ring phosphorus atoms. Fluorine chemical shifts range from 19.6 ppm (relative to $CFC1_3$) for the PFBr unit in $N_3P_3F_5Br$ to 71.9 ppm for the PF_2 group in $(NPF_2)_3$ [214, 230].

1.6.3 Synthesis of phosphazenes

The synthesis of the phosphazene skeleton can be accomplished by a number of routes. The cyclo- or polyphosphazenes formed by these direct synthesis methods are principally chloro, bromo, alkyl, or aryl derivatives. The majority of other phosphazenes are then synthesized by substitution reactions using the halogeno derivatives [214, 231].

Ammonium chloride reacts with phosphorus pentachloride in a boiling solvent, such as tetrachloroethane, to yield a mixture of cyclic and linear phosphazenes, with the concurrent evolution of hydrogen chloride. This reaction provides the most convenient route for the synthesis of chlorophosphazenes. These are themselves used as precursors for the preparation of nearly all organophosphazenes, and, the importance of this reaction cannot, therefore, be overemphasized. Since the initial report of this process in 1924**,** a considerable amount of research has been conducted to control the yields of specific chlorophosphazenes, to elucidate the reaction mechanism, and to develop a manufacturing process. At the present time, several companies produce chlorophosphazenes on a pilot plant or limited commercial basis, and it now seems clear that the technological future of phosphazene chemistry may depend on the efficiency and cost of these manufacturing processes [214, 232-237].

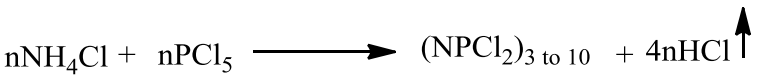

The laboratory preparation requires the reaction of approximately equimolar amounts of ammonium chloride and phosphorus pentachloride in boiling tetrachloroethane for ~7.5 h, followed by filtration to remove unreacted ammonium chloride. Removal of the solvent from the filtrate leaves an oily mixture of linear and cyclic phosphazenes, and the latter can be selectively removed by extraction with petroleum hydrocarbons. Typically, the cyclic chlorophosphazenes constitute ~60-70% of the total product, and, in this component, approximately 37% is $(NPCl_2)_3$, 28% is $(NPCl_2)_4$, and 35% is a mixture of higher cyclic chlorophosphazenes of formula $(NPCl)_n$. Pure trimer can be obtained by several fractional crystallizations from petroleum, by fractional sublimation, or by zone refining [214, 233, 238].

1.6.4 Applications of phosphazenes

The incorporation of phosphazenes into polymeric compositions is one of the most active areas of phosphazene application. Other research has been directed to the study of ethyleniminocyclophosphazenes as chemosterilant insecticides and as cancer chemotherapeutic agents [239,240]. Hexakis(amino)cyclotriphosphazene has been proposed as a high capacity fertilizer [241]. Alkoxyphosphazenes have proved to be valuable as flame

retardants for textiles [242]. Hexabromocyclotriphosphazene is used as a "getter" and bromine source in halogen lamps [243]. Phosphazene clathrates are investigated as substrates for the separation of organic compounds. At the present time, the technological opportunities in phosphazene chemistry appear to be expanding, and this field remains a fertile area for both fundamental and applied research [214].

1.7 Terminally functionalised polyisobutylene ligands

In synthesis and catalysis, interest in soluble polymer supports is increasing. Previously, most of the attention on polymer supports has focused on polystyrene with catalysts/reagents/ligands on pendant groups. Other soluble polar and nonpolar supports which are useful in catalysis have tuneable phase selective solubility that is altered by the identity of alkyl substituent groups. A lot of research has shown that such polymers can be recovered by liquid/liquid separations [244]. Terminally functionalized polymers are soluble alternatives to polymer supports with pendant groups. Poly(alkene oxide) (PEG) is the most common example of such a support. These linear polyethers are easier to characterize and can be recovered in the polar phase of a thermomorphic mixture [244].

However, PEG supports are more often recovered by less efficient solvent precipitation schemes. Solvent precipitation can be avoided by using terminally functionalized polyethylene (PE) oligomers. PE oligomers are recoverable by precipitation and filtration without excess solvent addition. However, PE's insolubility at < 50 °C and solubility only at > 75 °C in nonpolar solvents limit its utility. Bergbreiter et al. demonstrated that polyisobutylene (PIB) is a promising alternative to either PEG or PE [244]. Suitable terminally functionalized polyisobutylenes are easily prepared from commercially available materials. These readily soluble oligomers and the catalysts attached to them can be easily separated from products by liquid/liquid separation using a non-polar solvent after a reaction [244]. Amino functionalized PIB oligomers are investigated in this work as phase transfer agents in biphasic oxidations with hydrogen peroxide catalysed by POMs in collaboration with Prof. D.E. Bergbreiter's group (Texas A&M University, USA).

1.7.1 Synthesis of Terminally Functionalised Polyisobutylene

The synthesis of diethylamine terminated PIB oligomer is represented in Fig. 1.22. Vinyl-terminated PIB_{1000} (Glissopal 1000) (**1)** was obtained from BASF. This commercial sample, which contains some saturated PIB and a small amount of alkene isomer, was used without further purification [244, 245].

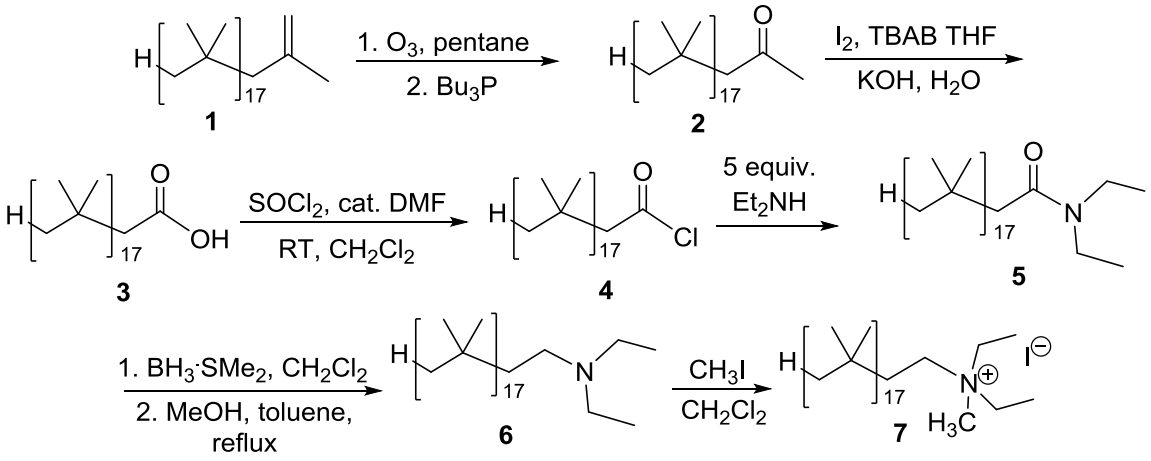

Fig. 1.22. Synthesis of a PIB_{1000}-amine and PIB_{1000}-quaternary ammonium salt [244, 245].

PIB_{1000}-$COCH_3$ (**2**). The starting vinyl-terminated PIB_{1000} (40.29 g, 40.29 mmol) Glissopal 1000) was dissolved in 200 mL of pentane. The resulting solution was cooled in an acetone-dry ice bath and was purged with oxygen for 10 min. Ozone was bubbled into the reaction mixture until the solution turned blue. Then the reaction mixture was purged with oxygen again to remove excess ozone from the solution until the solution became colorless. To reduce the ozonide, tributylphosphine (20 mL, 80 mmol) was added to the reaction mixture. The reaction mixture was stirred at room temperature under nitrogen for 24 h to complete this reaction. At this point, the reaction mixture was tested for peroxides with Baker Testrips. The solution was concentrated by removing pentane under reduced pressure only after the test was negative. The resulting mixture was dissolved in 200 mL of hexane, which was washed with 90% EtOH (4 x 50 mL) and brine (1 x 50mL). The organic phase was dried over anhydrous sodium sulfate and filtered. Hexane was removed under reduced pressure, and the crude product was purified with silica gel column chromatography to obtain an isolated yield of 90% (36.40 g, 36 mmol) [245].

PIB-$COOH_{1000}$ (**3**). PIB_{1000}-$COCH_3$ (2) (19.91 g, 19.91 mmol) was dissolved in 600 mL of THF. Iodine (19.20 g, 75.65 mmol) was added into the reaction mixture, followed by a solution of KOH (70.53 g, 1.07 mol) in 600 mL of deionized water. Tetrabutylammonium bromide (TBAB) (4.56 g, 14.15 mmol) was added into the reaction mixture and the resulting biphasic mixture was stirred for 48 h under nitrogen. After the iodoform reaction was complete, the aqueous layer was removed by extraction and THF was removed under reduced pressure. The crude product was dissolved in 150 mL of hexanes and this hexane solution was washed with 6 M HCl (2 x 40 mL), 90% EtOH (4 x 40 mL), and brine (1 x 40 mL). The organic phase was dried over anhydrous sodium sulfate and filtered and the solvent was removed under reduced pressure. The crude product was purified by silica gel chromatography to afford an isolated yield of 79% (15.66 g, 15.59 mmol) [245].

PIB_{1000}-COCl (**4**). PIB_{1000}-COOH (4.25 g, 4.23 mmol) was dissolved in 40 mL of dichloromethane. Thionyl chloride (1 mL, 13.77 mmol) and a catalytic amount of DMF (8 drops) were added and the reaction was stirred at room temperature under nitrogen for 24 h. The solvent was then removed under reduced pressure. The crude PIB_{1000}-COCl was used without further purification [245].

PIB_{1000}-$CON(CH_2CH_3)_2$ (**5**). PIB_{1000}-COCl (4.25 g, 4.16 mmol) was dissolved in 40 mL of dichloromethane. Diethylamine (2.50 mL, 21.28 mmol) was added into the solution, which was stirred at room temperature for 24 h. After the reaction was complete, the solvent was removed under reduced pressure. The viscous oil residue was dissolved in 80 mL of hexanes and this hexane solution was washed first with 90% EtOH (4 x 40 mL) and then brine (1 x 40 mL). The organic phase was dried with anhydrous sodium sulfate, filtered, and the solvent was removed by reduced pressure. The isolated yield of the amide product was 91% [245].

PIB_{1000}-$CH_2N(CH_2CH_3)_2$ (**6**). PIB_{1000}-$CON(CH_2CH_3)_2$ (21.46 g, 20.26 mmol) was dissolved in 200 mL of dichloromethane. The solution was placed under nitrogen for 15 min at which point 10 M $BH_3{\cdot}SMe_2$ (10.73 mL, 107.3 mmol) was added. The reaction was stirred at room temperature for 24 h. After the reaction was complete, solvent was removed under reduced pressure. The viscous residue was dissolved in 200 mL of toluene. Then 20 mL of methanol was added and the solution was stirred under reflux for 24 h to form trimethylborane. At this point, toluene was removed under reduced pressure and 150 mL of hexanes was used to dissolve the crude **6.** The hexane solution was washed with 90% EtOH (4 x 50 mL) and brine

(1 x 50 mL), dried with anhydrous sodium sulfate, filtered, and the solvent was removed under reduced pressure [245].

Two methods were used to purify PIB_{1000}-$CH_2N(CH_2CH_3)_2$. First, the amine could be purified using column chromatography (Brockmann aluminum oxide). Alternatively, a sequestration/release method we developed earlier using Amberlyst 15 could be used [245].

PIB_{1000}-$CH_2N(CH_2CH_3)_2CH_3I$ (**7**). PIB_{1000}-$CH_2N(CH_2CH_3)_2$ (3.6 g, 3.44 mmol) was dissolved in 30 mL of dichloromethane. Iodomethane (0.325 mL, 5.27 mmol) was added and the reaction solution was stirred at room temperature overnight. Dichloromethane was removed from the product ammonium salt by reduced pressure and the crude product was purified by aluminum oxide column chromatography to afford the ammonium salt **7** [245].

1.8 Objectives of this thesis and outline

It has been extensively documented that POMs, especially those comprising Keggin type polyanions $[XM_{12}O_{40}]^{m-}$ {X = P^{V} (m = 3) and Si^{IV} (m = 4)}, serve as precursors of highly efficient catalysts for environmentally benign biphasic oxidations with hydrogen peroxide. Oxidative desulfurization catalysed by POM using aqueous H_2O_2 as a "green" oxidant in a two-phase system has been developed as a promising method for deep desulfurization of transportation fuel.

Biphasic oxidations in a water–organic system are particularly attractive, as such systems facilitate product/catalyst separation. These reactions typically involve phase-transfer catalysis with peroxo polyanion transport through the water-organic interface and require an efficient agent to move the peroxo polyanions from the aqueous phase into the organic phase. The primary objective of this project is to investigate hexa-alkyl(amino)cyclotriphosphazenes as novel phase transfer agents for biphasic oxidation of benzothiophenes to sulfones catalysed by Keggin type POMs. In particular, we focus on the oxidation of dibenzothiophene (DBT) which is typically employed as a model reaction for catalyst testing. We also aim to gain an insight into phase behaviour of POM-phosphazene catalysts and reaction mechanism.

Terminally functionalized polyisobutylene (PIB) derivatives readily soluble in nonpolar solvents like heptane have been demonstrated to have the potential to improve the recovery and recycling of homogeneous catalysts. In this work, in collaboration with Prof. D.E. Bergbreiter group (Texas A&M University, USA), we investigate the use of amine terminated PIB oligomer as a solubilizing agent for Keggin POM catalysts in oxidative desulfurization with hydrogen peroxide in a heptane-water two-phase system. It is demonstrated that the PIB oligomer-bound Keggin polyoxometalates are efficient and recyclable catalysts for environmentally benign biphasic oxidation of benzothiophene derivatives with hydrogen peroxide to the corresponding sulfones.

Chapter 1 presents definitions and an outline account of the environmental background of fuel sulfur regulations and desulfurization technologies, in addition to a brief introduction to heteropoly acids, phosphazenes and PIB oligomers. The literature on the oxidative desulfurization catalysed by POM in two-phase systems is reviewed.

Chapter 2 provides a description of the methods which were used in catalyst preparation. The techniques of catalyst characterisation and the two-phase catalytic reaction testing procedures are described.

In chapter 3, the results of catalyst characterisation techniques are elucidated and there follows a description of the structure and phosphazene characterisation.

Chapter 4 reports an investigation of the catalytic performance of $H_3PW_{12}O_{40}$, $H_3PMo_{12}O_{40}$ and $H_4SiW_{12}O_{40}$ polyoxometalates and various phosphazenes in two-phase oxidative desulfurization reaction. The possible reaction pathways are suggested.

Chapter 5 reports an examination of the catalytic activity of polyisobutylene oligomer-bound polyoxometalates for oxidative desulfurization.

Finally, **Chapter 6** draws conclusions from the results of the catalytic study and the characterisation of the catalysts.

References

1. Wikipedia, http:// http://en.wikipedia.org/wiki/Liquid_fuel, (accessed January 2015).
2. G. E. Likens, F. H. Bormann, N. M. Johnson, Enviro. **14 (**1972) 33.
3. EPA, http://www.epa.gov/acidrain/, (accessed October 2014).
4. United Nations, http://www.unece.org/env/lrtap/welcome.html, (accessed December 2013).
5. Dieslnet, https://www.dieselnet.com/tech/env_effect.php, (accessed 2004).
6. Explainthatstuff, http://www.explainthatstuff.com/air-pollution-introduction.html, (accessed October 2010).
7. Y. Hu, Q. He, Z. Zhang, N. Ding, B. Hu, Chem. Commun. **47** (2011) 12194.
8. I. Babich, J. Moulijn, Fuel **82** (2003) 607.
9. Transportpolicy, http://transportpolicy.net/index.php?title=Main_Page, (accessed October 2013).
10. EPA, http://www.epa.gov/OTAQ/fuels/dieselfuels/index.htm, (accessed October 2012).
11. J. Speight, The Chemistry and Technology of Petrolum, CRC Press, Boca Raton, 4th Ed. 2007.
12. Simetric, http://www.Simetric. Co. Uk, (accessed September 2012).
13. J. G. Speight, D. I. Exall, Refining Used Lubricating Oils, CRC Press, New York, 2002.
14. EPA, http://www.epa.gov/otaq/marine.htm, (accessed December 2014).
15. Upstreampumping, http://upstreampumping.com/article/well-completion-stimulation/understandnonroad diesel-engine-emissions-regulations, (accessed August 2011).
16. R. Kapichak, A Basic Overview of Transportation Conformity and State Implementation Plans, EPA, United State, 2008.
17. C. Ueno, Understanding Tier 4 Interim and Tier 4 Final EPA regulations for generator set applications, MTU Onsite Energy, Mankato, 2010.

18. I. Mochida, K. H. Choi, J. Jpn Pet. Inst. **47** (2004) 145.

19. H. Topsøe, B. S. Clausen, F. E. Massoth, Catal. Sci. Tech. **11** (1996) 310.

20. R. Colvile, E. Hutchinson, J. Mindell, Atmos. Environ. **35** (2001) 1537.

21. J. Ancheyta, J. G. Speight, The Desulfurization of Heavy Oils and Residua, CRC Press, New York, 2000.

22. U. S. Climate Action Report, Third National Communication of the United of America, Washington, 2002.

23. I. V. Babich, J. A. Moulijn, Fuel **82** (2003) 607.

24. C. Byrns, W. E. Bradley, M. W. Lee, Ind. Eng. Chem. **35** (1943) 1160.

25. L. Z. Pillon, Interfacial Properties of Petroleum Products, CRC Press, New York, 2007.

26. A. Rothlishberger, R. Prins, J. Catal. **235** (2005) 229.

27. Z. Jiang, Y. Liu, X. Sun, F. Tian, F. Sun, C. Linang, W. You, C. Han, C. Li, Langmuir **19** (2003) 731.

28. X. Ma, K. Sakanishi, I. Mochida, Ind. Eng. Chem. Res. **33** (1994) 218.

29. R. Shafi, G. J. Hutcnings, Catal. Today **59** (2000) 423.

30. C. Song, X. Ma, Appl. Catal. B: Environ. **41** (2003) 207.

31. S. K. Beg, S. K. Maty, U. T. Turaga, Energy Fuels **18** (2004) 1227.

32. J. G. Michael, C. C. Bruce, Ind. Eng. Chem. Res. **30** (1991) 202.

33. K. Heeyeon, J. Jung, S. Lee, M. Heup, Appl. Catal. B: Environ. **44** (2003) 287

34. I. V. Babich, J. A. Moulijn, Fuel **52** (2003) 607.

35. U.S. Energy Information Administration. The Transition to Ultra-Low-Sulfur Diesel Fuel: Effects on Prices and Supply, (2001) 13.

36. K. G. Knudsen, B. H. Cooper, H. Topsøe, Appl. Catal. A: Gen. **189** (1999) 205.

37. P. T. Vasudevan, J. L. G. Fierro, Catal. Rev. Sci. Eng. **38** (1996) 161.

38. B. C. Gates, H. Topsøe, Polyhedron **16** (1997) 3213.

39. C. Song, Catal. Today **86** (2003) 211.

40. J. J. Phillipson, Chemical Engineers Meeting, Houston, TX, 1971.

41. C. G. Frye, J. F. Mosby, Chem. Eng. Prog. **63** (1967) 66.

42. D. R. Kilanowski, H. Teeuwen, V. H. J. De Beer, B. C. Gates, B. C. A. Schuit, H. Kwart, J. Catal. **55** (1978) 129.

43. M. Houalla, D. H. Broderick, A. V. Sapre, N. K. Nag, V. H. J. De Beer, B. C. Gates, H. Kwart, J. Catal. **61** (1980) 523.

44. M. J. Girgis, B. C. Gates, Ind. Eng. Chem. **30** (1991) 2021.

45. P. T. Vasudevan, J. L. G. Fierro, Catal. Rev.-Sci. Eng. **38** (1996) 161.

46. B. C. Gates, H. **16** (1997) 3213.

47. C. Song, Am. Chem. Soc., Div. Fuel Chem. Prepr. **47** (2002) 438.

48. D. J. Monticello, Chemtech **28** (1998) 38.

49. B. L. McFarland, D. J. Boron, W. Deever, J. A. Meyer, A. R. Johnson, R. M. Atlas, Crit. Rev. Microbiol. **24** (1998) 99.

50. M. Ayala, R. Tinoco, V. Hernández, P. Bremauntz, R. Vazquez-Duhalt, Fuel Process Technol. **57** (1998) 101.

51. K. A. Gray, O. S. Pogrebinsky, G. T. Mranchko, L. Xi, D. J. Monticello, C. H. Squires, Nat. Biotechnol. **14** (1996) 1705.

52. J. R. Gallagher, E. S. Olson, D. C. Stanley, FEMS Microbiol. Lett. **107** (1993) 31.

53. L. Setti, P. Faarinelli, S. Di Martino, S. Frassinetti, G. Lanzarini, P. G. Pifferi, Appl. Microbiol. Biotechnol. **52** (1999) 111.

54. B. L. McFarland, Curr. Opin. Microbiol. **2** (1999) 257.

55. K. A. Gray, G. T. Mrachko, C. H. Squires, Curr. Opin. Biotechnol. **6** (2003) 229.

56. K. A. Gray, O. S. Pogrebinsky, G. T. Mrachko, X. Lei, D. J. Monticello, C. H. Squires, Biotechnol. **14** (1996) 1705.

57. G. Mohebali, A. S. Ball, Microbiology **154** (2008) 2169.

58. V. C. Srivastava, RSC Advan. **2** (2012) 759.

59. A. Srivastav, V. C. Srivastava, J. Hazard. Mater. **170** (2009) 1133.

60. V. Selvavathi, V. Chidambaram, A. Meenakshisundaram, B. Sairam, B. Sivasankar, Catal. Today **141** (2009) 99.

61. M. V. Landau, M. Herskowitz, T. Hoffman, D. Fucks, E. Liverts, D. Vingurt, N. Froumin, Ind. Eng. Chem. Res. **48** (2009) 5239.

62. Z. Y. Zhang, T. B. Shi, C. Z. Jia, W. J. Ji, Y. Chen, M. Y. He, Appl. Catal. B: Environ. **82** (2008) 1.

63. J. H. Kim, X. Ma, A. Zhou, C. Song, Catal. Today **111** (2006) 74.

64. X. Ma, L. Sun, C. Song, Catal. Today **77** (2002) 107.

65. W. Wang, J. C. T. Kwak, Colloid Surf. A **156** (1999) 95.

66. E. Baumgarten, J. Colloid Interface Sci. **194** (1997) 1.

67. T. P. Tranior, G. E. Brown Jr., G. A. Parks, J. Colloid Interface Sci. **231** (2000) 359.

68. M. H. Ali, A. Al-Maliki, B. El-Ali, G. Martinie, M. N. Siddiqui, Fuel **85** (2006) 1354.

69. I. V. Babich, J. A. Moulijn, Fuel **82** (2003) 607.

70. H. Vasile, F. Francois, B. Jacques, J. Catal. **198** (2000) 179.

71. R. T. Yang, F. H. Yang, A. Takahashi, A. J. H. Maldonado, US Patent, 7029574, 2002.

72. R. F. Zaykina, Y. A. Zaykin, T. B. Mamaonava, N. K. Nadirov, Radiat. Phys. Chem. **63** (2002) 621.

73. H. Mei, B. W. Mei, T. F. Yen, Fuel **82** (2003) 405.

74. G. Yu, S. Lu, H. Chen and Z. Zhu, Carbon **43** (2005) 2285.

75. H. Lu, J. Gao, Z. Jiang, F. Jing, Y. Yang, G. Wang, C. Li, J. Catal. **239** (2006) 369.

76. L. Yang, J. Li, X. Yuan, J. Shen, Y. Qi, J. Mol. Catal. A: Chem. **262** (2007) 114.

77. G. E. Dolbear, E. R. Skov, Am. Chem. Soc, Div. Pet. Chem. 45 (2000) 375.

78. W. Gore, US Patent, 6274785, 2001.

79. Attar, W. H. Corcoran, Ind. Eng. Chem. Prod. Res. Dev. **17** (1978), 102.

80. S. Liu, B. Wang, B. Cui, L. Sun, Fuel **87** (2008) 422.

81. J. P. Nehlsen, Ph.D. Dissertation, Princeton University, 2006.

82. G. M. K. Abotsi, A. W. Scaroni, Fuel Process. Technol. **22** (1989) 107.

83. Y. Shiraishi, T. Naito, T. Hirai, I. Komasawa, Ind. Eng. Chem. Res. **41** (2002) 4376.

84. S. T. Patrick, R. K. James, W. E. John, Ind. Eng. Chem. Res. **29** (1990) 321.

85. S. Kumar, V. C. Srivastava, R. P. Badoni, Fuel Proc. Technol. **10** (2011) 1016.

86. F. M. Collins, A. R. Lucy, C. Sharp, J. Mol. Catal. A: Chem. **117** (1997) 397.

87. M. J. Grassman, M. Siskin, D. T. Ferrughelli, M. K. Lee, US Patent, 5910440, 1999.

88. T. F. Yen, S. H. Lu, US Patent, 6402939, 2002.

89. C. Lanju, G. U. O. Shaohui, Z. H. A. O. Dishun, Chin. J. Chem. Eng. **15** (2007) 520.

90. F. Al-Shahrani, T. Xiao, A. Simon, S. Barri, Z. Jiang, H. Shi, G. Martinie, L. H. M. Green, Appl. Catal. B: Environ. **73** (2007) 311

91. K. Yazu, Y. Yamamoto, T. Furuya, K. Miki, K. Ukegawa, Energy Fuels **15** (2001) 1535.

92. S. Herbstman, J. Patel, In: Symposium on Upgrading of Synthetic Crudes, American Chemical Society: Kansas City, 1982.

93. N. D'Alessandro, T. Lucia, B. Monica, D. Milena, B. Mario, M. Antonino, New J. Chem. **27** (2003) 989.

94. J. L. G. Gutierrez, A. G. Fuentes, M. E. Hernandez-Teran, P. Garcia, F. Murrieta-Guevara and F. Jimenez-Cruz, Appl. Catal. A: Gen. **334** (2008) 366.

95. L. C. Caero, H. Gomez-Bernal, A. Fraustro-Cuevas, D. H. Guerra-Gomez, R. Cuevas-Garcia, Catal. Today **133** (2008) 244.

96. T. I. Collins, Science **291** (2001) 48.

97. T. J. Collins, Nature **414** (2001) 161.

98. R. F. Zaykina, Y. A. Zaykin, G. Mirkin, N. K. Nadirov, Radiat. Phys. Chem. **63** (2002) 617.

99. N. K. Nadirov, R. F. Zaykina, Y. A. Zaykin, T. B. Mamonova, C. F. Bakirova, Oil Gas Kazakhstan **3** (1998) 129.

100. Y. Zaykin, R. F. Zaykina, N. K. Nadirov, T. B. Mamonova, Oil Gas Kazakhstan **4** (1998) 91.

101. L. H. Thompson, L. K. Doraiswamy, Ind. Eng. Chem. Res. **38** (1999) 1215.

102. Y. T. Shah, A. B. Pandit, V. S. Moholkar, Cavitation Reaction Engineering, Plenum publishers, New York, 1999.

103. T. F. Yen, R. D. Gilbert, J. H. Fendler, Membrane mimetic chemistry and its applications, Plenum Press, New York, 1994.

104. Y. Shiraishi, Y. Taki, T. Hirai, I. Komasawa, Ind. Eng. Chem. Res. **38** (1999) 3310.

105. S. Yasuhiro, T. Kenya, H. Takayuki, K. Isao, Ind. Eng. Chem. Res. **39** (2000) 2826.

106. T. Hirai, K. Ogawa, I. Komasawa, Ind. Eng. Chem. Res. **35** (1996) 586.

107. T. Hirai, Y. Shiraishi, I. Komasawa, J. Chem. Eng. Jpn **30** (1997) 173.

108. T. Hirai, Y. Shiraishi, K. Ogawa, I. Komasawa, Ind. Eng. Chem. Res. **36** (1997) 530.

109. Y. Shiraishi, T. Hirai, I. Komasawa, Ind. Eng. Chem. Res. **38** (1999) 3300.

110. A. Ibrahim, S. B. Xian, Z. Wei, Pet. Sci. Technol. **21** (2003) 1555.

111. Y. Shiraishi, T. Hirai, I. Komasawa, Ind. Eng. Chem. Res. **40** (2001) 293.

112. A. Ibrahim, S. B. Xian, Z. Wei, Pet. Sci. Technol. **22** (2004) 287.

113. K. Yazu, Y. Yamamoto, T. Furuya, K. Miki, K. Ukegawa, Energy Fuels **15** (2001) 1535.

114. W. Wang, S. Wang, H. Liu, Z. Wang, Fuel **86** (2007) 2747.

115. W. Wang, S. Wang, Y. Wang, H. Liu, Z. Wang, Fuel Process. Technol. **88** (2007) 1002.

116. W. Y. Liu, Z. L. Lei, I. K. Wang, Energy Fuels **15** (2001) 38.

117. G. M. K. Abotsi, A. W. Scaroni, Fuel Process. Technol. **22** (1989) 107.

118. W. Gore, US Patent, 6274785, 2001.

119. H. Zhao, S. Q. Xia, P. S. Ma, J. Chem. Technol. Biotechnol. **80** (2005) 1089.

120. G. Yu, X. Li, X. Liu, C. Asumana, X. Chen, Ind. Eng. Chem. Res. **50** (2011) 2236.

121. K. Kendra-Krolik, M. Fabrice, J. -N. Jaubert, Ind. Eng. Chem. Res. **50** (2011) 2296.

122. L. Alonso, A. Arce, M. Francisco, O. Rodriguez, A. Soto, AIChE J. **53** (2007) 3108.

123. L. Alonso, A. Arce, M. Francisco, A. Soto, Fluid Phase Equilib. **263** (2008) 176.

124. L. Alonso, A. Arce, M. Francisco, A. Soto, J. Chem. Thermodyn. **40** (2008) 966.

125. A. Bosmann, L. Datsevich, A. Jess, A. Lauter, C. Schmitz, P. Wasserscheid, Chem. Commun. **23** (2001) 2494.

126. X. M. Chu, Y. F. Hu, J. G. Li, Q. Q. Liang, Y. S. Liu, X. M. Zhang, X. M. Peng, W. J. Yue, Chin. J. Chem. Eng. **16** (2008) 881.

127. J. Esser, P. Wasserscheid, A. Jess, Green Chem. **6** (2004) 316.

128. H. S. Gao, Y. G. Li, J. M. Wu, Y. Wu, M. F. Luo, Q. Li, J. M. Xing, H. Z. Liu, Energy Fuels **23** (2009) 2690.

129. H. S. Gao, M. F. Luo, J. M. Xing, Y. Wu, Y. G. Li, W. L. Li, Q. F. Liu, H. Z. Liu, Ind. Eng. Chem. Res. **47** (2008) 8384.

130. Q. X. Guo, X. D. Tang, J. Southwest Pet. Univ. China **29** (2007) 95.

131. J. D. Holbrey, I. Lopez-Martin, G. Rothenberg, K. R. Seddon, G. Silvero, X. Zheng, Green Chem. **10** (2008) 87.

132. C. P. Huang, B. H. Chen, J. Zhang, Z. C. Liu, Y. X. Li, Energy Fuels **18** (2004) 1862.

133. X. C Jiang, Y. Nie, C. X. Li, Z. H. Wang, Fuel **87** (2008) 79.

134. N. H. Ko, J. S. Le, E. S. Huh, H. Lee, K. D. Jung, H. S. Kim, M. Cheong, Energy Fuels **22** (2008) 1687.

135. Y. Nie, C. X. Li, H. Meng, Z. H. Wang, Fuel Process. Technol. **89** (2008) 978.

136. Y. Nie, C. X. Li, A. J. Sun, H. Meng, Z. H. Wang, Energy Fuels **5** (2006) 2083.

137. Y. Nie, C. X. Li, Z. H. Wang, Ind. Eng. Chem. Res. **46** (2007) 5108.

138. J. Planeta, P. Karasek, M. Roth, Green Chem. **8** (2006) 70.

139. J. L. Wang, D. S. Zhao, E. P. Zhou, D. Zhi, J. Fuel Chem. Technol. **35** (2007) 293.

140. Q. B. Wang, K. F Liu, X. P. Zhang, S. J. Zhang, Appl. Chem. Ind. China **37** (2008) 7.

141. S. G. Zhang, Z. C. Zhang, Green Chem. **4** (2002) 376.

142. S. G. Zhang, Q.L. Zhang and Z. C. Zhang, Ind. Eng. Chem. Res. **43** (2004) 614.

143. H. C. Zhou, N. Chen, F. Shi, Y. Q. Deng, J. Mol. Catal. A: Chem. **19** (2005) 95.

144. C. Phillips, Energy Fuels **22** (2008) 1774.

145. J. Eber, P. Wasserscheid, A. Jess, Green Chem. **6** (2004) 316.

146. X. C Jiang, Y. Nie, C. X. Li, Z. H. Wang, Fuel **87** (2008) 79.

147. N. H. Ko, J. S. Le, E. S. Huh, H. Lee, K. D. Jung, H. S. Kim, M. Cheong, Energy Fuels **22** (2008) 1687.

148. Y. Nie, C. X. Li, H. Meng, Z. H. Wang, Fuel Process. Technol. **89** (2008) 978.

149. R. P. Swatloski, J. D. Holbrey, R. D. Rogers, Green Chem. **5** (2003) 361.

150. J. Feng, C. X. Li, H. Meng, Z. H. Wang, Petrochem. Technol. **35** (2006) 272.

151. U. Domanska, M. Krolikowski, K. Slesinska, J. Chem. Thermodyn. **41** (2009) 1303.

152. M. T. Pope, Heteropoly and Isopoly Oxometalates, Springer-Verlag, Berlin, 1983.

153. J. B. Moffat, Metal – Oxygen Clusters: The Surface and Catalytic Properties of Heteropoly Oxometalates, Klumer Academic/ Plenum Publishers, New York, 2001.

154. I. V. Kozhevnikov, in: Polyoxometalate Molecular Science, ed. J.J.Borrás-Almenar et al., Kluwer Academic Publishers, Netherlands, 2003, 351.

155. I .V. Kozhevnikov, Catalysts for Fine Chemicals. Vol. 2. Catalysis by Polyoxometalates, Wiley, Chichester, 2002.

156. T. Okuhara, N. Mizuno, M. Misono, Adv. Catal. **41** (1996) 113.

157. I. V. Kozhevnikov, Chem. Rev. **98** (1998) 171.

158. N. Mizuno, M. Misono, Chem. Rev. **98** (1998) 199.

159. K. I. Matveev, Kinet. Katal. **18** (1977) 862.

160. I. V. Kozhevnikov, K. I. Matveev, Russ. Chem. Rev. **51** (1982) 1075.

161. I.V. Kozhevnikov, K. I. Matveev, Appl. Catal. **5** (1983) 135.

162. I. V. Kozhevnikov, Russ. Chem. Rev. **56** (1987) 811.

163. M. Misono, Chem. Comm. **13** (2001) 1141.

164. A. Corma, Chem. Rev. **95** (1995) 559.

165. C. L.Hill, C.M. Prosser-McCartha, Coord. Chem. Rev. **143** (1995) 407.

166. J. J. Berzelius, Poggendorffs Ann. Phys. Chem. **6** (1826) 369.

167. L. Svanberg, H. J. Struve, Pract. Chem. **61** (1854) 449.

168. C. Marignac, J. Pract. Chem. **77** (1862) 417.

169. J. F. Keggin, Proc. Roy. Soc. London Ser.A, **144** (1934) 75.

170. H. T. Evans, Jr., J. Am. Chem. Soc. **70** (1948) 1291.

171. B. Dawson, Acta Crystallogr. **6** (1953) 113.

172. L. C. W. Baker, D. C. Glick, Chem. Rev. **98** (1998) 3.

173. M. T. Pope, A. Müller, Angew. Chem. Int. Ed. Engl. **30** (1991) 34.

174. G. M. Brown, M.-R. Noe-Spirlet, W.R. Bushing, H.A. Levy, Acta Crystallogr. Sect. B **33** (1977) 1038.

175. I. V. Kozhevnikov, A. Sinnema, R. J. J. Jansen, H. van Bekkum, Mendeleev Commun. (1994) 92.

176. I. V. Kozhevnikov, A. Sinnema, R. J. J. Jansen, H. van Bekkum, Catal. Lett. **27** (1994) 187.

177. I. V. Kozhevnikov, A. Sinnema, H. van Bekkum, Catal. Lett. **34** (1995) 213.

178. I. V. Kozhevnikov, A. Sinnema, H. van Bekkum, M. Fournier, Catal. Lett. **41** (1996) 153.

179. P. Souchay, Ions Mineraux Condenses, Masson, Paris, 1969.

180. G. A. Tsigdinos, Top. Curr. Chem. **76** (1978) 1.

181. V. F. Chuvaev, K. I. Popov, V. I. Spitsyn, Dokl. Akad. Nauk. SSSR **255** (1980) 892.

182. J. B. Moffat, In: Acidity and Basicity of Solids: Theory, Assessment and Utility, ed. J. Fraissard, I. Petrokis, Kluwer, Dordrecht 1993.

183. S. D. Naik, L. K. Doraiswamy, React. Kinet. Catal. **44 (**1998) 3.

184. M. J. Jarrouse, C. R. Acad. Sci. Ser. **232** (1951) 1424.

185. A. Brandstorm, Phys. Org. Chem. **15** (1977) 267.

186. M, Makosza, Pure. Appl. Chem. **43** (1975) 439.

187. C. M. Starks, J. Am. Chem. Soc. **93** (1971) 195.

188. N. Mizuno, K. Yamaguchi, K. Kamata, Coord. Chem. Rev. **249 (**2005) 1944.

189. M. Beller, C. Bolm, Transition Metals for Organic Synthesis, Wiley-VCH, Weinheim 1998.

190. M. Beller, C. Bolm, Transition Metals for Organic Synthesis, Wiley-VCH, Weinheim, 1998.

191. G. Franz, R. A, Sheldon, In Ulmann's Encyclopedia of Industrial Chemistry, 5th ed.; VCH, Weinheim, 1991.

192. R. A. Sheldonvan, M. C. A. Vliet, In: Fine Chemicals through Heterogeneous Catalysis, Wiley, Weinheim, 2001.

193. Y. Ishii, K. Yamawaki, T. Ura, H. Yamada, T. Yoshida, M. Ogawa, J. Org. Chem. **53** (1988) 3587.

194. N. Mizuno, K. Yamaguchi, K. Kamatab, Coord. Chem. Rev. **249** (2005) 1944.

195. C. Venturello, R. D'Aloisio, J. C. J. Bart, M. Ricci, J. Mol. Catal. **32** (1985) 107.

196. C. Aubry, G. Chottard, N. Platzer, J.-M. Br´egeault, R. Thouvenot, F. Chauveau, C. Huet, H. Ledon, Inorg. Chem. **30** (1991) 4409.

197. A. C. Dengel, W. P. Griffith, B. C. Parkin, J. Chem. Soc., Dalton Trans. (1993) 2683.

198. L. Salles, C. Aubry, R. Thouvenot, F. Robert, C. Dor´emieux-Morin, G. Chottard, H. Ledon, Y. Jeannin, J.-M. Br´egeault, Inorg. Chem. **33** (1994) 871.

199. D. C. Duncan, R. C. Chambers, E. Hecht, C. L. Hill, J. Am. Chem. Soc. **117** (1995) 681.

200. W. P. Griffith, R.G.H. Moreea, H.I.S. Nogueira, Polyhedron **15** (1996) 3493.

201. N. M. Gresley, W. P. Griffith, A. C. Laemmel, H. I. S. Nogueira, B. C. Parkin, J. Mol. Catal. A: Chem. **117** (1997) 185.

202. W.P. Griffith, N. Morley-Smith, H.I.S. Nogueira, A.G.F. Shoair, M. Suriaatmaja, A.J.P. White, D.J. Williams, J. Organomet. Chem. **607** (2000) 146.

203. J. M. Martin, M. C. –Sanchez, J. L. G. Fierro, Green Chem. **6** (2004) 557.

204. R. Noyori, M. Aoki and K. Sato, Chem. Commun. 2003, 1977.

205. C. Li, Z. Jiang, J. Gao, Y. Yang, S. Wang, F. Tian, F. Sun, X. Sun, P. Ying, C. Han, Chem. Eur. J. **10** (2004) 2277.

206. H. Lu, Jinbo Gao, Z. Jiang, F. Jing, Y.Yang, G. Wang, C. Li, J. Catal. **239** (2006) 369.

207. X. Jiang, H. Li, W. Zhu, L. He, H. Shu, J. Lu, Fuel **88** (2009) 431.

208. H. Lu, J. Gao, Z. Jiang, F. Jing, Y. Yang, G. Wang, J. Catal. **239** (2006) 369.

209. J. Gao, S. Wang, Z. Jiang, H. Lu, Y. Yang, F. Jing, J. Mol. Catal. A: Chem. **258** (2006) 261.

210. H. R. Allcock, Chemistry and Applications of Polyphosphazenes, Wiley-Interscience, Hoboken, NJ, 2003.

211. H. R. Allcock, In Phosphorus-Nitrogen Compounds, Academic Press, New York, 1972.

212. J. C. van, A. Vos, Recl. Trav. Chim. **82** (1963) 246.

213. C. Voswijk, J. C. van, Recl. Trav. Chim. **93** (1974) 120.

214. H. R. Allcock, Chem. Rev. **72** (1972) 315.

215. H. M. McGeachin, F. R. Tromans, J. Chem. Soc. (1961) 4777.

216. A. W. Schlueter, R. A. Jacobson, J. Chem. Soc. A (1968) 2317.

217. A. J. Wagner, A. Vos, Acta Crysfallogr. Sect. B **24** (1968) 707.

218. H. Zoer, A. J. Wagner, Acta Crystallogr. Sect. B **28** (1972) 252.

219. N. L. Paddock, J. Trotter, S. H. Whitlow, J. Chem. Soc. A (1968) 2227.

220. H. R. Allcock, G. F. Konopski, R. L. Kugel, E. G. Stroh, Chem. Commun. (1970) 985.

221. H. R. Allcock, R. L. Kugel, E. G. Stroh, Inorg. Chem. **11** (1972) 1120.

222. E. Hobbs, D. E. C. Corbridge, B. Raistrick, Acta Crystallogr. **6** (1953) 621.

223. L. G. Hoard, R. A. Jacobson, J. Chem. Soc. A (1966) 1203.

224. H. Hess, D. Forst, Z. Anorg. Allg. Chem. **342** (1966) 240.

225. P. T. Clarke, H. S. Turner, R. J. Warne. J. Chem. Soc. (1965) 6421.

226. G. A. Wiegers, A. Vos, Acta Crystallogr. **16** (1963) 152.

227. J. Trotter, S. H. Whitlow, N. L. Paddock, Chem. Commun. (1969) 695.

228. J. Trotter, S. H. Whitlow, J. Chem. Soc. A (1970) 460.

229. R. Keat, S, K. Ray, R. A. Shaw, J. Chem. Soc. (1965) 7193.

230. G. Allen, D. J. Oldfield, N. L. Paddock, F. Rallo, J. Serregi, S. M. Todd, Chem. Ind. (1965) 1032.

231. H. Saito, M. Kajiwara, J. Chem. Soc. Jap. Ind. Chem. Sect. **66** (1963) 618.

232. R. Steinman, F. B. Schirmer, L. F. Audrieth, J. Am. Chem. Soc. **64** (1942) 2377.

233. L. G. Lund, N. L. Paddock, J**.** E. Proctor, H. T. Searle, J. Chem. Soc. (1960) 2542.

234. F. G. R. Gimblett, Chem. Ind. (1958) 365.

235. M. Becke-Goehring, K. Koch, Chem. Ber. **92** (1959) 1188.

236. M. Becke-Goehring, E. Fluck, Angew. Chem. **74** (1962) 382.

237. M. Becke-Goehring, W. Lehr, Z. Anorg. Allg. Chem. **327** (1964) 128.

238. K. S. Brenner, J. Chromafogr. **57** (1971) 131.

239. R. Ratz, E. Kober, C. Grundmann, G. Ottmann, Inorg. Chem. **3** (1964) 757.

240. V. A. Chernov, V. B. Lytkina, S. I. Sergievskaya, A. A. Kropacheva, V. A. Parshina, L. E. Sventsitkaya, Farmakol. Toksikol. **22** (1959) 365.

241. Z. T. Wakefield, B. B. Luff, J. J. Kohler, J. Chem. Eng. Data **15** (1970) 314.

242. L. E. A. Godfrey, J. W. Schappel, Ind. Eng. Chem., Prod. Res. Develop. **9** (1970) 426.

243. J. M. Rees, Lighting Res. Technol. **2** (1970) 257.

244. D. E. Bergbreiter, J. Li, Chem. Commun. (2004) 42.

245. R. Yahya, M. Craven, E. F. Kozhevnikova, A. Steiner, P. Samunual, I. V. Kozhevnikov, D. E. Bergbreiter, Catal. Sci. Technol. **5** (2015) 818.

Chapter 2. Experimental

2.1 Introduction

This chapter describes the experimental processes that were followed in the study of the biphasic oxidation of sulfur compounds with H_2O_2 catalysed by polyoxomelate-phosphazene aggregates. The catalysts were formed *in situ* by adding pre-determined ratios of the substituents to the reaction mixture. Various commercially available polyoxometalates were used as active catalysts in these systems whereas different organoaminocyclophosphazenes were prepared from hexachlorocyclotriphosphazene for use as phase transfer agents. All of the catalysts were characterised by means of various techniques to determine properties such as their structure, bonding, thermal stability, water content, elemental composition and impurities. This chapter also describes, in detail, a variety of reaction procedures and conditions for the liquid phase oxidation of sulfur compounds as well as GC calibration of the substrates and products obtained. Finally, calculation of the activation energy for the oxidation of dibenzothiophene (based on the conversion of (H_2O_2/dibenzothiophene)) is detailed.

2.2 Chemicals and solvents

Dibenzothiophene ($C_{12}H_8S$, 98%), dibenzothiophene sulfone ($C_{12}H_8SO_2$, 97%), benzothiophene (C_8H_6S, 98%), benzothiophene sulfone ($C_8H_6SO_2$, 97%) and 4,6-dimethyldibenzothiophene ($C_{14}H_{12}S$, 97%) were purchased from Sigma/Aldrich and used without further treatment. Toluene (Aldrich, 99%) was used as a solvent and dodecane (Aldrich, 99%) and undecane (Aldrich, 99%) as an internal standard for GC analysis.

Polyoxometalates tested in this work were commercially available compounds. The following polyoxometalate compounds were obtained from Sigma/Aldrich and were used without further treatment: phosphotungstic acid hydrate ($H_3PW_{12}O_{40}.20H_2O$, 99%), silicotungstic acid hydrate ($H_4SiW_{12}O_{40}.20H_2O$, 99.9%) and phosphomolybdic acid hydrate ($H_3PMo_{12}O_{40}.20H_2O$, 99.9%). Hydrogen peroxide (30 wt.% H_2O_2, Sigma/Aldrich) was used in excess as an oxidant; its concentration in the reaction mixture was monitored before and after each reaction by titration with standardised 0.005 M $KMnO_4$ as detailed below.

Determination of the concentration of H_2O_2 in reaction solution was necessary to figure out if the H_2O_2 had decomposed. One method that can accomplish this is the method of titration by permanganate, in which a solution of known concentration permanganate is allowed to react with a solution of unknown concentration of H_2O_2. This is an oxidation/reduction reaction rather than an acid/base reaction. A sulfuric acid solution (H_2SO_4) is used to provide an acidic environment for the titration with permanganate.

$$2KMnO_4(aq) + 5H_2O_2(aq) + 3H_2SO_4(aq) \longrightarrow 2MnSO_4(aq) + K_2SO_4(aq) + 5O_2(g) + 8H_2O$$

In this reaction, the faint pink color of the permanganate ion is used as an indicator rather than using an additional dye to determine the end point. In essence, the permanganate in the $KMnO_4$ solution acts as its own indicator. The Mn^{2+} ion is actually colorless, but when MnO_4^- is in excess, the solution will turn from colorless to pink, indicating that the equivalence point has been reached.

When performing a titration, it is necessary to first determine the concentration of the known permanganate solution as accurately as possible. This process is referred to as standardization. Solid $KMnO_4$ contains traces of other impurities, such as MnO_2, so a solution of known concentration cannot be made by simply measuring out a certain number of grams of $KMnO_4$ and dissolving it in the appropriate amount of water. To determine the concentration of the $KMnO_4$, it is titrated against an appropriate standard, such as solid oxalic acid, $H_2C_2O_4$, whose mass can be measured very precisely. By using the stoichiometry of the standardization reaction, the concentration of the titrant solution can be determined accurately.

$$2MnO^{4-} + 5H_2C_2O_4 + 6H^+ \longrightarrow 2Mn^{2+} + 10CO_2(g) + 8H_2O$$

2.3 Preparation of cyclophosphazenes

2.3.1 Preparation benzylaminocyclotriphosphazene

Dry toluene (200 mL) was added to hexachlorocyclophosphazene (10 g, 28.8 mmol) in a 1 L flask followed by triethylamine (50 mL, 358 mmol) and benzylamine (50 mL, 578 mmol). The mixture, which formed a white precipitate, was refluxed for ca. 24 h until the reaction had gone to completion (checked with ^{31}P NMR). The mixture was cooled to room temperature to produce a white precipitate (triethylamine hydrochloride), which was filtered off by suction using a Büchner funnel. Filtration was repeated 2 more times to ensure the precipitate was removed from the solution. The solvent was removed on a rotary evaporator to give a yellow/brown oil. Hexane (200 mL) was added to the oil and stirred for 15 min resulting in a white precipitate. The hexane was then decanted off and petroleum ether (200 mL, b.p., 40-60 ^{o}C) was added to the precipitate and refluxed for 15 min. The white powder was isolated by filtration using a Büchner funnel in 85% yield (18.94 g; m.p., 83 ^{o}C). A ^{31}P NMR spectrum (toluene, $CDCl_3$ lock): δ_{ppm} 17.4 ppm (s, P-BzPN). Anal. Calcd for $(PhCH_2NH)_6P_3N_3$: C, 65.37; H, 6.23; N, 16.34. Found: C, 65.17; H, 6.24; N, 16.09.

2.3.2 Preparation of other alkylaminophosphazenes

Isobutylamine (60 mL, 575 mmol) was added to a stirred solution of hexachlorocyclophosphazene (10 g, 28.8 mmol) in toluene (200 mL) in a 500 mL flask. The mixture, which formed a white precipitate, was refluxed for ca. 24 h until the reaction had gone to completion (checked with ^{31}P NMR). Aqueous KOH (30%) was added and stirred for 30 min before the mixture was transferred into a separating funnel. The organic layer was then separated and distilled to remove most of the solvent. The remaining solvent was removed under vacuum to produce a white solid which was re-crystallised from n-pentane to afford the product in 97% yield (15.8 g; m.p., 60.5 ^{o}C). A ^{31}P NMR spectrum (toluene, $CDCl_3$ lock): δ_{ppm} 19.6 (s, P-iBuPN). Anal. Calcd for $(iBuNH)_6P_3N_3$: C, 50.77; H, 10.65; N, 22.20. Found: C, 50.21; H, 10.53; N, 21.95; IR ν/cm^{-1} 3220 (N-H), 2957 (CH_3), 2869 (CH_2), 1402 (C-C), 1105 (C-N).

Hexa(isopropylamino)cyclotriphosphazene was synthesised from isopropylamine and hexachlorocyclophosphazene similarly to iBuPN in 87% yield (m.p., 76 ^{o}C). A ^{31}P NMR

spectrum (toluene, $CDCl_3$ lock): δ_{ppm} 15.1 (s, P-iPrPN). Anal. Calcd $(iPrNH)_6P_3N_3$: C, 44.17; H, 10.01; N, 25.80. Found: C, 43.15; H, 9.82; N, 25.51; IR ν/cm^{-1} 3212 (N-H), 2962 (C-H), 1400 (C-C), 1076 (C-N).

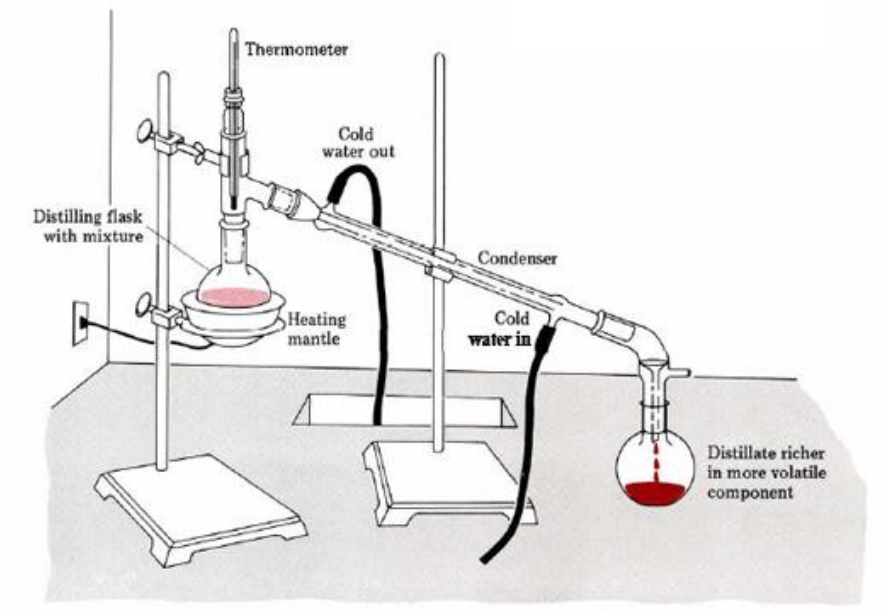

Fig. 2.1 Laboratory display of distillation

2.4 Techniques

2.4.1 Gas chromatography

Gas chromatography (GC) is widely used for the separation and quantitative analysis of mixtures of volatile compounds [3-6]. The sample to be analyzed is volatilized and swept by a stream of carrier gas through a heated column containing an absorbent support impregnated with a non-volatile liquid, which acts as the stationary phase. The carrier gas is required to be inert to the column and components of the sample. Nitrogen, helium, argon or hydrogen may be used. Capillary column GC, in which the stationary phase is bonded to the walls of a long capillary tube, permits far greater selectivity. However, sample injection into capillary systems is much more difficult due to the small sample loading required on the column and the low flow rates used. The most widely used method of placing samples onto the column is a *split/splitless injection*. For this purpose 0.1-1.0 μl sample is injected into a glass-lined heated injection port, where it vaporizes and mixes with carrier gas; a preset proportion, normally between 1% and 10%, is allowed to pass into the column and the rest is vented to

the atmosphere. The split-splitless vaporizing injector for capillary columns is shown in Fig. 2.2. The ratio of the split flow rate to the column flow rate is called the *split ratio*.

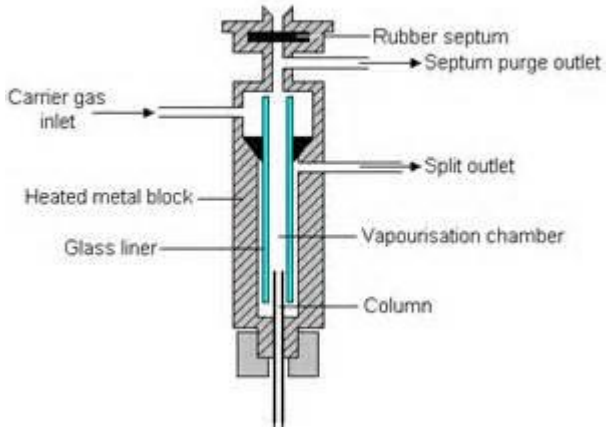

Fig. 2.2 Split-splitless vaporizing injector [4].

The components of the gas mixture distribute between the stationary phase of the column and the carrier gas due to a combination of volatility and the degree with which they interact with the stationary phase. The separated components are then eluted from the column and pass over a detector. Various types of detector may be used. One of the most common detectors is the *flame ionisation detector* (FID) which is particularly useful for analyzing organic compounds. The basis of the FID is that the effluent from the column is mixed with hydrogen and burnt in air to produce a flame that has sufficient energy to ionize solute molecules with low ionization potentials. The charged particles, formed when an organic species is burnt in the detector, migrate towards the collector electrode under the influence of a polarizing electric field applied to the jet of the detector (Fig. 2.3). The burner jet is the negative electrode whereas the anode is usually a wire or grid extending into the tip of the flame. The quantity of charge produced is proportional to the amount of compound present. The resulting current is amplified and plotted on the screen as a chromatogram. The lapsed time between injection onto the column and the exit of a particular component is referred to as the *retention time* and is diagnostically useful for a given column and set of conditions. A schematic representation for the operation procedure of a typical gas chromatograph is represented diagrammatically in Fig. 2.4.

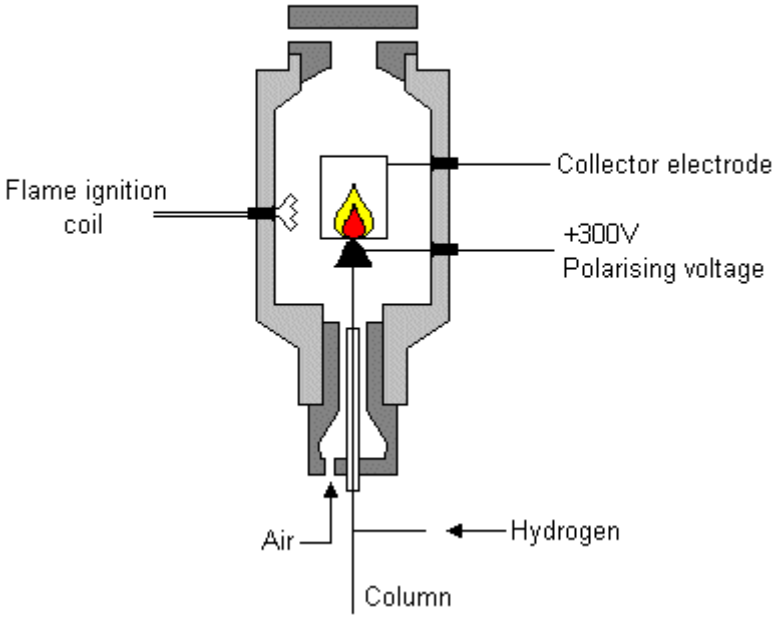

Fig. 2.3 Flame ionisation detector [5].

In this work, reactions were monitored by gas chromatography using a Varian CP-3380 gas chromatograph equipped with FID using a BP1 capillary non-polar column (25 m length, 0.32 mm internal diameter, 0.5 μm film thickness). N_2 was employed as the carrier gas at a flow rate of 2 ml/min. Nitrogen was also used as the make-up gas at a flow rate of 30 ml/min. The split ratio and split vent flow were 20 and 40 ml/min, respectively. The detector and injector temperature was set at 250°C. The FID enables compounds that ionize in a hydrogen flame to be detected. The hydrogen (30 ml/min) introduced into the elute from the column is burnt in air (300 ml/min) introduced into the base of the detector to form a stable, noise-free flame. The temperature of the column oven was set at 140^{o}C for 0.5 min and increased to 250^{o}C for 6 min. The products were identified by comparison with authentic samples and by gas chromatography-mass spectrometry (GC-MS).

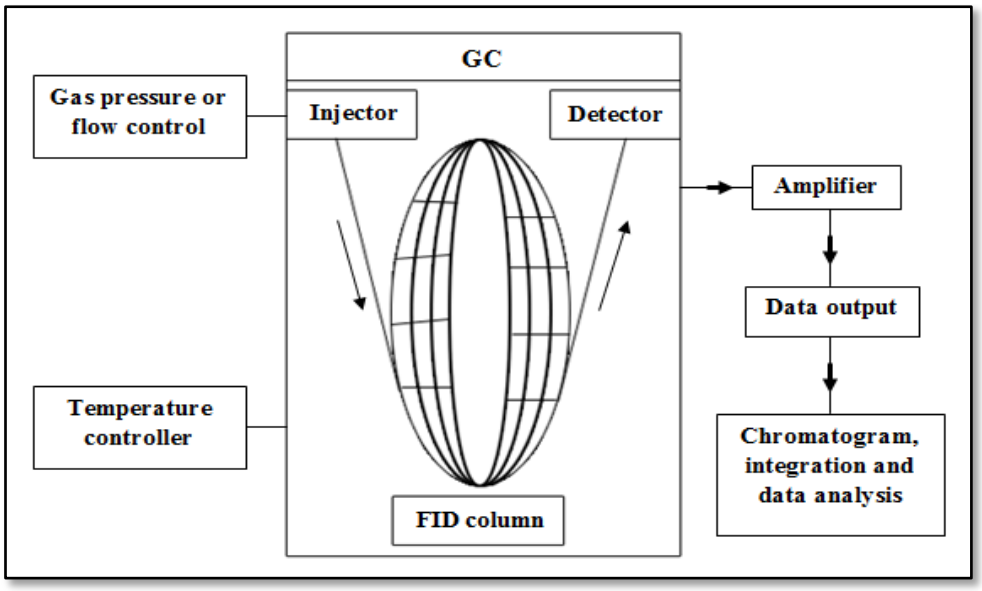

Fig. 2.4 Schematic representation for the operation procedure of a typical gas chromatograph [5].

2.4.2 GC calibration

Quantitative measurements depend upon correlation of peak areas with the amount or concentration of solutes in various samples. But equal areas for different solutes do not necessarily indicate that equal quantities of those substances are present, as the magnitude of the recorded peaks depends upon the response characteristics of the detector to those substances. The height and area of chromatographic peaks are affected not only by the amount of sample but also by fluctuations of the carrier gas flow rate, the column and detector temperatures, etc. Using the internal standard method, in which a known amount of a reference substance is added to the sample to be analysed, the effect of these variations can be eliminated.

For quantitative gas chromatographic analysis, retention times and calibration factors were determined for each compound under specified analysis conditions using commercially available reagents and analytical standards. Suitable standards (dodecane and undecane) were chosen as an internal standard for different reaction mixtures. The standard peak should be eluted close to the components to be measured and its peak area should also be similar. Calibration factors were measured experimentally by making several solutions of a known

concentration of the compound and the internal standard in dodecane and undecane. The calibrations were plotted in accordance with Eq. 2.1:

$$\mathbf{M/M_o = K \times S/S_o} \qquad (2.1)$$

Here $\mathbf{M/M_o}$ is the molar ratio of the analysed compound and internal standard, $\mathbf{S/S_o}$ is the ratio of area counts of the corresponding peaks and **K** is the molar calibration factor.

If authentic materials - and hence the calibrations - are not available, it may be assumed that isomers or compounds of the same structural type will have similar calibration factors and, therefore, the relative peak areas can be compared [6].

The retention times and the molar calibration factors for dibenzothiophen, dibenzothiophen sulfone, benzothiophene, benzothiophene sulfone and 4,6-dimethyldibenzothiophene are in Table 2.1. These values were measured by GC under conditions shown in Fig. 2.5. Typical GC traces for sulfur compounds are shown in Fig. 2.6-2.8. The calibration plots (Eq. 2.1) for this system are shown in Fig. 2.9-2.13. The calibrations were done in the same concentration ranges as those employed in the reactions. The average error of the **K** values obtained is ≤ 2%.

Table 2.1. Sulfur compounds. GC retention times and calibration factors.[a]

No.	Compound	Retention time (min)	Calibration factor (**K**)
1	Dibenzothiophene	6.56-6.60	1.078
2	Dibenzothiophene sulfone	9.14-9.18	1.666
3	Benzothiophene	3.33-3.34	1.476
4	Benzothiophene sulfone	5.30-5.31	1.799
5	4,6-Dimethyldibenzothiophene	8.04-8.05	0.971
6	Toluene	2.3-2.5	Solvent
7	Heptane	2.17	Solvent
8	Dodecane (standard)	3.29-3.30	1.00
9	Undecane (standard)	2.89-2.90	1.00

[a]The conditions of GC analysis are shown in Fig. 2.4. The average error of **K** is ≤ 2%.

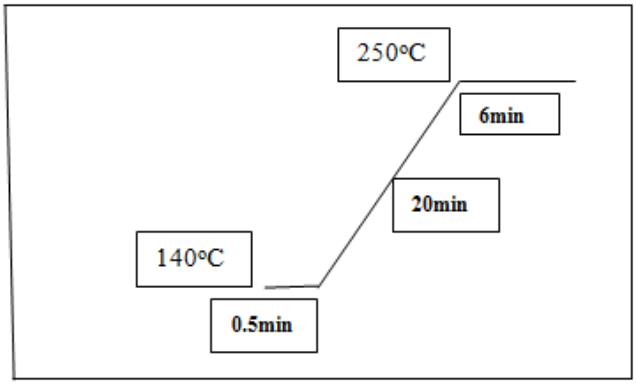

Fig. 2.5 Conditions of GC analysis for oxidative desulfurization of sulfur compounds.

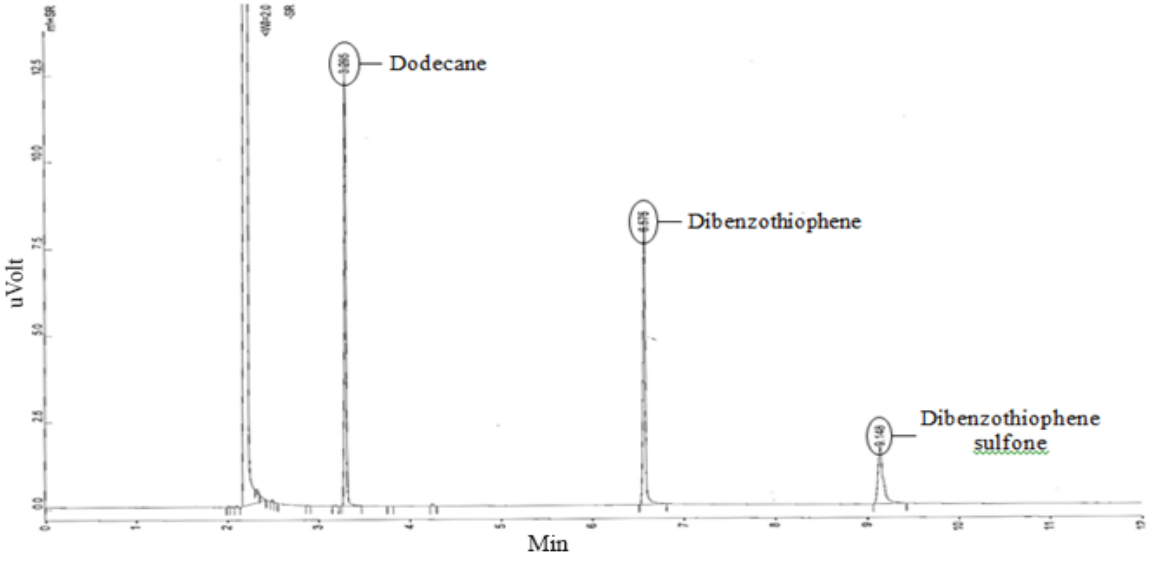

Fig. 2.6 Typical GC trace for dibenzothiophene oxidation to dibenzothiophene sulfone.

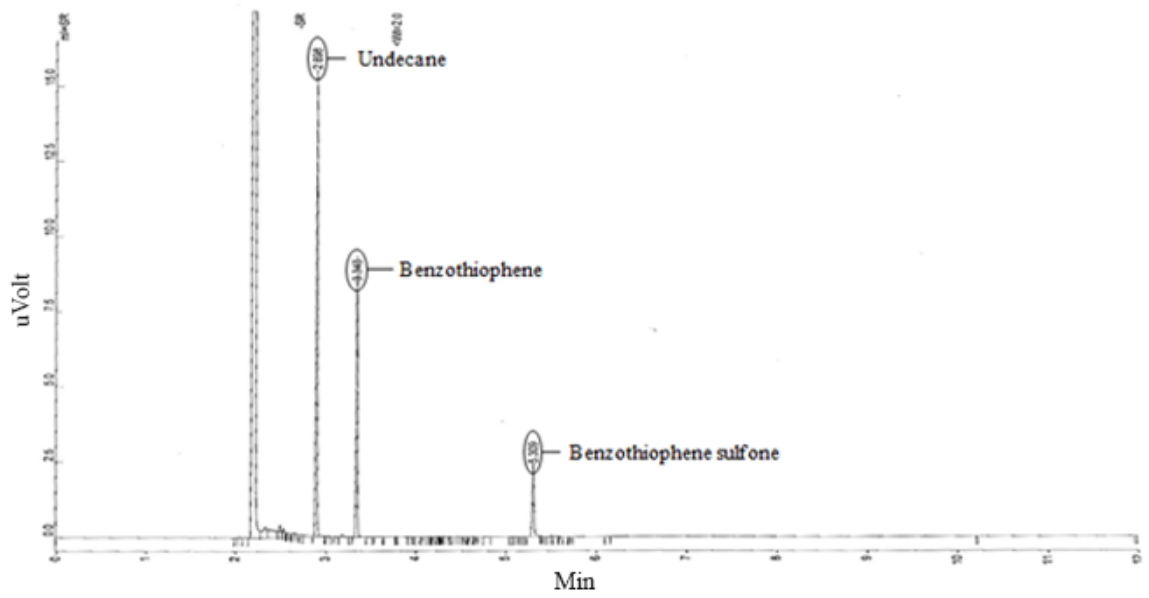

Fig. 2.7 Typical GC trace for benzothiophene oxidation to benzothiophene sulfone.

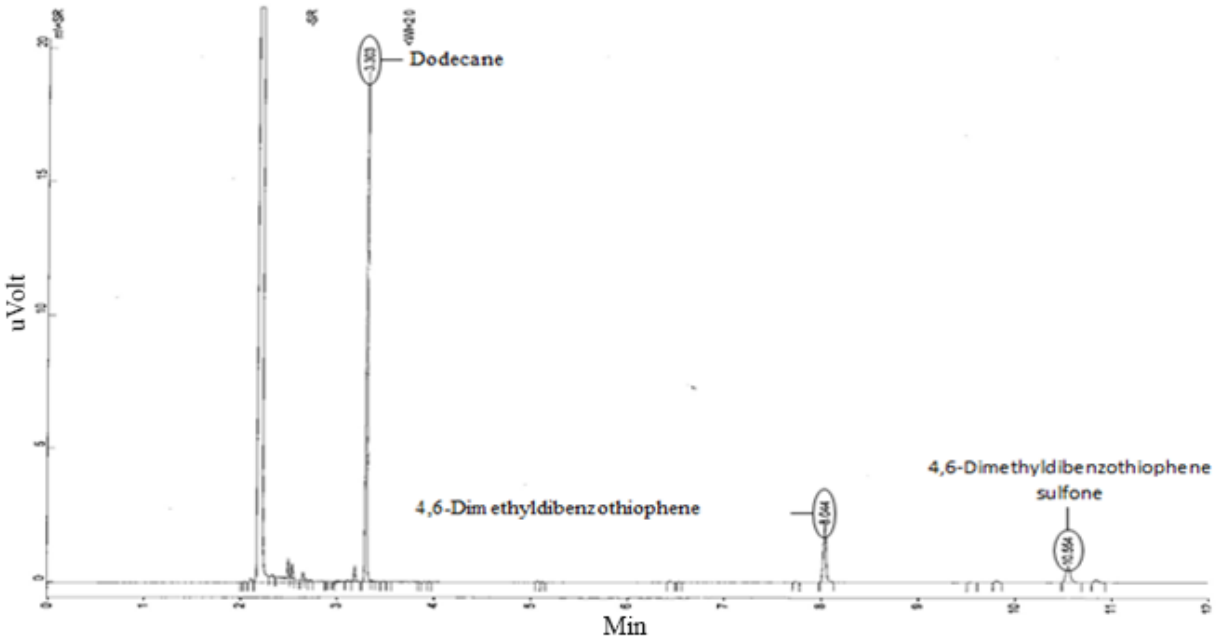

Fig. 2.8 Typical GC trace for 4,6-dimethyldibenzothiophene oxidation.

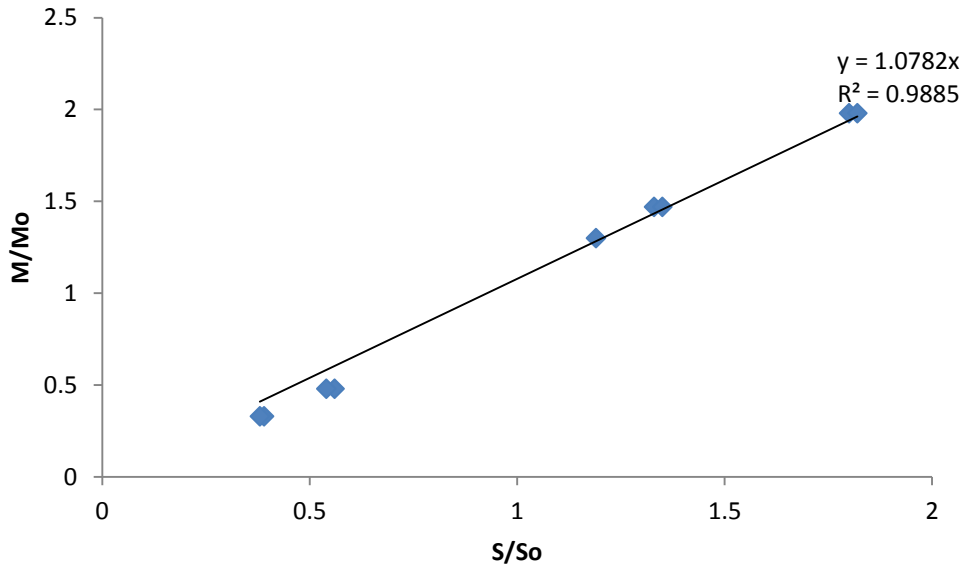

Fig. 2.9 Calibration for dibenzothiophene with dodecane as a standard.

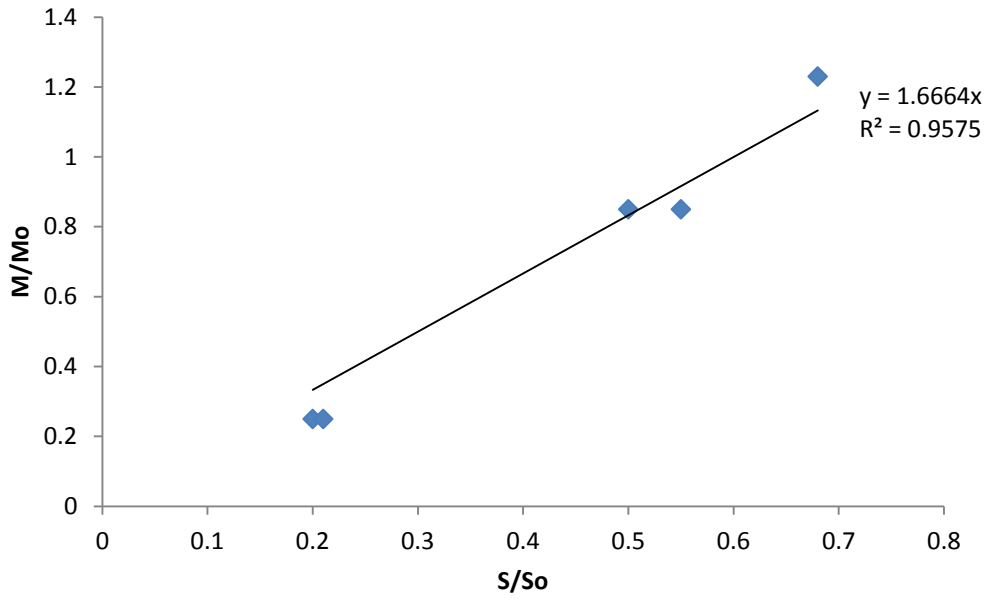

Fig. 2.10 Calibration for dibenzothiophene sulfone with dodecane as a standard.

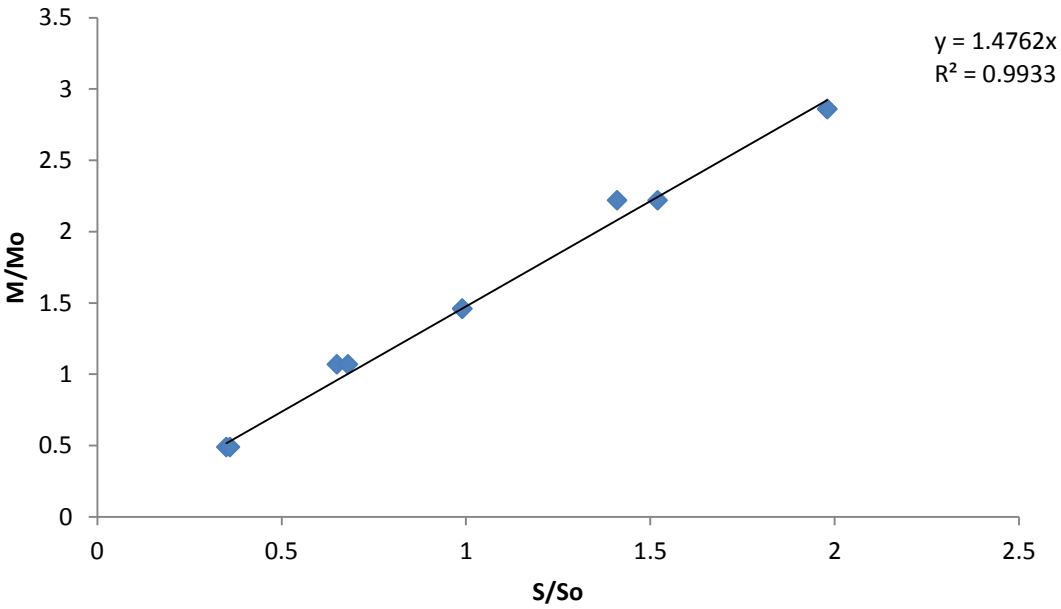

Fig. 2.11 Calibration for benzothiophene with undecane as a standard.

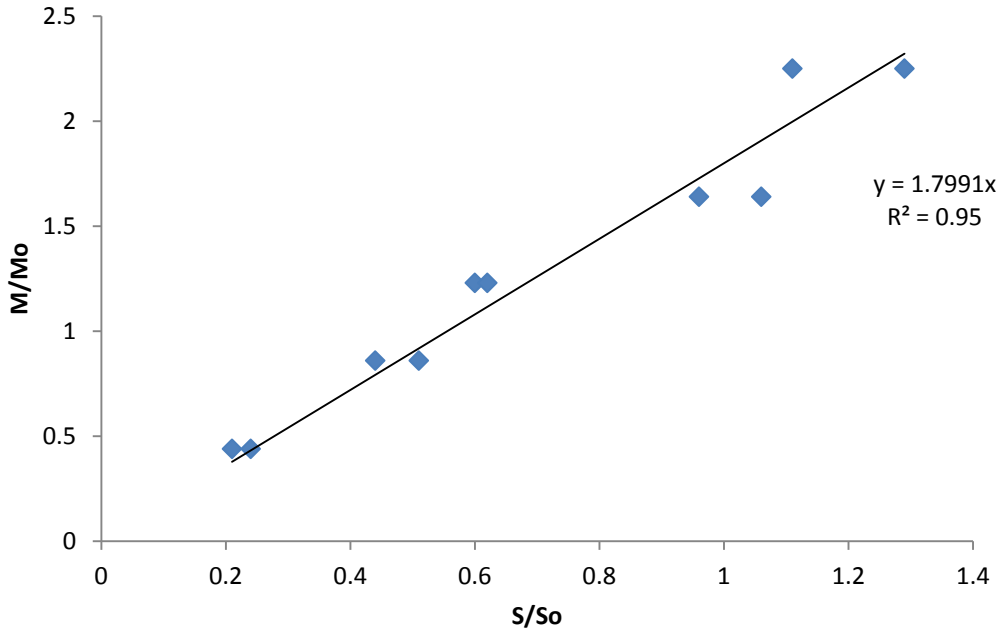

Fig. 2.12 Calibration for benzothiophene sulfone with undecane as a standard.

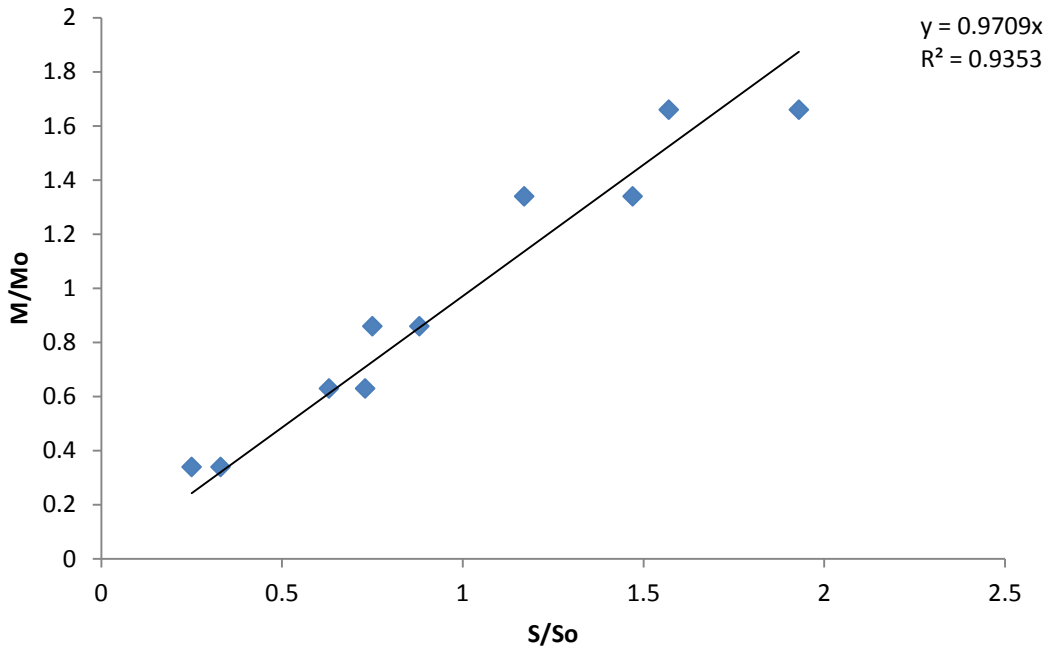

Fig. 2.13 Calibration for 4,6-dimethyldibenzothiophene with dodecane as a standard.

2.4.3 Elemental analysis

One of the most important quantitative applications of gas chromatography is the determination of elements like carbon, hydrogen, nitrogen and sulfur in organic compounds [4]. Although the dedicated elemental analysers vary from each other, they do follow well-established procedures. The weighed samples are placed into a reactor heated at ca. 1000°C and through which flows a constant stream of helium gas. When the samples are introduced, the helium stream is temporarily enriched with pure oxygen and flash combustion occurs followed by some steps to obtain quantitative combustion. Finally, the mixture of gasses so obtained passes through a Porapak chromatographic column and quantified using a GC detector.

Elemental microanalyses of our samples were obtained by submission to the CHN Micro-analysis Service in the University of Liverpool Chemistry Department.

2.4.4 Spectroscopic techniques

Molecular spectroscopic analysis methods are based on interactions between molecules and light quanta with different energy levels [8-10]. They are named after the spectral region and imply different effects on the molecules, depending on the energy, such as electron excitation, molecular vibration and molecular rotation (Fig. 2.14). The following values are used to characterize an electromagnetic wave: the wave number is the reciprocal wavelength (**1/λ** in cm^{-1}); the frequency **ν** indicates the number of vibrations of an electric or magnetic field per unit time (in s^{-1} or Hz).

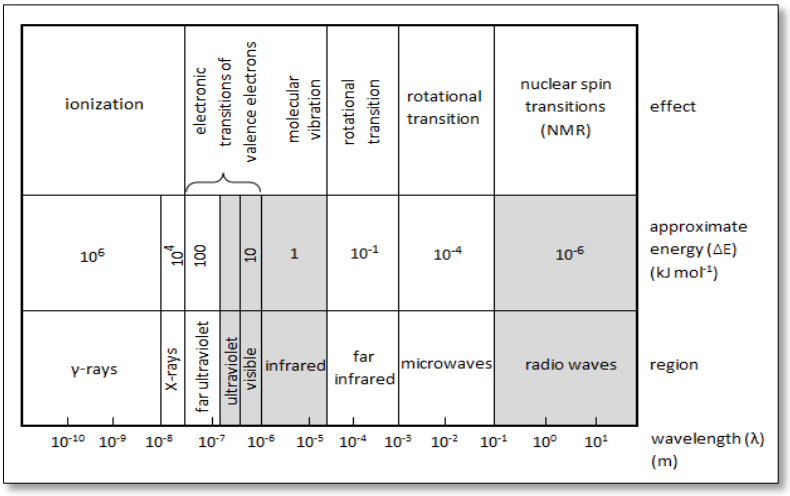

Fig. 2.14 The electromagnetic spectrum [9].

2.4.4.1 Fourier transform infrared spectroscopy (FTIR)

Infrared spectroscopy is an important method for obtaining information about the structural framework of materials [4-7]. It is known that molecules are capable of vibrating. Vibration can be excited by the absorption of electromagnetic radiation. Observation of the frequencies at which absorption occurs gives information about the structure of the molecule. Most IR spectrometers operate on the double beam principle, and a typical example of such a spectrometer is shown schematically in Fig. 2.15.

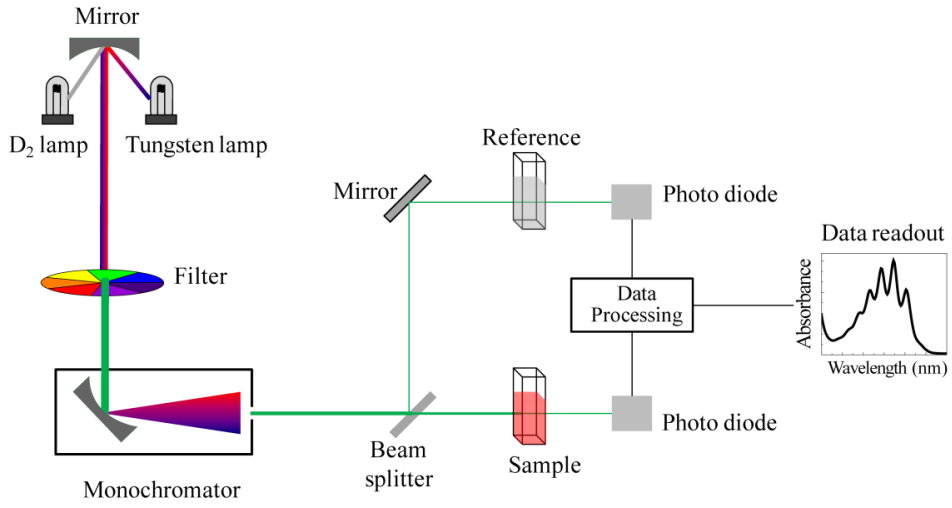

Fig. 2.15 Schematic representation of a double-beam IR spectrometer [6].

A more sophisticated type of IR spectroscopy, known as Fourier transform infrared (FTIR) spectroscopy, has been developed [5-7]. Although the final spectrum looks almost identical to one that is obtained on a double beam instrument, the spectrometer operates on an entirely different principle. Light, often from a laser source, covering the whole range of IR frequencies, is passed through the sample. A second beam, which has travelled along a longer path length, is combined with the first beam to produce a complex interference pattern. The on-board microcomputer performs a Fourier transformation on a series of these interference patterns to convert them into a conventional plot of absorption against frequency. FTIR has many advantages over the traditional method: sensitivity (very small sample can be examined), resolution (not dependent on optical properties of grating, slits and prisms), time (the whole spectral range is measured in a few seconds).

In our work, the diffuse reflectance technique, commonly called DRIFT, was used for recording the FTIR spectra of catalysts. DRIFT measures the radiation which is reflected from the sample in all directions [4]. Diffusely scattered light can be collected directly from a sample. The technique is particularly suitable for sampling powders or fibres. The design employs 4 flat and 2 aspherical reflectors, plus an alignment mirror (Fig. 2.16). Access to the sample is from the top, by sliding the ellipsoids out of the way (sample cup is removable for filling). Particles that are highly absorbing may produce totally absorbing peaks in the resulting spectrum because little energy is released from the sample. Highly absorbing

material can be mixed with a diffusely scattering matrix, such as KBr, which lowers absorption and improves throughput.

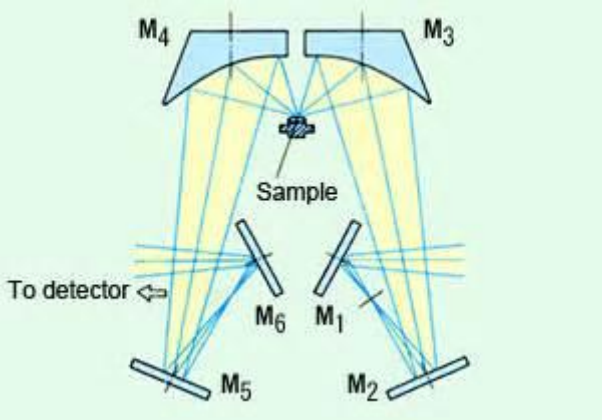

Fig. 2.16 Scheme of the diffuse reflectance accessory [6].

Samples were set as loose powders by mixing 2 mg of catalyst (which was previously dried at 150ºC/0.5 Torr/1.5 h) with 100 mg of dried KBr powder (2 wt %) and grinding thoroughly for 1-2 min. All the measurements were performed at room temperature under dry nitrogen flow. The infrared spectra were collected using a Nicolet Model Nexus FTIR-Raman spectrometer. Spectra were recorded using either absorbance **A** or percentage transmittance **T (A = log 1/T)**. The scanning limits were in the range of 4000 to 400 cm^{-1}. As an example, the IR spectrum obtained for bulk $H_3PW_{12}O_{40}$ is represented in Fig. 2.17.

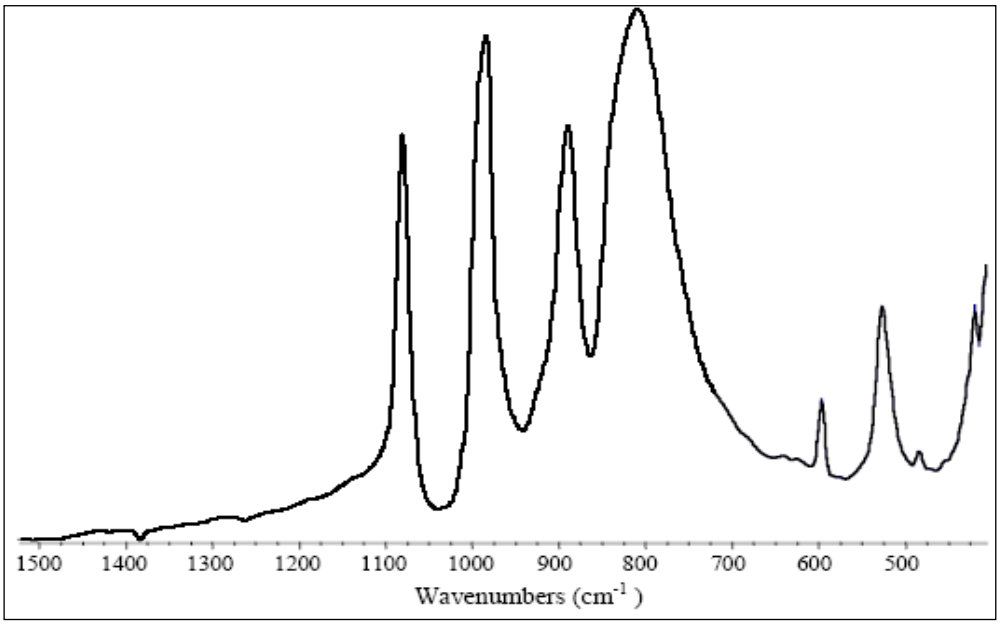

Fig. 2.17 FTIR spectrum of $H_3PW_{12}O_{40}$.

In the case of heteropoly compounds, the frequencies of molecular vibrations in the mid-infrared region (1200-500 cm^{-1}) reveal information on the primary structure of the heteropoly compounds. The FTIR data obtained are discussed in Section 3.3.

2.4.4.2 UV-Vis spectroscopy

Like IR spectrometers, most UV spectrometers operate on the double-beam principle, with one beam passing through the sample and the other through a reference cell [5-7]. After passing through the monochromator and the cells, the light from the source arrives at the detector which measures the ratio of the intensity of the reference beam (the incident intensity, $\mathbf{I_o}$) to the intensity of the sample beam (the transmitted intensity, **I**). On most machines the output from the detector is automatically converted into the absorbance $\mathbf{A = \log I_o/I = \log 1/T}$. The absorbance of a sample is proportional to its concentration, **c**, and to the path length, **ℓ**, and is given by an equation, usually called the Lambert-Beer law:

$$\mathbf{A = \varepsilon c \ell} \qquad (2.2)$$

Typically, a standard UV cell with **ℓ** = 1 cm is used, hence **A = εc**. The constant ***ε*** (molar extinction coefficient) is a measure of how strongly the compound absorbs at a given wavelength. Provided that the concentration of the sample is known, **ε** is readily calculated. Conversely, if the **ε** value for a compound is known at a given wavelength, measuring the absorbance at this wavelength permits the determination of the concentration of the sample. Absorption maxima and molar extinction coefficient are characteristics of an absorption spectrum.

In this work, the UV spectroscopy was used for measuring the concentration of $H_3PW_{12}O_{40}$ and $H_3PMo_{12}O_{40}$ in solution. The amount of $H_3PW_{12}O_{40}$ in DCE aqueous solution was measured with a VARIAN Cary 50 UV spectrophotometer in 1 cm quartz cuvette at a wavelength of 265 nm. The UV spectrum of the $PW_{12}O_{40}^{3-}$ anion in aqueous solution usually consists of one broad peak (Fig. 2.18).

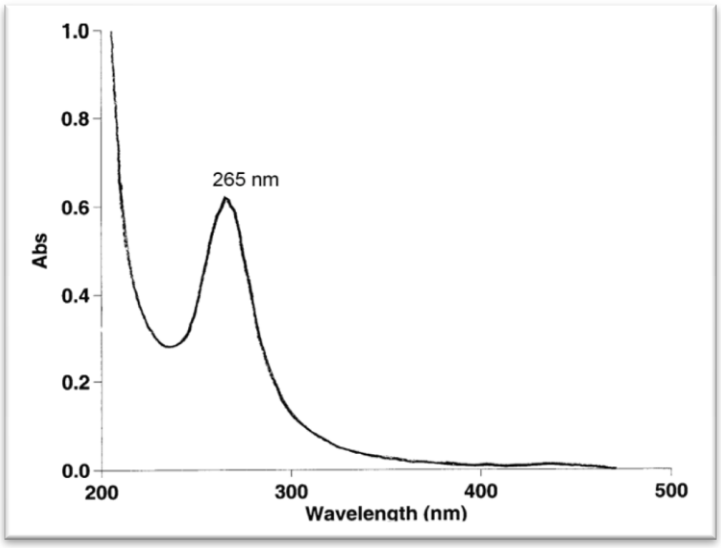

Fig. 2.18 UV spectrum of $H_3PW_{12}O_{40}$ in aqueous solution.

2.4.4.3 Nuclear magnetic resonance (NMR)

NMR spectroscopy is a fundamental technique for structural elucidation. It measures the absorption of electromagnetic radiation in the radiofrequency region of 4 MHz to 750 MHz, which corresponds to a wavelength of about 75 m to 0.4 m [5,6]. The NMR differs from other kinds of absorption spectroscopy with respect to the requirement for the sample to be subjected to an external magnetic field (Fig. 2.19).

Nuclear resonance comes about because the nuclei of at least one of the isotopes of most elements possess magnetic moments. The magnetic moment arises because the nucleus may have “spin” and is also charged. When placed in a constant magnetic field, the energy of the nuclear magnetic moment depends on the orientation of the nucleus with respect to that field, and on the microscopic nuclear scale only certain energies are permitted (that is, the energy is quantized). Application of electromagnetic radiation at a suitable frequency can stimulate transitions between the nuclear energy levels, which provide the basis for any form of spectroscopy.

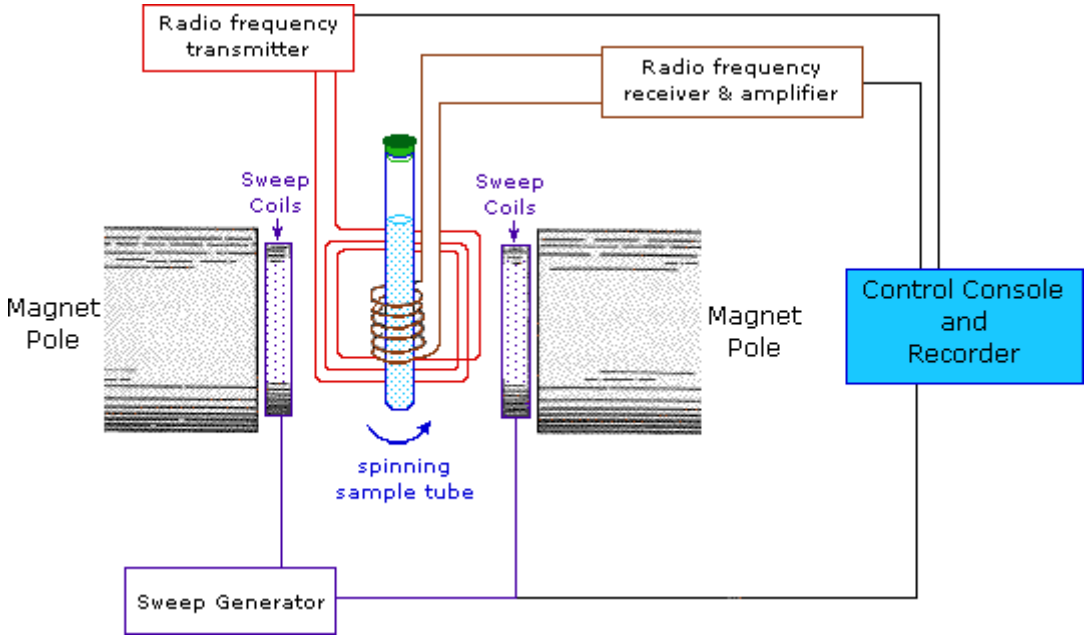

Fig. 2.19 Scheme of NMR spectrometer [6].

The different resonance frequency for each chemically distinct nucleus is identified in an NMR spectrum with the term chemical shift. The chemical shift of a nucleus is the difference between its resonance frequency and that of a reference standard. The fact that chemical shifts reflect the chemical environments of nuclei is obviously useful to structure determination.

Solid-state and solution NMR spectroscopies are powerful methods to investigate the primary structure of heteropoly compounds. Use of nuclei, such as ^{1}H, ^{17}O, ^{31}P, ^{51}V, ^{183}W as well as many others, proved particularly effective in polyoxometalate chemistry [1,2,5,7,11,17,19-38]. For heteropoly phosphates, ^{31}P NMR, both solid-state and solution, is the most useful method for structural characterisation due to the high sensitivity of this technique [1,11,40]. Misono et al. [7] studied the states and dynamics of protons and water in HPW using solid-state NMR. The ^{31}P spectra of $HPW \cdot nH_2O$ hydrates (n = 0-6) which were prepared from the hexahydrate by evacuation at 100-150°C are shown in Fig. 2.20. It can be seen that the chemical shift and peak width are dependent on water content. Hexahydrate of HPW gave a single peak at – 15.6 ppm that is consistent with the crystal structure in which all polyanions are equally hydrogen bonded by $H_5O_2^+$ cations [7].

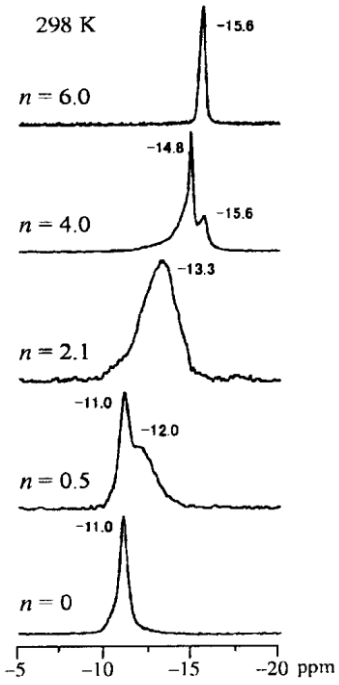

Fig. 2.20 ^{31}P NMR spectra of $H_3PW_{12}O_{40}\cdot nH_2O$ with a variety of hydration states ($0 \leq n \leq 6$) measured at 25°C [2].

2.4.5 Thermal gravimetric analysis

Most chemical compounds decompose and lose some weight when heated. TGA monitors the change in weight of substance as a function of temperature or time as the sample is subjected to a controlled temperature program. TGA is used to rank materials in order of their thermal stability by comparing their loss of weight versus temperature. Other TGA applications include the determination of moisture and coke percentage as well as the oxidation temperature of samples [9]. A derivative thermogravimetric weight loss curve (DTG) can be used to show the point at which the weight loss becomes most apparent. TGA consists of an extremely sensitive pan balance (generally platinum) and an accurate, draft-free furnace.

In this study, TGA was mainly used to measure the percentage by mass of physisorbed water in materials in order for the correct amount of reactants to be used in the catalyst synthesis (Figure 2.22). A Perkin Elmer TGA 7 instrument was used to perform the thermogravimetric

experiments using a heating rate of 20 ºC per minute to raise the temperature from room temperature to 700 ºC, under nitrogen gas flow. Figure 2.21 is an example of a typical TGA curve for $H_3PW_{12}O_{40}$.

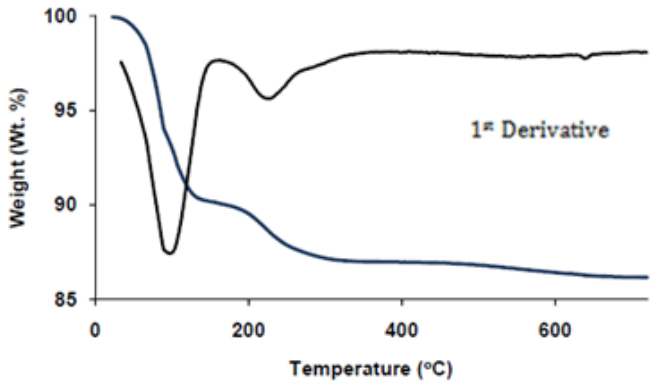

Fig. 2.21 Thermogravimetric analysis of $H_3PW_{12}O_{40}$.

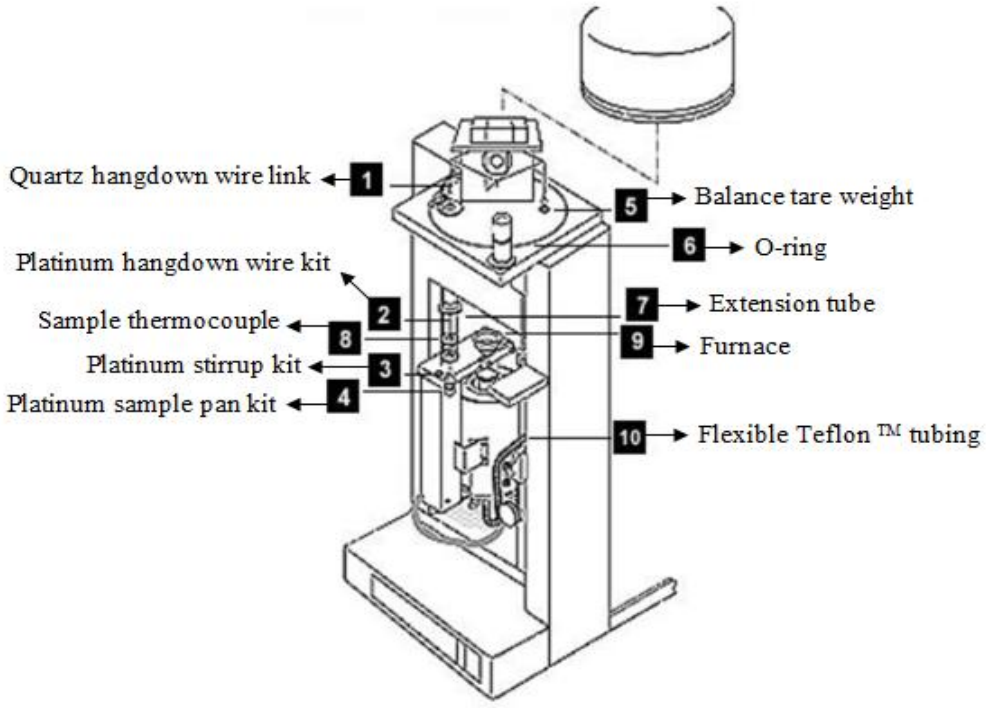

Fig. 2.22 Perkin Elmer TGA 7 instrument.

2.5 Reaction procedure

2.5.1 General procedure

The oxidation of dibenzothiophene was carried out in 50 ml three-necked jacketed glass reactor connected to a Grant heating circulator to control the reaction temperature. Samples withdrawn during reaction were spun in a centrifuge and were injected into the GC for analysis.

2.5.1.1 First procedure

The Grant water heating circulator was first heated up and stabilized to the desired reaction temperature (25-60^{o}C). Then, sulfur compounds (0.5 mmol) and standard (0.4 mmol) were dissolved in a flask in solvent (10 ml). After withdrawing the first sample (0 min reaction time) phase transfer agent (0.0023 mmol) was added to the mixture. Hydrogen peroxide (30 wt.%, 0.15 ml, 1.5 mmol) was then added to the reactor. Finally, polyoxometalate catalyst (0.0056 mmol) was added to the reactor to initiate the reaction. Reaction samples were withdrawn at 2, 5, 10, 20, 30, 60, 90 and 120 min and submitted for GC analysis.

2.5.1.2 Second procedure

The Grant water heating circulator was first heated up and stabilized to the desired reaction temperature (25-60^{o}C). Then, solvent (5 ml), phase transfer agent (0.0023 mmol), hydrogen peroxide (30 wt.%, 0.15 ml, 1.5 mmol) and polyoxometalate catalyst (0.0056 mmol) were added to the vessel and stirred for 5 min. Finally, sulfur compound(s) (0.5 mmol) and standard (0.4 mmol) were dissolved in solvent (5 ml) and added to reaction mixture.

For oxidation of sulfur compounds, a polar capillary GC column ZB-WAX, 30 m × 0.32 mm was used. The products were identified by comparison with authentic compounds and by GC-MS (Sections 2.3.1 and 2.3.2).

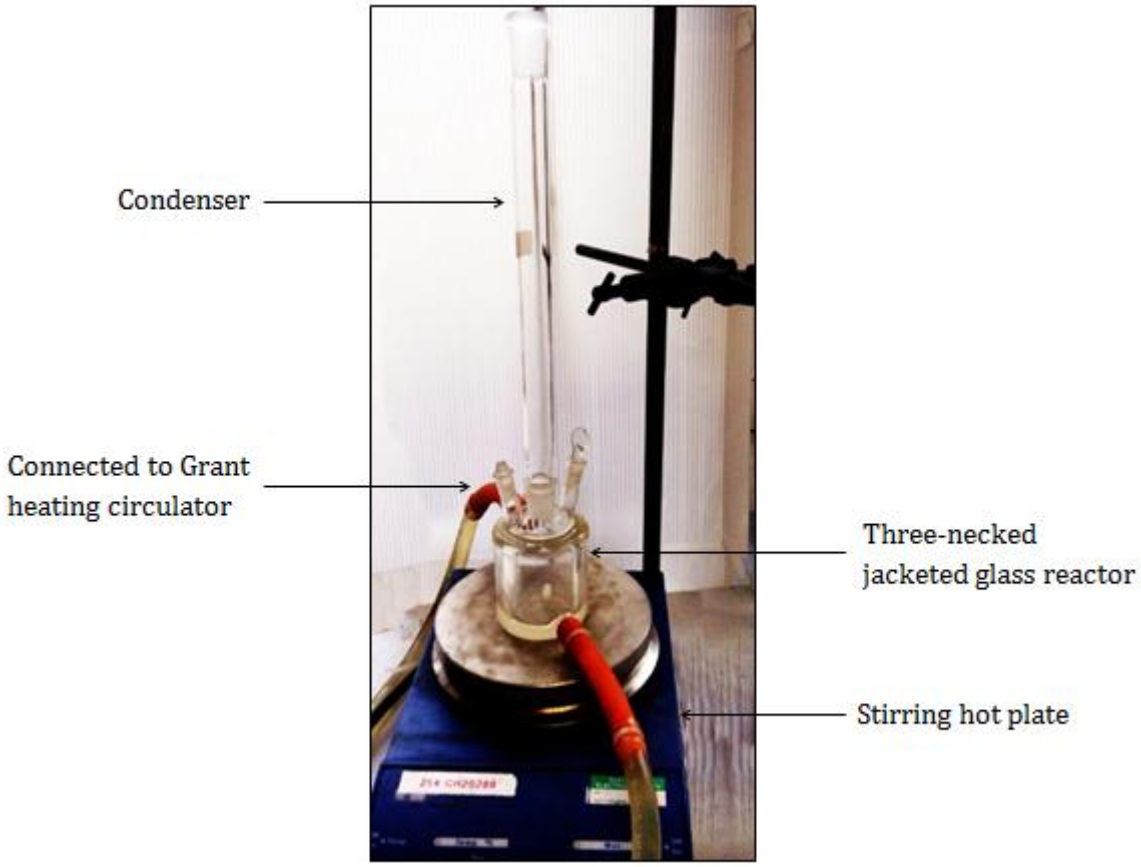

Fig. 2.23 Set-up of reaction equipment.

2.5.2 Catalyst reuse

The oxidation of sulfur compounds was carried out as described in Section 2.4.1, with different ratios of phase transfer agent to polyoxometalate. Catalyst reuse studies were carried out on a scale up to 50 ml of the initial reaction mixture. After each run, the catalyst was either added to the reaction mixture and new cycle was then run or the solvent was evaporated using a pump evaporator, then worked up by one of the procedures specified in Section(4.3).

2.5.3 Activation energy of dibenzothiophene oxidation

The activation energy, E_a, of dibenzothiophene oxidation was measured under differential conditions at a dibenzothiophene conversion < 10%. The reaction rate becomes linearly proportional to the change in conversion. Therefore, the activation energy can be calculated directly from the incremental change in conversion [9]. The activation energy was calculated using the Arrhenius equation (Equations 2.11 and 2.12).

$$k = A\exp\{-E_a/RT\} \qquad (2.11)$$

$$\ln k = -E_a/RT + \ln A \qquad (2.12)$$

Here, k is the reaction rate constant, A is the pre-exponential factor, E_a is the activation energy, R is the gas constant and T is the absolute temperature. A plot of ln(*conversion*) against $1/T$ gives a straight line, from which the activation energy can be determined under differential conditions. Thus, when the conversion log was plotted against the inverse of the temperature (K) and a straight line drawn through the plots, the gradient of this line represented $-E_a/R$, from which the activation energy could be reduced [10]. In this study, the activation energy for the oxidation of dibenzothiophene in liquid phase is presented in Chapter 4, Section 4.5.

References

1. J. F. Bickley, R. Bonar-Law, G. T. Lawson, P. I. Richards, F. Rivals, A. Steiner, S. Zacchini, Dalton Trans. (2003) 1235.
2. H. R. Allcock, T. J. Fuller, K. Matsumura, Inorg. Chem. **21** (1982) 515.
3. I. A. Fowlis, Gas Chromatography, ACOL-Wiley, Chichester, 1995.
4. J. Mendham, R. C. Denney, J. D. Barnes, M.J.K. Thomas, Vogel's Textbook of Quantitative Chemical Analysis, Pearson Education Ltd., 2000.
5. L. M. Harwood, C. J. Moody, J. M. Percy, Experimental Organic Chemistry: Standard and Microscale, Blackwell Science, 2001.
6. G. Schwedt, The Essential Guide to Analytical Chemistry, John Wiley & Sons, Chichester, England, 1997.
7. M. R. H. Siddiqui, S. Holmes, H. He, W. Smith, E. N. Coker, M. P. Atkins, I.V. Kozhevnikov, Catal. Lett. **66** (2000) 53.
8. E. F. Kozhevnikova, E. Rafiee, I.V. Kozhevnikov, Appl. Catal. A **260** (2004) 25.
9. S. Vyazovkin, Thermochimica Acta **236** (1994) 1.
10. R. Hetterley, Ph.D Thesis, Department of Chemistry, University of Liverpool, UK, 2008.

Chapter 3. Catalyst characterisation

In this Chapter, the characterisation of catalysts that were prepared and used in this work is presented and discussed. The main techniques used are described in Chapter 2. The catalysts under study include bulk Keggin heteropoly acids $H_3PW_{12}O_{40}$, $H_3PMo_{12}O_{40}$ and $H_4SiW_{12}O_{40}$. Phosphazene characterisation is also discussed using various techniques such as elemental CHN analysis, ^{31}P NMR and UV-Vis spectroscopy.

3.1 Characterisation of heteropoly acids

3.1.1 Thermogravimetric analysis of HPA

Thermogravimetric analysis (TGA) was used to determine both the water content and the thermal stability of each catalyst. Generally, solid heteropoly compounds (i.e. heteropoly acids and salts) accommodate a large amount of water of crystallisation (up to 30 molecules per Keggin unit). Depending on the amount of hydration water and on the counter-cation, several crystallographic arrangements exist (Table 3.1).

Table 3.1 Crystal structures of 12-tungstophosphoric acid hydrates [1].

Hydrate	Crystal type
$H_3PW_{12}O_{40}\cdot 29\ H_2O$	cubic
$H_3PW_{12}O_{40}\cdot 21\ H_2O$	orthorhombic
$H_3PW_{12}O_{40}\cdot 14\ H_2O$	triclinic
$H_3PW_{12}O_{40}\cdot 6\ H_2O$	cubic

The TGA and derivative thermogravimetric analysis (DTG) results for bulk HPAs (HPW, HSiW and HPMo) are summarised in Table 3.2; description of how these techniques were applied is outlined in Section 2.3.7.1. It should be noted that the results for the bulk HPW and HPMo are very close to the results obtained by other researches [1-11].

Table 3.2 Summary of TGA results.

Sample	Temperature range, °C	Weight loss, %	Number of H_2O molecules
$H_3PW_{12}O_{40}$	30 – 150	9.80	17.40
	150 - 300	3.30	5.40
	300 – 600	0.90	1.50
$H_4SiW_{12}O_{40}$	30 – 150	1.00	17.70
	150 - 300	3.50	5.80
	300 – 600	1.00	1.90
$H_3PMo_{12}O_{40}$	30 – 150	12.30	4.20
	150 - 300	2.30	2.40
	300 – 600	1.40	1.40

The thermal behavior of HPA catalysts has already been the subject of many investigations [1-3]. Three stages of weight loss have been found upon TG analysis of solid HPW hydrates [1-3,10-11].

First, water of crystallisation evolves when the temperature is raised from room temperature to 100-150°C (Fig. 3.1). These waters are hydrogen-bonded together and are often zeolitic, i.e. easily and reversibly removable from the solid. The hydration-dehydration process is frequently accompanied by changing (expanding or shrinking) the volume of the crystal cell. It should be noted that the amount of crystallisation water is not easy to control in the synthesis and depends on the conditions under which the acid is prepared. In our case, the first weight loss corresponded to 17.4, 17.7 and 4.2 molecules of water per Keggin unit (KU) for commercial HPW, HSiW and HPMo respectively (Table 3.2).

In the second stage, about 2-6 molecules of water are lost, showing a peak in the temperature range of 150-300°C centred at about 200-220°C (Fig. 3.1). These stronger bound waters are suggested to hydrate the three acidic protons in HPW, forming dioxonium ions $H_5O_2^+$ [12].

The third step at ca. 450°C (Fig. 3.1) corresponds to the loss of all acidic protons to evolve ~1.5 water molecules per KU for HPW and HPMo, and ~2 water molecules per KU for HSiW. This water is suggested to form as a result of the extraction of oxygen from the anion

by the protons, apparently without collapse of the Keggin structure of the anion but with some rearrangement of its secondary structure [11].

$$H_3PW_{12}O_{40} \rightarrow PW_{12}O_{38.5} + 1.5\ H_2O \qquad (3.1)$$

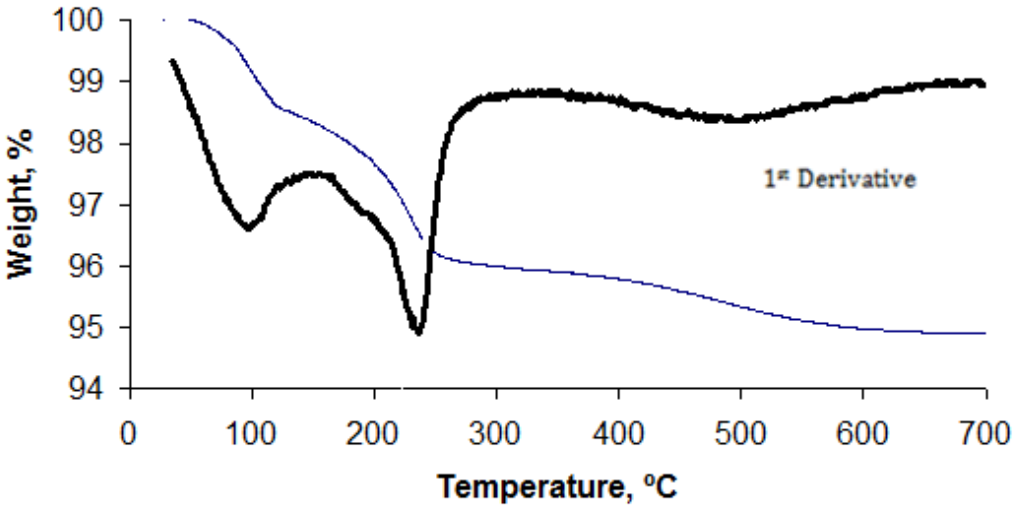

Figure 3.1 TGA analysis of $H_3PW_{12}O_{40}$ hydrate.

A mechanism involving the protonation of the bridging oxygen atom has been suggested for the deprotonation of HPW as a step preceding the decomposition of HPW [11,13] (Fig. 3.2). The decomposition of the Keggin structure to the constituent oxides WO_3 and P_2O_5 occurs above 550°C [11].

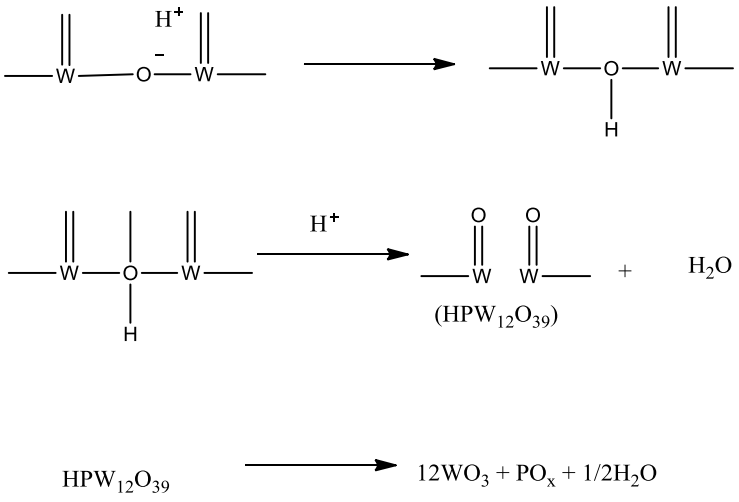

Fig. 3.2. Mechanism for the thermal decomposition of HPW.

The deprotonation step allows us to calculate the number of protons in HPA. Our values are in agreement with the expected number of protons for the three different HPWs analysed, i.e. 1.5 H_2O were lost in the temperature range of 300-600°C for HPW and HPMo (Table 3.2), which corresponds to 3 H^+ per KU, whereas in the same temperature range 1.9 H_2O were lost from HSiW, which corresponds to ~4 H^+ per KU.

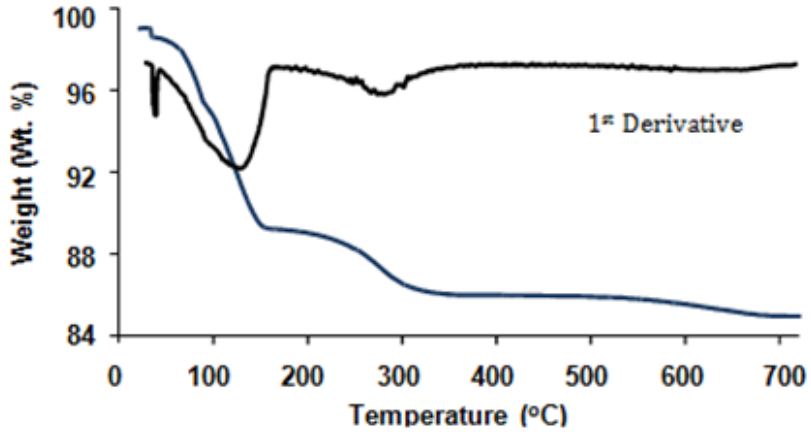

Figure 3.3 TGA analysis of $H_4SiW_{12}O_{40}$.

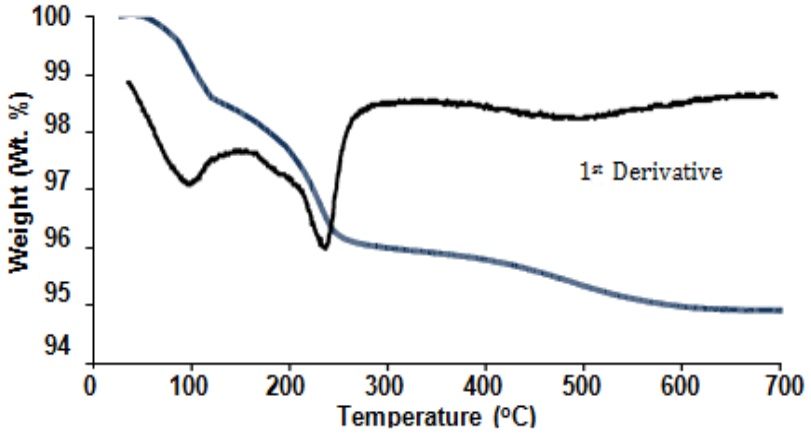

Figure 3.4 TGA analysis of $H_3PMo_{12}O_{40}$.

3.1.2 Infrared spectroscopy of HPA

The general procedure for FTIR measurements is described in Section 2.3.6.1. Infrared spectroscopy is one of the most frequently employed techniques for the characterisation of polyoxometalates as a consequence of the characteristic peaks of their structure ([11] and

references therein). Most of the characteristic bands of the Keggin anion are found in the HPA fingerprint region (1200-500 cm^{-1}) ([11, 35-40] and references therein). The IR spectra of bulk HPW, HPMo and HSiW recorded in this work show bands characteristic of Keggin anions in the region below 1200 cm^{-1} (Fig. 3.5-3.6). These spectra were measured as described in Section 2.3.6.1 and were in good agreement with data from the literature [11,14-19]. The results are summarized in Table 3.3. The spectrum for bulk HPW shows bands which coincide with those in the literature assigned by Choi *et al.* [15] and Southward *et al.* [13]. Interestingly, an analysis of the fingerprint bands for the Keggin unit in Southward *et al.* work showed a variation of band maxima with pre-treatment conditions and counter cations [13]. These bands was assigned to the stretching vibrations P-O_a, W-O_d, W-O_b-W, W-O_c-W and bending vibration O_a-P-O_a, respectively. The subscripts indicate oxygen bridging the W and the heteroatom: (a) corner sharing, (b) edge sharing oxygen, (c) belonging to octahedra WO_6 and (d) terminal oxygen.

Table 3.3 FTIR spectra of bulk HPW, HPMo and HSiW, (M=Mo, W and X=P, Si).

POMs	**FTIR band frequencies (cm^{-1})**		
	P-O	**M=O**	**M-O-M, M-O-X**
HPW	1080	982	893, 812
HPMo	1060	955	876, 800
HSiW	1015	976	885, 770

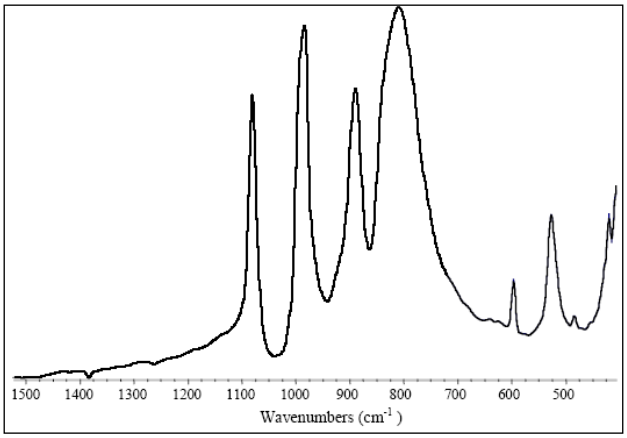

Figure 3.5 FTIR spectrum of bulk $H_3PW_{12}O_{40}$, showing characteristic Keggin structure bands.

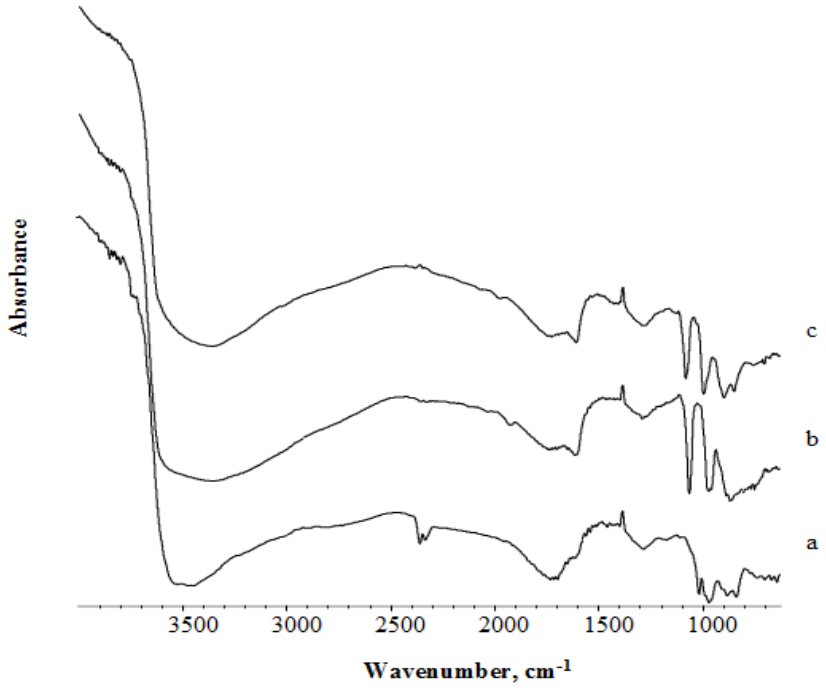

Fig. 3.6 FTIR spectra of bulk (a) HSiW, (b) HPMo and (c) HPW.

3.2 Phase transfer agent characterisation

3.2.1 Elemental CHN analysis of phosphazenes

Combustion analysis is a valuable method of measuring the amount of C, H and N in solid samples. It was used in this work to measure the C, H and N content during the preparation of phase transfer catalysts in order to ensure the reaction had gone to completion. It was carried out on a Thermo Flash EA 1112 series analyzer, which is available in the Department of Chemistry at Liverpool University.

The microanalysis results for all phosphazenes synthesized during this project are summarised in Table. 3.4. Reasonable results were obtained for all phosphazenes apart from diethylphosphazene, dibutylphosphazene and dihexylphosphazene. The experimental C and N values for these compounds differ significantly from the corresponding theoretical values indicating substitution of dialkylamines may be incomplete under the synthetic conditions used.

Table 3.4 Summary of CHN microanalysis.

Compound	Theory	Analysis
Benzylphosphazene		
C	65.62	64.84
H	6.25	6.31
N	16.41	15.92
Isobutylphosphazene		
C	50.77	50.21
H	10.65	10.53
N	22.20	21.95
Isopropylphosphazene		
C	44.17	43.15
H	10.01	9.82
N	25.80	25.51
Diethylphosphazene		
C	51.06	36.57
H	10.64	7.82
N	22.34	19.10
Hexylphosphazene		
C	59.02	57.48
H	11.48	11.31
N	17.21	16.22
Butylphosphazene		
C	51.06	53.79
H	10.64	11.16
N	22.34	21.00
Dibutylphosphazene		
C	64.00	57.84
H	12.00	10.92
N	14.00	12.87
Dihexylphosphazene		
C	69.90	73.25
H	12.62	13.67
N	10.19	8.00

3.2.2 ^{31}P NMR

To obtain structural information about a N-hexaclorocyclotriphosphazene $(PNCl_2)_{3,}$ one dimensional ^{31}P and ^{15}N NMR have been utilized [39]. One large singlet at ~17 ppm due to

BzPN has been reported. The three phosphorus atoms are chemically equivalent due to the ring symmetry [39]. The triplet arises due to one bond ^{31}P-^{15}N coupling with a coupling constant (J) value of 22.9 Hz. Each triplet is further split into two doublets by three bonds ^{31}P-^{15}N coupling (J=18.2 Hz) [39].

Our ^{31}P NMR spectra were recorded on a Bruker Avance DMX 400 spectrometer. The chemical shifts were found to be range between 13 ppm to 22 ppm. For example, ^{31}P NMR spectrum for isobutylphosphazene in toluene showed a single peak at 19.6 ppm and for benzylphosphazene at 17.4 ppm (Fig. 3.8 and 3.9) in agreement with the literature [39].

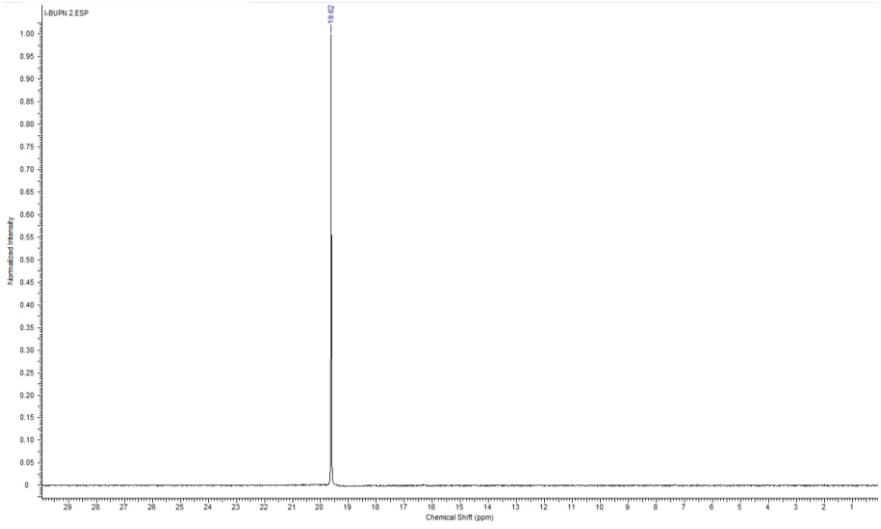

Fig. 3.7 ^{31}P NMR of iBuPN in toluene solution.

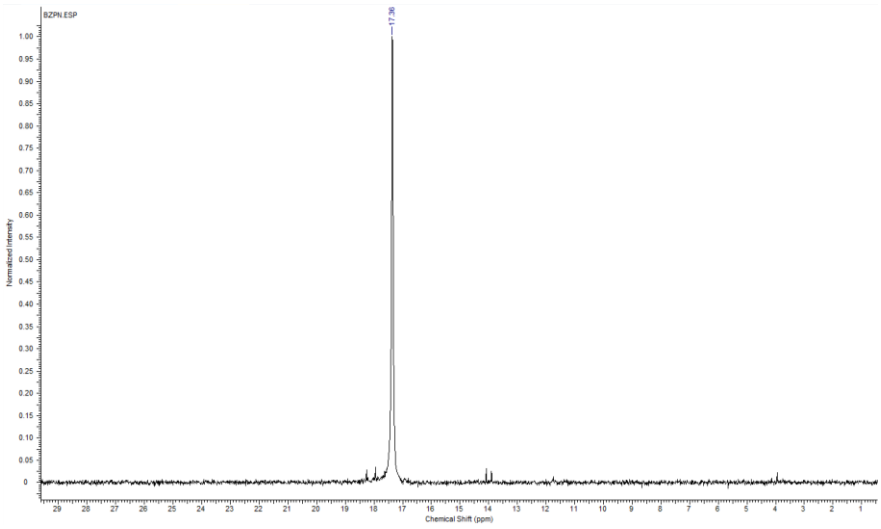

Fig. 3.8 ^{31}P NMR of BzPN in toluene solution.

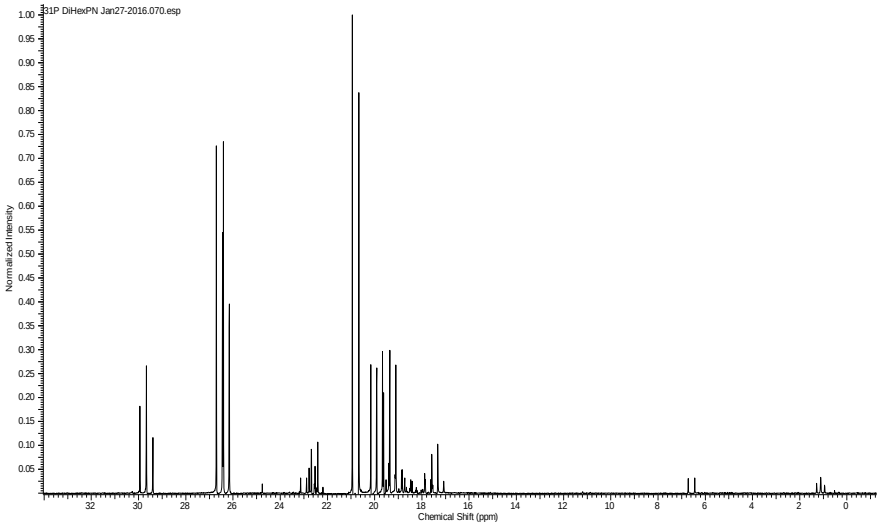

Fig. 3.9 ^{31}P NMR of DiHexPN in toluene solution.

On the other hand, the ^{31}P NMR spectrum of our DiHexPN sample (Fig. 3.9) showed that the sample contained a complex mixture of phosphazenes rather than the individual DiHexPN.

3.2.3 UV-Vis Spectroscopy study of POM phase transfer

For the UV-Vis study of POM phase transfer facilitated by alkylaminophosphazenes RPN, $H_3PW_{12}O_{40}$ (0.648 10^{-3} mmol), H_2O (0.5 mL) and BzPN in 1,2-dichloroethane (DCE) (10 mL) were added to a stoppered test tube and shaken vigorously at room temperature (~20 ^{o}C). The mixture was then left to settle for 2 h at room temperature. An aliquot of the organic phase was taken, spun in a centrifuge and analysed via UV-Vis spectroscopy at 268 nm (Fig. 3.10, 3.12) using a 1-cm quartz cell. POM phase transfer in the DCE – H_2O – H_2O_2 system was monitored similarly at 292 nm and different ratios of PW-BzPN (1:6), (1:4), (1:2) and (1:1) (Fig. 3.11, 3.13).

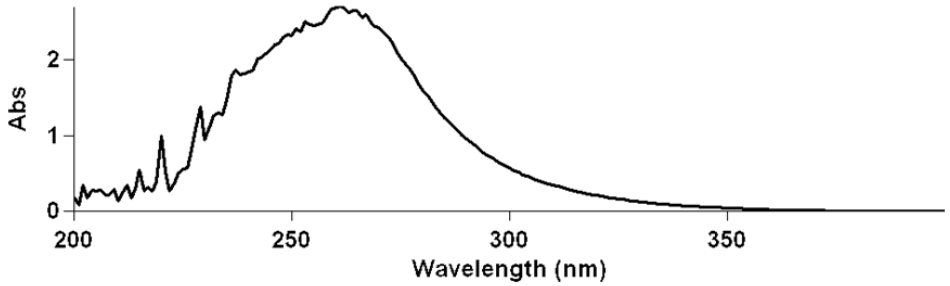

Fig. 3.10 UV-Vis spectrum of DCE phase after shaking the PW-BzPN (1:6)/DCE-H_2O system {PW (6.48 10^{-3} mmol), BzPN (38.9 10^{-3} mmol), DCE (10 mL), H_2O (0.5 mL)}. DCE phase was diluted 1:10 with fresh DCE. The band is peaked at 268 nm due to the presence of POM species in the DCE phase as a result of phase transfer facilitated by RPN.

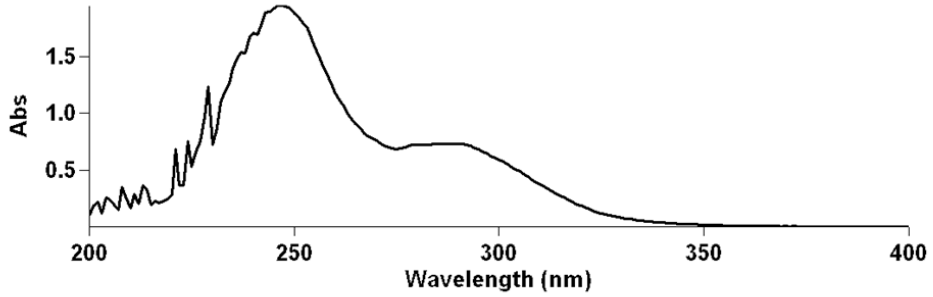

Fig. 3.11 UV-Vis spectrum of DCE phase after shaking the PW-BzPN (1:6)/DCE-H_2O_2-H_2O system {PW (6.48 10^{-3} mmol), BzPN (38.9 10^{-3} mmol), H_2O_2 (1.01 mmol), DCE (10 mL), H_2O (0.3 mL)}. DCE phase was diluted 1:10 with fresh DCE. The two bands are peaked at 250 and 292 nm.

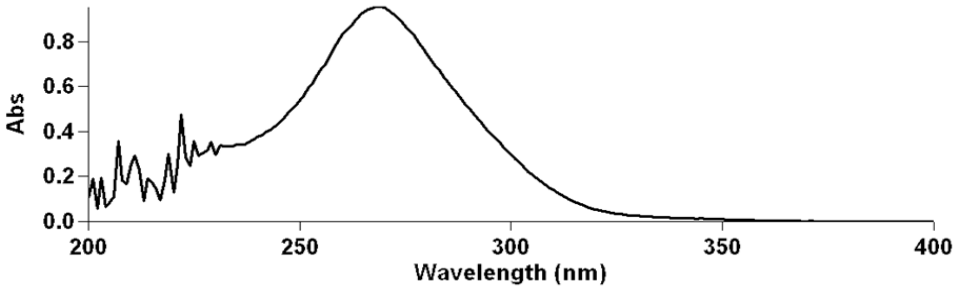

Fig. 3.12 UV-Vis spectrum of DCE phase after shaking the PW-BzPN (1:1)/DCE-H_2O system {PW (6.48 10^{-3} mmol), BzPN (38.9 10^{-3} mmol), DCE (10 mL), H_2O (0.5 mL)}. DCE phase was diluted 1:10 with fresh DCE. The band is peaked at 268 nm.

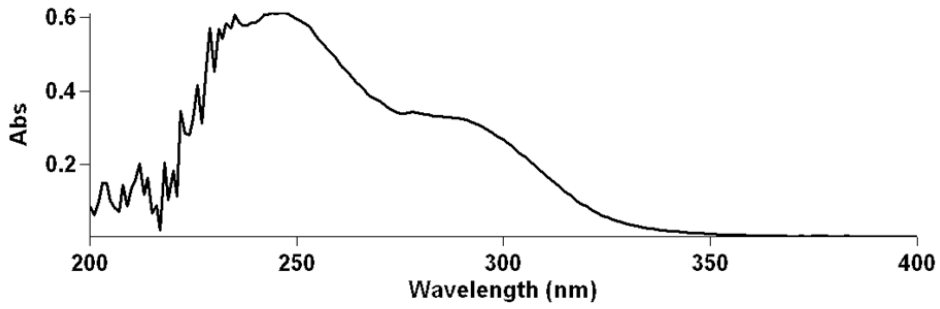

Fig. 3.13 UV-Vis spectrum of DCE phase after shaking the PW-BzPN (1:1)/DCE-H_2O_2-H_2O system {PW (6.48 10^{-3} mmol), BzPN (38.9 10^{-3} mmol), H_2O_2 (1.01 mmol), DCE (10 mL), H_2O (0.3 mL)}. DCE phase was diluted 1:10 with fresh DCE. The two bands are peaked at 250 and 292 nm.

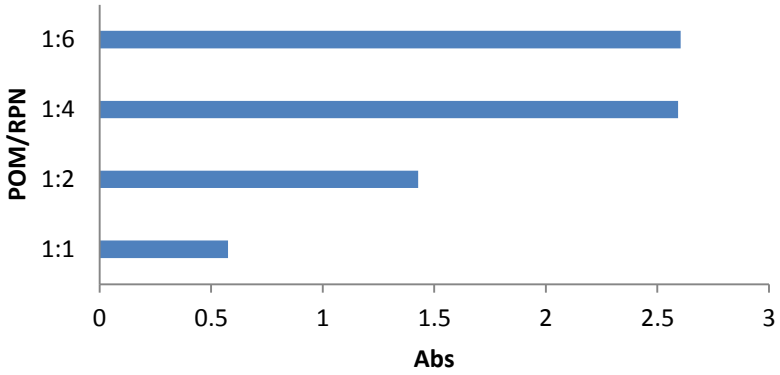

Fig. 3.14 UV-Vis study of POM phase transfer in DCE-H_2O system facilitated by RPN at 268 nm.

The absorption UV-Vis spectrum of DCE phase after shaking the PW-BzPN /DCE-H_2O system is illustrated in Fig. 3.14 with molar ratio [PW/RPN]: [1:6, 1:4, 1:2 and 1:1]. As shown in Fig. 3.10 and 3.12, the UV-vis absorption spectra display one intense absorption (λ_{max}) in the range of 260–270 nm.

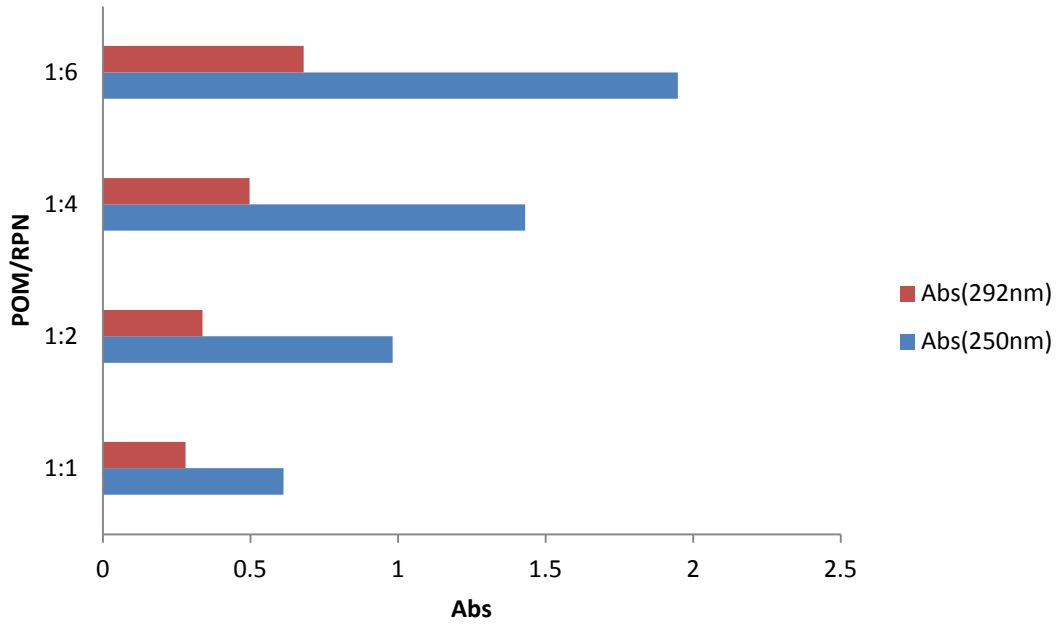

Fig. 3.15 UV-Vis study of POM phase transfer in DCE-H_2O_2-H_2O system facilitated by RPN at 250 and 292 nm.

UV-vis spectrum of DCE phase after shaking the PW-BzPN /DCE-H_2O_2-H_2O shows two bands at 250 and 292 nm. The first band is assigned to the combination of POM and the second one is peroxo species.

Phase transfer of $H_3PMo_{12}O_{40}$ was also carried out using the same procedure as outlined above. Peaks in the UV-Vis spectrum were identified at 248 and 315 nm (Fig. 3.16, 3.18). POM phase transfer in the DCE – H_2O – H_2O_2 system was monitored similarly at 247 nm (Fig. 3.17, 3.19).

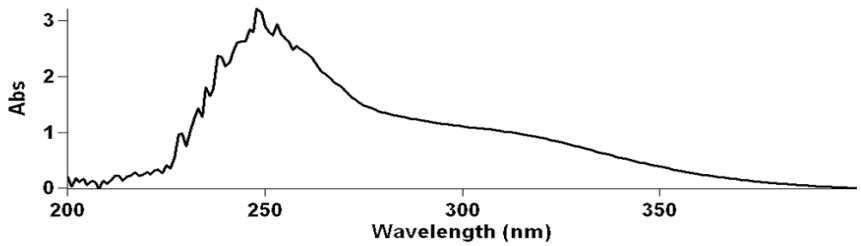

Fig. 3.16 UV-Vis spectrum of DCE phase after shaking the PMo-BzPN (1:6)/DCE-H_2O system {PW (6.48 10^{-3} mmol), BzPN (38.9 10^{-3} mmol), DCE (10 mL), H_2O (0.5 mL)}. DCE phase was diluted 1:10 with fresh DCE. The two bands are peaked at 248 and 315 nm.

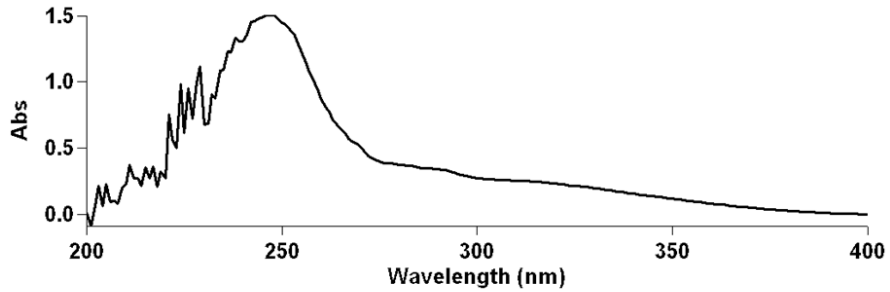

Fig. 3.17 UV-Vis spectrum of DCE phase after shaking the PMo-BzPN (1:6)/DCE-H_2O_2-H_2O system {PW (6.48 10^{-3} mmol), BzPN (38.9 10^{-3} mmol), H_2O_2 (1.01 mmol), DCE (10 mL), H_2O (0.3 mL)}. DCE phase was diluted 1:10 with fresh DCE. The band is peaked at 247 nm.

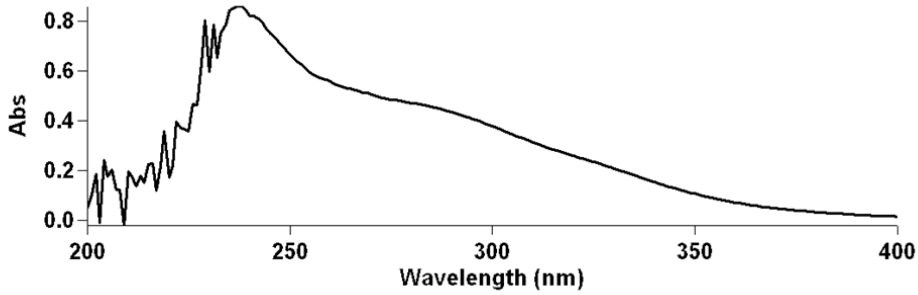

Fig. 3.18 UV-Vis spectrum of DCE phase after shaking the PMo-BzPN (1:1)/DCE-H_2O system {PW (6.48 10^{-3} mmol), BzPN (38.9 10^{-3} mmol), DCE (10 mL), H_2O (0.5 mL)}. DCE phase was diluted 1:10 with fresh DCE. The two bands are peaked at 248 and 315 nm.

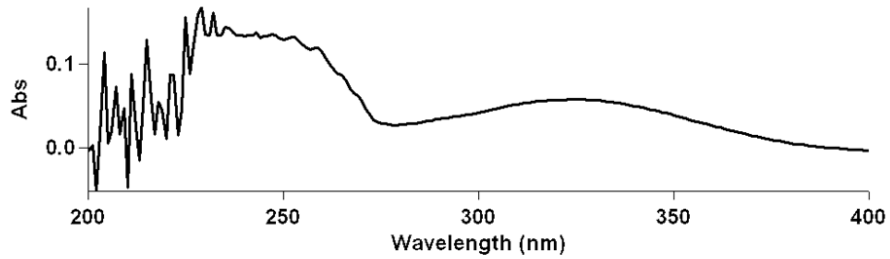

Fig. 3.19 UV-Vis spectrum of DCE phase after shaking the PMo-BzPN (1:1)/DCE-H_2O_2-H_2O system {PW (6.48 10^{-3} mmol), BzPN (38.9 10^{-3} mmol), H_2O_2 (1.01 mmol), DCE (10 mL), H_2O (0.3 mL)}. DCE phase was diluted 1:10 with fresh DCE. The band is peaked at 247 nm.

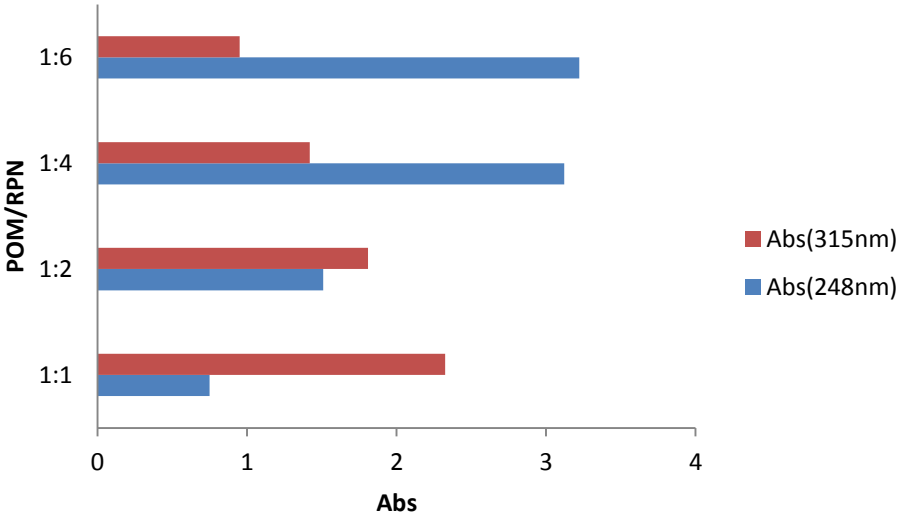

Fig. 3.20 UV-Vis study of PMo phase transfer in DCE-H_2O system facilitated by RPN at 248 and 315 nm.

From Fig. 3.20, it may be concluded that the absorption band at 315 nm is not relevant to PMo phase transfer in the DCE-H_2O two-phase system.

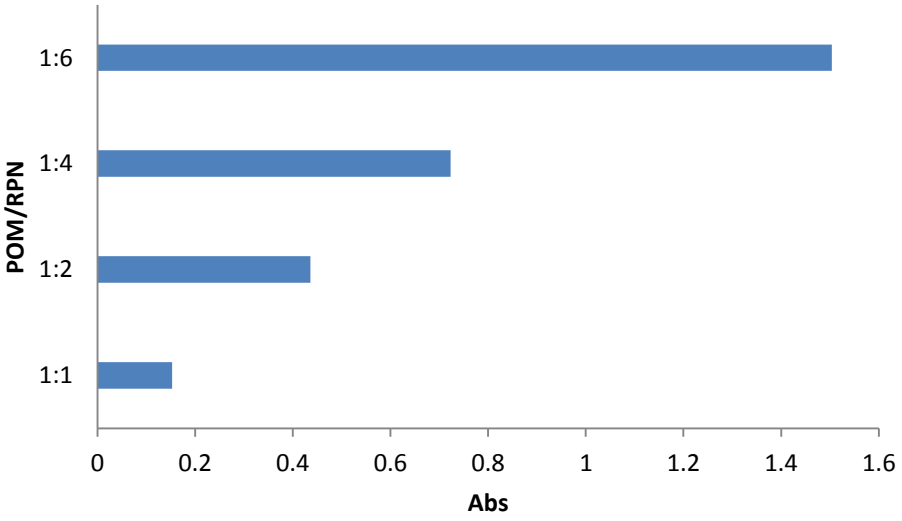

Fig. 3.21 UV-Vis study of PMo phase transfer in DCE-H_2O_2-H_2O system facilitated by RPN at 247 nm.

References

1. I. V. Kozhevnikov, Catalysts for Fine Chemicals, Catalysis by Polyoxometalates, vol. 2, Wiley, Chichester, 2002.
2. M. Misono, Chem. Comm. (2001) 1141.
3. C. Xian, D. Daichun, N. Jianping, J. Youming, Z. Jing, Q. Yixiang, Thermochim. Acta **292** (1997) 45.
4. V. V. Khakhinov, L. V. Tumurova, J. Thermal Anal. **53** (1998) 235.
5. N. Essayem, Y. Y. Tong, H. Jobic, J. C. Vedrine, Appl. Catal. A **194-195** (2000) 109.
6. M. Varga, B. Török, Á. Molnár, J. Therm. Analysis **53** (1998) 207.
7. S. Uchida, K. Inumara, M. Misono, J. Phys. Chem. B **104** (2000) 8108.
8. B. B. Bardin, R. J. Davis, Appl. Catal. **200** (2000) 219.
9. J. Kaur, K. Griffin, B. Harrison, I. V. Kozhevnikov, J. Catal. **208** (2002) 448.
10. N. Essayem, G. Couduier, M. Fournier, J. C. Védrine, Catal. Lett. **34** (1995) 223.
11. J. B. Moffat, Metal – Oxygen Clusters: The Surface and Catalytic Properties of Heteropoly Oxometalates, Klumer Academic/ Plenum Publishers, New York, 2001.
12. G. M. Brown, M. R. Noe-Spirlet, W. R. Bushing, H. A. Levy, Acta Cryst. B **33** (1977) 1038.
13. B. W .L. Southward, J. S. Vaughan, C. T. O'Connor, J. Catal. **153** (1995) 293.
14. N. Essayem, R. Frety, G. Coudurier, J.C. Vedrine, J. Chem. Soc. Faraday Trans. **93** (1997) 3243.
15. S. Choi, Y. Wang, Z. Nie, J. Liu, C. H. F. Peden, Catal. Today **55** (2000) 117.
16. T. Nakato, M. Kimura, S. Nakata, T. Okuhara, Langmuir **14** (1998) 319.
17. Catalyst Characterization: Physical Techniques for Solid Materials. Edited by B. Imelic, J. C. Vedrine, Plenum Press, New York, 1994.
18. C. Trolliet, G. Coudurier, J. C. Vedrine, Top. Catal. **15** (2001) 73.
19. M. T. Pope, Heteropoly and Isopoly Oxometalates, Springer-Verlag, Berlin, 1983.
20. N. Mizuno, M. Misono, Adv. Catal. **41** (1996) 113.
21. Y. Kanda, K. Y. Lee, S. Nakata, S. Asaoka, M. Misono, Chem. Lett. (1988) 139.
22. V. I. Spitsyn, V. F. Chuvaev, S. A. Bakhcisaraitseva, Dokl. Akad. Nauk SSSR, **165** (1965) 1126.
23. S. Gao, J. B. Moffat, Catal. Lett. **42** (1996) 105.
24. L. C. Jozefowicz, H. G. Karge, E. Vasilyeva, J. B. Moffat, Microporous Mater. **1** (1993) 313.

25. R. Massart, R. Contant, J. M. Fruchart, J. P. Ciabrini, M. Fournier, Inorg. Chem. **16** (1977) 2916.
26. R. Thouvenot, M. Fournier, C. Rocchiccioli-Deltcheff, J. Chem. Soc. **87** (1991) 2829.
27. F. Lefebvre, J. Chem. Soc. Chem. Commun. (1992) 756.
28. K. Mohana Rao, R. Gobetto, A. Iannibello, A. Zecchina, J. Catal. **119** (1989) 512.
29. J. C. Edwards, C. Y. Thiel, B. J. C Benas, J. F. Knifton, Catal. Lett. **51** (1998) 77.
30. A. Ghanbari-Siahkali, A. Philippou, J. Dwyer, M. W. Anderson, Appl. Catal. **192** (2000) 57.
31. T. Blasco, A. Corma, A. Martinez, P. Martinez-Escolano, J. Catal. **177** (1998) 306.
32. V. M. Mastikhin, V. V. Terskikh, M.N. Timofeeva, O. P. Krivoruchko, J. Mol. Catal. **95** (1995) 135.
33. V. M. Mastikhin, S. M. Kulikov, A.V. Nosov, I. V. Kozhevnikov, I. L. Mudrakovsky, M. N. Timofeeva, J. Mol. Catal. **60** (1990) 65.
34. I. V. Kozhevnikov, A. Sinnema, R. J. J. Jansen, H. van Bekkum, Catal. Lett. **27** (1994) 187.
35. I. V.Kozhevnikov, A. Sinnema, H. van Bekkum, M. Fournier, Catal. Lett. **41** (1996) 153.
36. I. V. Kozhevnikov, K.R. Kloetstra, A. Sinnema, H. W. Zandbergen, H. van Bekkum, J. Mol. Catal. A, **114** (1996) 287.
37. I. V. Kozhevnikov, Chem. Rev. **98** (1998) 171.
38. E. F. Kozhevnikova, J. Quartararo, I. V. Kozhevnikov, Appl. Catal. **245** (2003) 69.
39. D. Banerjee, Ph.D Thesis, Department of Chemistry, University of Akron, US, 2005.

Chapter 4. Polyoxometalate–phosphazene aggregates as catalysts for oxidative desulfurization

Sulfur present in crude oils not only poisons the catalysts used in oil refining industries, it also causes a series of environmental problems among which acid rain is the most common [1]. It is therefore unsurprising that the removal of sulfur from oil products has attracted growing attention in the past few decades [1,2]. Hydrodesulfurization (HDS) technology has become a very efficient method for the removal of mercaptans, sulfides and disulfides [1,2]. However, operation at high temperature and high hydrogen pressure creates many problems, including high investment costs, high operating costs and reduction of the length of the catalyst life [3,4,5]. Besides, HDS has some inherent problems in the treatment of aromatic sulfur compounds, such as dibenzothiophene (DBT), and their methylated derivatives [6,7].

Oxidative desulfurization (ODS) is considered one of the most promising processes to reduce refractory sulfur-containing compounds (dibenzothiophene and alkylated dibenzothiophene) [8]. Typical oxidising agents used for ODS include H_2O_2 [8,9], peracids [8,10], t-BuOOH [8,11], and O_2 or O_3 [8,12]. The reaction can be carried out in non-acidic media in the presence of catalytic amounts of a transition metal, e.g. Mo, W or V on several supports [8,13, 14]. For example, phosphotungstic acid – the main substituent of which is tungsten oxide – can catalyse the oxidation of dibenzothiophene with H_2O_2 in the presence or absence of a phase transfer agent in an oil/acetic acid biphasic system [8,15,16].

Indeed, polyoxometalates are a valuable class of inorganic compounds because of their tuneable size and charge, and the inclusion of a variety of transition metals [8,17]. Different polyoxometalate catalyst precursors with a phase transfer agent were reported for oxidative desulfurization of dibenzothiophene with H_2O_2 [8,18]. It was reported that a $[(C_{18}H_{37})_2N(CH_3)_2]_3[PW_{12}O_{40}]$ catalyst, assembled in an emulsion in diesel, could selectively oxidise DBT and its derivatives into their corresponding sulfones using H_2O_2 [8,19].

In the search for highly active catalysts for environmentally benign biphasic oxidations with hydrogen peroxide we have investigated aggregates comprising Keggin type polyanions $[XM_{12}O_{40}]^{m-}$ {X = P^{5+} (m = 3) and Si^{4+} (m = 4)} and lipophilic cyclophosphazene cations $[(RNH)_6P_3N_3H_n]^{n+}$ (n = 1 or 2). Cyclic and polymeric phosphazenes are renowned for their chemical and thermal robustness [22]. They have been used as high performance elastomers, fire retardants, polymeric electrolytes and also for biomedical applications [23]. Cyclophosphazenes with amino substituents $\{(RNH)_6P_3N_3$, labeled from here RPN} are strong bases; one or two ring N-centres can be protonated in the presence of Brønsted acids yielding mono and dications, $RPNH^+$ and $RPNH_2^{2+}$, respectively (Scheme 4.1) [24]. These compounds are easy to prepare on a large scale in one-step reactions from commercially available hexachloro cyclotriphosphazene and a wide range of primary amines [25]. Their phosphazene backbone is remarkably inert even towards concentrated acids and bases at elevated temperatures [26]. These compounds are highly soluble in non-polar solvents, but at the same time provide multiple hydrogen bonding sites, which makes them versatile building blocks for supramolecular assemblies [27].

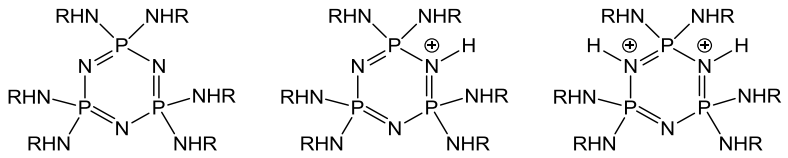

Scheme 4.1 Aminocyclophosphazene (RPN) and its mono ($RPNH^+$) and diprotonated ($RPNH_2^{2+}$) cations.

4.1 Oxidation of benzothiophenes catalysed by POM-RPN aggregates

Oxidative desulfurization catalyzed by tungsten POMs using 30% H_2O_2 as a ‘‘green’’ oxidant has been developed as a promising method for deep desulfurization of transportation fuel [22,29]. The oxidation of dibenzothiophene (Eqn. 4.1) is typically employed as a model reaction for catalyst testing.

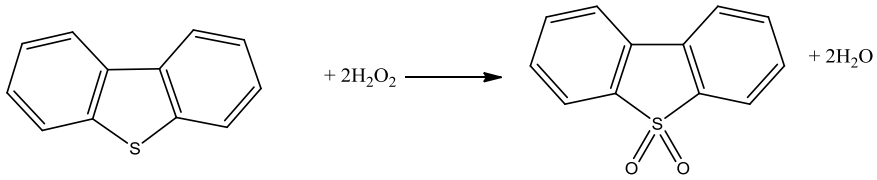

(4.1)

The oxidation of dibenzothiophene was carried out in a 50 ml three-necked, jacketed glass reactor connected to a Grant heating circulator to control the reaction temperature. Samples withdrawn during the reaction were injected into the GC for analysis. POM–RPN aggregates can be introduced in the reaction system as pre-synthesized compounds, however, in these reactions POM and RPN components were usually added separately to form the active catalyst in situ. POM–RPN aggregates were found to be highly active catalysts for DBT oxidation with H_2O_2 in a biphasic system, e.g. toluene–water, yielding DBT sulfone as the sole product.

4.1.1 Blank reaction

Blank experiments in the absence of phase transfer agent were carried out under optimal conditions (see Chapter 2): at 60^{o}C, DBT (0.5 mmol) and dodecane (GC internal standard, 0.4 mmol) were dissolved in a flask in 10 ml of toluene. After withdrawing the first sample (zero reaction time), hydrogen peroxide (30 wt.%, 0.15 ml) was then added to the reactor. Finally, polyoxometalate catalyst (0.0056 mmol) was added to the reactor to initiate the reaction. When the experiment was carried out reaction samples were withdrawn at 2, 5, 10, 20, 30, 60, 90 and 120 min and subjected to the GC analysis. No reaction was found to occur in the absence of phase transfer agent.

4.1.2 Effect of RPN and temperature on the oxidation of dibenzothiophene

Catalyst activity was found to increase with the size of the R group in RPN in line with increasing phase-transfer efficiency of RPN: iPr < iBu < Bz (Table 4.1) at molar ratios:

DBT/PW = 90:1, RPN/PW=4:1; 0.5 h reaction time. DBT sulfone was the only reaction product observed.

Temperature is an important parameter that can also play an important role in the oxidative desulfurization process. The influence of reaction temperature on the oxidation of DBT by RPN-POM in the presence of H_2O_2. It can be seen that when the reaction temperature was increased from 25 ^oC to 60 ^oC, the DBD conversion increased and could reach 100% after 20 min at 60 ^oC with BzPN as a phase transfer agent. Therefore, a high temperature is beneficial for the removal of DBT by RPN-POM in the presence of H_2O_2. No H_2O_2 decomposition was observed under these conditions, as was established by post reaction titration with permanganate. This might be because the rate of the reaction was faster than the decomposition of H_2O_2 in the temperature range 25-60 ^oC.

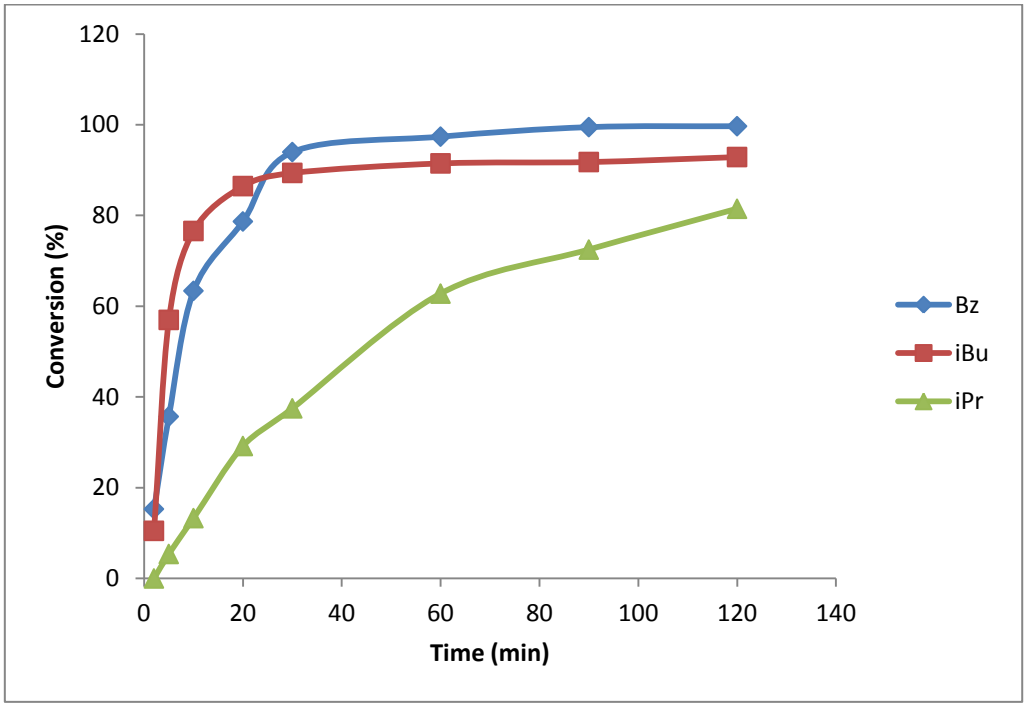

Fig. 4.1 Effect of RPN on DBT conversion (40 ^oC, toluene (10 mL), DBT (0.50 mmol, 1 wt%), aqueous 30% H_2O_2 (1 mL); molar ratios: RPN/POM= 4:1, DBT/POM = 90:1, DBT/H_2O_2 = 1:20).

Fig. 4.1 shows comparative results for phosphazene activity at 40 ^oC, demonstrating that increasing the size of the alkyl group increased the activity of the catalyst, with BzPN showing the highest efficiency. These phosphazenes were also tested at 25 and 60 ^oC (Fig.

4.2 and Fig. 4.3, respectively) and exhibited a moderate to good catalytic activity in the oxidation of dibenzothiophene.

Table 4.1 Effect of temperature and RPN on oxidation of DBT by H_2O_2 in toluene-H_2O two-phase system in the presence of PW catalysts.

R in RPN	**DBT/H_2O_2 (mol/mol)**	**Temp. (^oC)**	**Conv. (%)**	**H_2O_2 efficiency (%)**
Bz	1:20	40	94.0	>99
iBu	1:20	40	89.4	>99
iPr	1:20	40	37.5	>99
Bz	1:20	25	63.9	>99
iBu	1:20	25	69.6	>99
iPr	1:20	25	9.6	>99
Bz	1:3	60	91.0	>99
Hex	1:3	60	59.8	>99
DiHex	1:3	60	76.8	>99
DiEt	1:3	60	15.5	>99
DiBu	1:3	60	47.6	>99
Hex	1:3	40	54.4	>99
DiHex	1:3	40	55.0	>99
DiEt	1:3	40	0	>99
DiBu	1:3	40	16.3	>99

Toluene (10 mL), DBT (0.50 mmol, 1 wt%), aqueous 30% H_2O_2 (0.15 mL); molar ratios: DBT/PW = 90:1, RPN/PW=4:1; 0.5 h reaction time. DBT sulfone was the only reaction product observed.

As mentioned in the previous chapter, the experimental C and N analysis for diethylphosphazene, dibutylphosphazene and dihexylphosphazene differed significantly from the corresponding theoretical values indicating substitution of dialkylamines may be incomplete under the synthetic conditions used. Nonetheless, these compounds were tested as phase transfer catalysts at 60 ^oC and 40^oC (Fig. 4.3 and Fig. 4.4 respectively) and showed activity of the order DiEth < DiBut < DiHex < He.

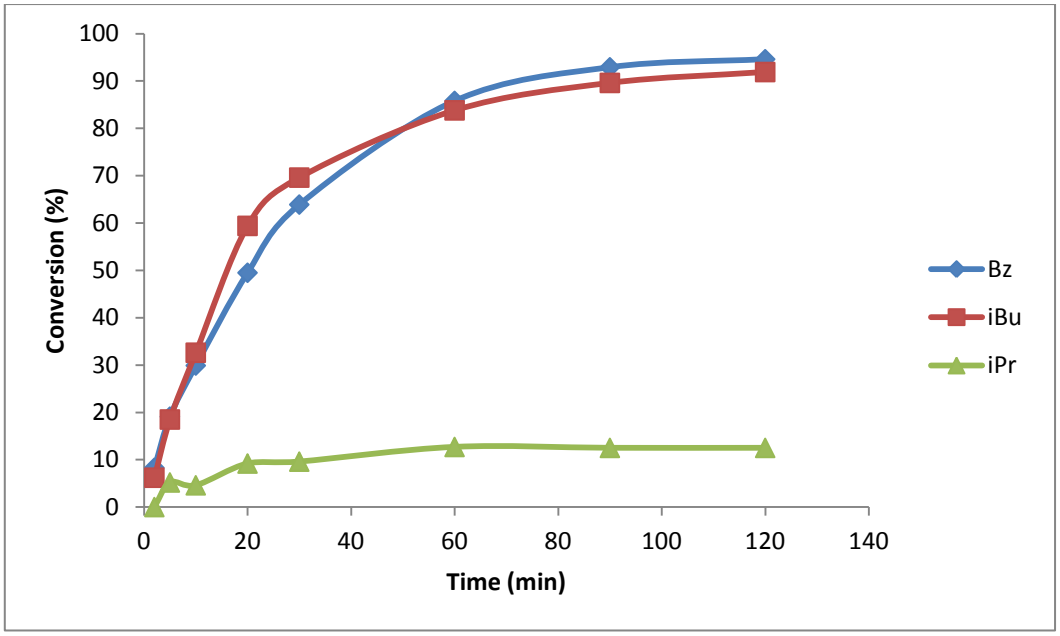

Fig. 4.2 Effect of RPN on DBT conversion (25 ^{o}C, Toluene (10 mL), DBT (0.50 mmol, 1 wt%), aqueous 30% H_2O_2 (1 mL); molar ratios: RPN/POM= 4:1, DBT/POM = 90:1, DBT/H_2O_2 = 1:20).

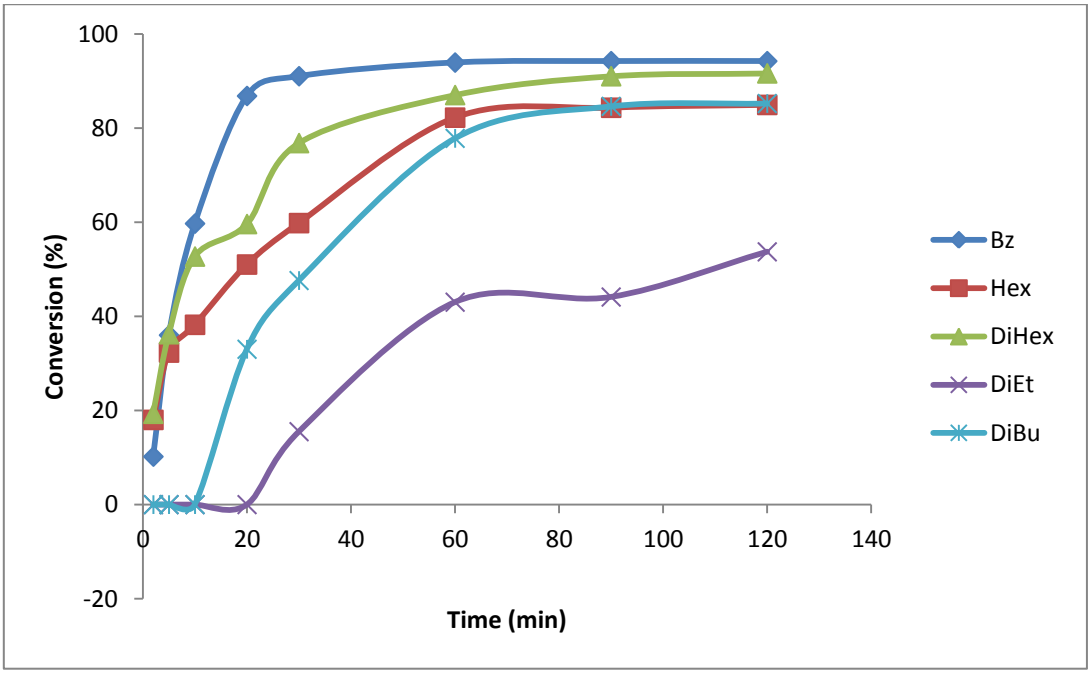

Fig. 4.3 Effect of RPN on DBT conversion (60 ^{o}C, toluene (10 mL), DBT (0.50 mmol, 1 wt%), aqueous 30% H_2O_2 (0.15 mL); molar ratios: RPN/POM= 4:1, DBT/POM = 90:1, DBT/H_2O_2 = 1:3).

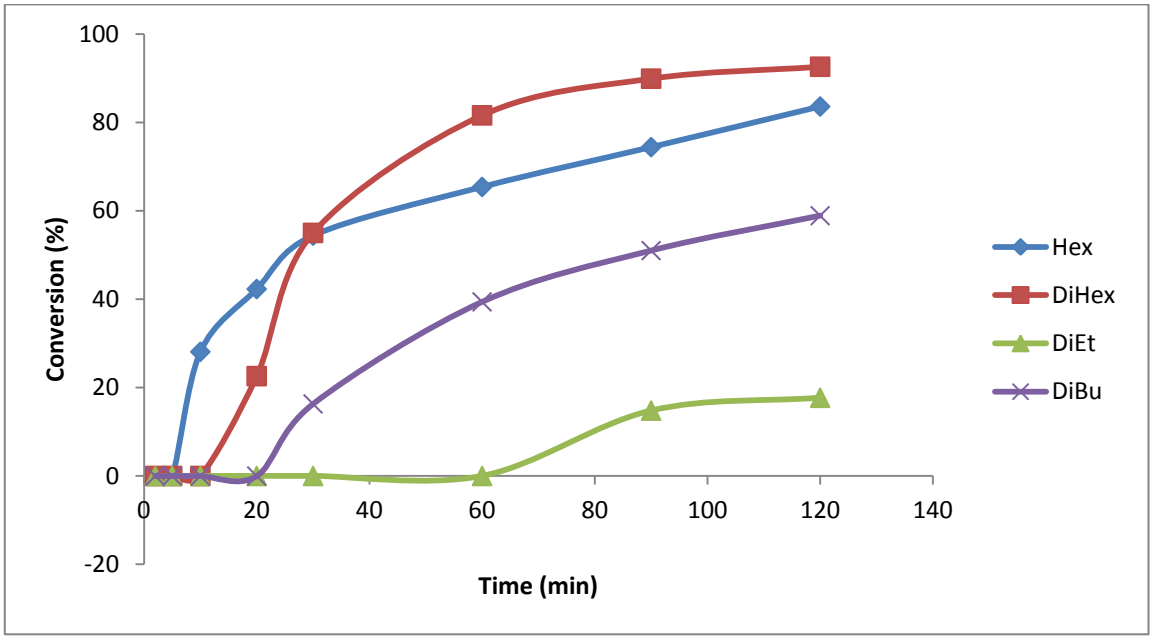

Fig. 4.4 Effect of RPN on DBT conversion (40 ^{o}C, toluene (10 mL), DBT (0.50 mmol, 1 wt%), aqueous 30% H_2O_2 (0.15 mL); molar ratios: RPN/POM= 4:1, DBT/POM = 90:1, DBT/H_2O_2 = 1:3).

4.1.3 Effect of POM on the oxidation of dibenzothiophene

PMo exhibited a higher activity than PW (Table 4.2), whereas SiW showed no activity before 60 min. The latter is in agreement with the well-known stability of SiW to degradation in solution, meaning more time is needed to form active peroxo species.

Indeed, Fig. 4.5 shows SiW needs time to form active peroxo species which is evident by the induction period up to 90 min, after which dibenzothiophene begins to oxidise in the presence of active species to form sulfone. PMo was found to be the best catalyst at 60 ^{o}C and 40 ^{o}C as indicated in Fig. 4.5 and Fig. 4.6.

Table 4.2 Oxidation of DBT by H_2O_2 in toluene-H_2O two-phase system in the presence of RPN-bound POM catalysts.

POM	DBT/H_2O_2 (mol/mol)	Temp. (^oC)	Conv. (%)	H_2O_2 efficiency (%)
PW	1:3	60	91.0	>99
PMo	1:3	60	99.5	>99
SiW	1:3	60	0	
PW	1:20	60	96.1	>99
PMo	1:20	60	100	>99

Toluene (10 mL), DBT (0.50 mmol, 1 wt%), aqueous 30% H_2O_2 (0.15 mL); molar ratios: DBT/POM = 90:1, 0.5 h reaction time. DBT sulfone was the only reaction product observed.

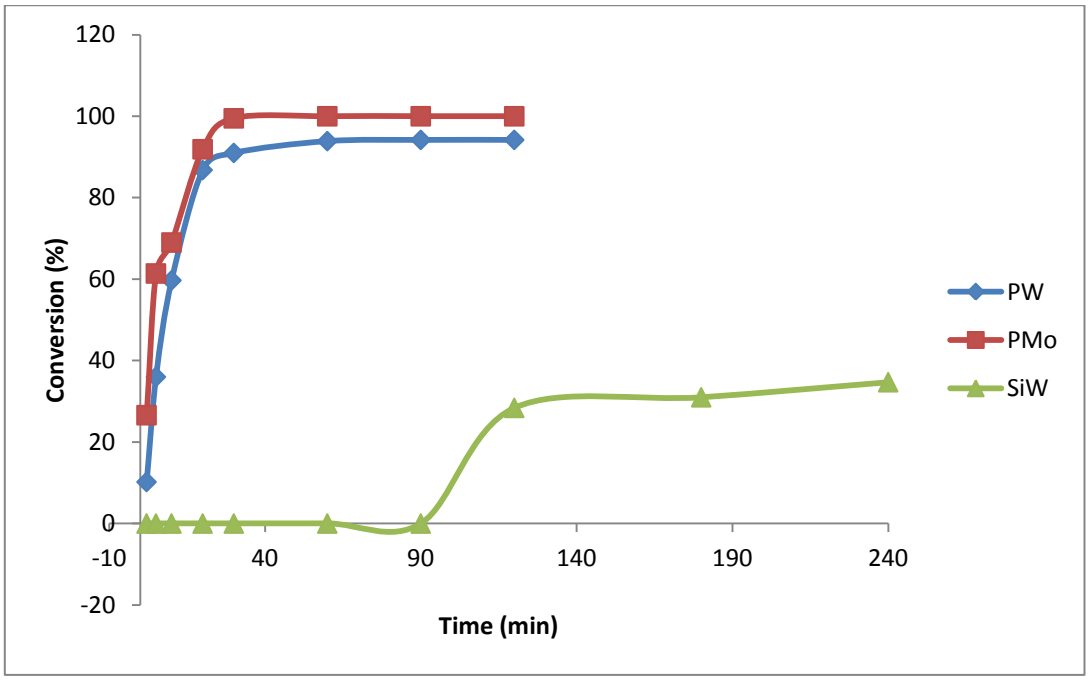

Fig. 4.5 Effect of POM on DBT conversion (60 ^oC, Toluene (10 mL), DBT (0.50 mmol, 1 wt%), aqueous 30% H_2O_2 (0.15 mL); molar ratios: RPN/POM= 4:1, DBT/POM = 90:1, DBT/H_2O_2 = 1:3).

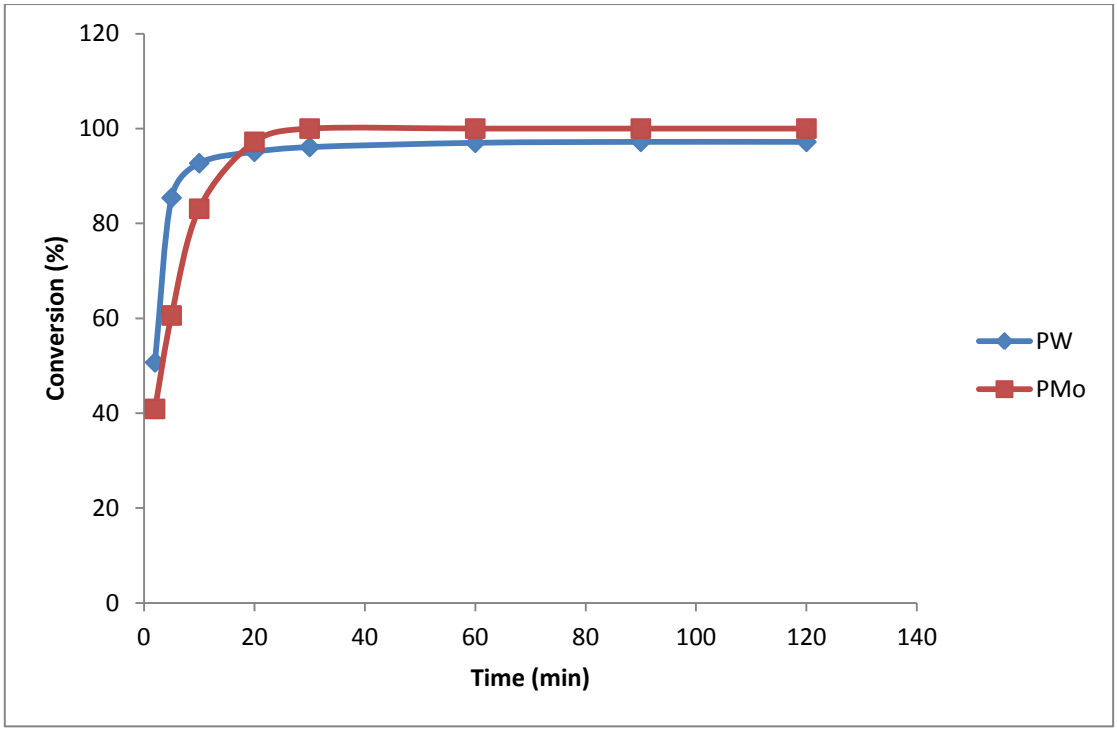

Fig. 4.6 Effect of POM on DBT conversion (60 ^{o}C, toluene (10 mL), DBT (0.50 mmol, 1 wt%), aqueous 30% H_2O_2 (0.15 mL); molar ratios: RPN/POM= 4:1, DBT/POM = 90:1, DBT/H_2O_2 = 1:20).

4.1.4 Effect of the nature of substrate

The structure of the substrate is a critical factor affecting sulfur removal in the desulfurization process. In this connection, the activity of BzPN-POM was studied with different substrates such as BT, DBT and 4,6-DMDBT. As shown in Fig. 4.6 and 4.7, the oxidation of these substrates followed the order of DBT > 4,6-DMDBT > BT. Therefore, it was clearly demonstrated that DBT was easier to oxidise than BT at 60 ^{o}C. This might be because the electron density on the sulfur atom of BT is lower than that of DBT [30–33]. Therefore, it is more difficult to remove BT among other sulfur-containing compounds [33].

Table 4.3 Oxidation of different benzothiophenes by H_2O_2 in toluene-H_2O two-phase system in the presence of BzPN-bound POM catalysts.

POM	Substrate	Temp. (^oC)	Conv. (%)	H_2O_2 efficiency (%)
PW	DBT	60	100	>99
PW	BT	60	55.1	>99
PW	4,6-DMDBT	60	81.3	>99
PMo	DBT	60	100	>99
PMo	BT	60	56.0	>99
PMo	4,6-DMDBT	60	92.4	>99

Toluene (10 mL), DBT (0.50 mmol, 1 wt%), aqueous 30% H_2O_2 (0.15 mL); molar ratios: substrate/POM = 90:1, BzPN/POM:6:1,substrate/H_2O_2 = 1:3; 0.5 h reaction time. Sulfones were the only reaction products observed.

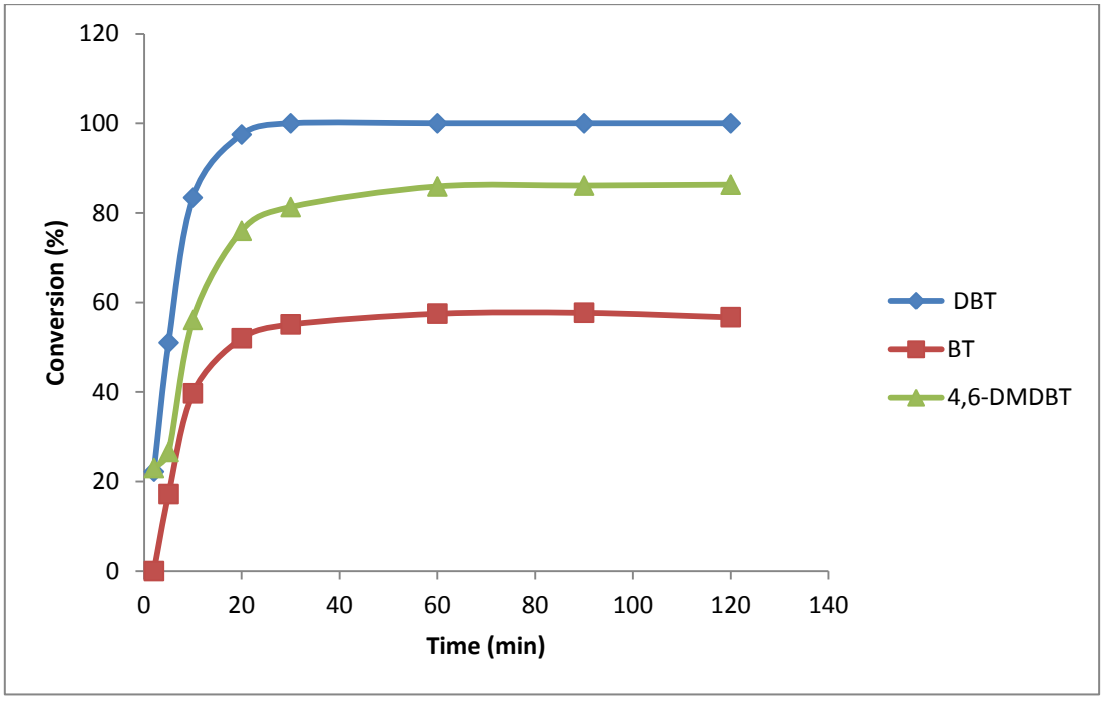

Fig. 4.7 Effect of substrate on oxidation using $H_3PW_{12}O_{40}$ (60 ^oC, toluene (10 mL), substrate (0.50 mmol, 1 wt%), aqueous 30% H_2O_2 (0.15 mL); molar ratios: BzPN/POM= 6:1, substrate/POM = 90:1, substrate/H_2O_2 = 1:3).

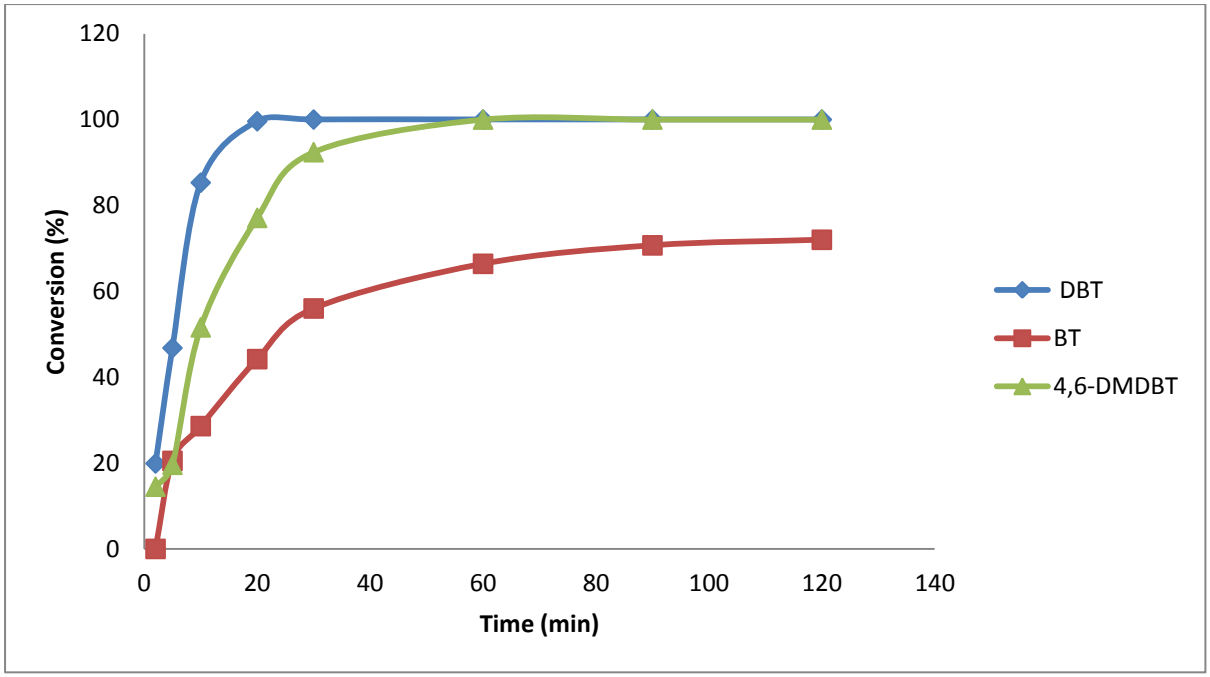

Fig. 4.8 Effect of substrate on oxidation using $H_3PMo_{12}O_{40}$ (60 ^oC, toluene (10 mL), substrate (0.50 mmol, 1 wt%), aqueous 30% H_2O_2 (0.15 mL); molar ratios: BzPN/POM= 6:1, substrate/POM = 90:1, substrate/H_2O_2 = 1:3).

4.1.5 Effect of [H_2O_2]/[DBT] ratio

In order to investigate the influence of the amount of the oxidant (H_2O_2) on sulfur removal, the oxidation of DBT in the BzPN-POM-H_2O_2 system under various O/S (oxidant/sulfur) molar ratios was carried out at 60 ^oC. The data are plotted in Fig. 4.9 and 4.10. It can be seen that when the O/S molar ratio was 6/1, DBT oxidation can reach 100 % in 30 min. However, when the O/S molar ratio decreased to 2/1, DBT conversion decreased to around 50% with PW, which might be because the [H_2O_2] is not high enough in the solution. Therefore, with the sulfur removal taken into consideration, the optimal molar ratio of O/S was 3/1 in the present study [34].

From Table 4.4, reaction solution diluted with water (1:1) gave a slight increase in conversion to 95.8% compared with 91.0% for non-diluted one.

Table 4.4 Effect of $[H_2O_2]/[DBT]$ ratio on oxidation of DBT by H_2O_2 in toluene-H_2O two-phase system in the presence of BzPN-bound POM catalysts.

POM	DBT/H_2O_2 (mol/mol)	Temp. (^oC)	Conv. (%)	H_2O_2 efficiency (%)
PW	1:20	60	95.8	>99
PMo	1:20	60	100	>99
PW	1:3	60	91.0	>99
PMo	1:3	60	99.5	>99
PW	1:2	60	48.9	>99
PW	1:3 diluted 1:1	60	95.8	>99

Toluene (10 mL), DBT (0.50 mmol, 1 wt%), aqueous 30% H_2O_2 (0.15 mL); molar ratios: DBT/POM = 90:1, BzPN/POM:4:1, 0.5 h reaction time. DBT sulfone was the only reaction product observed.

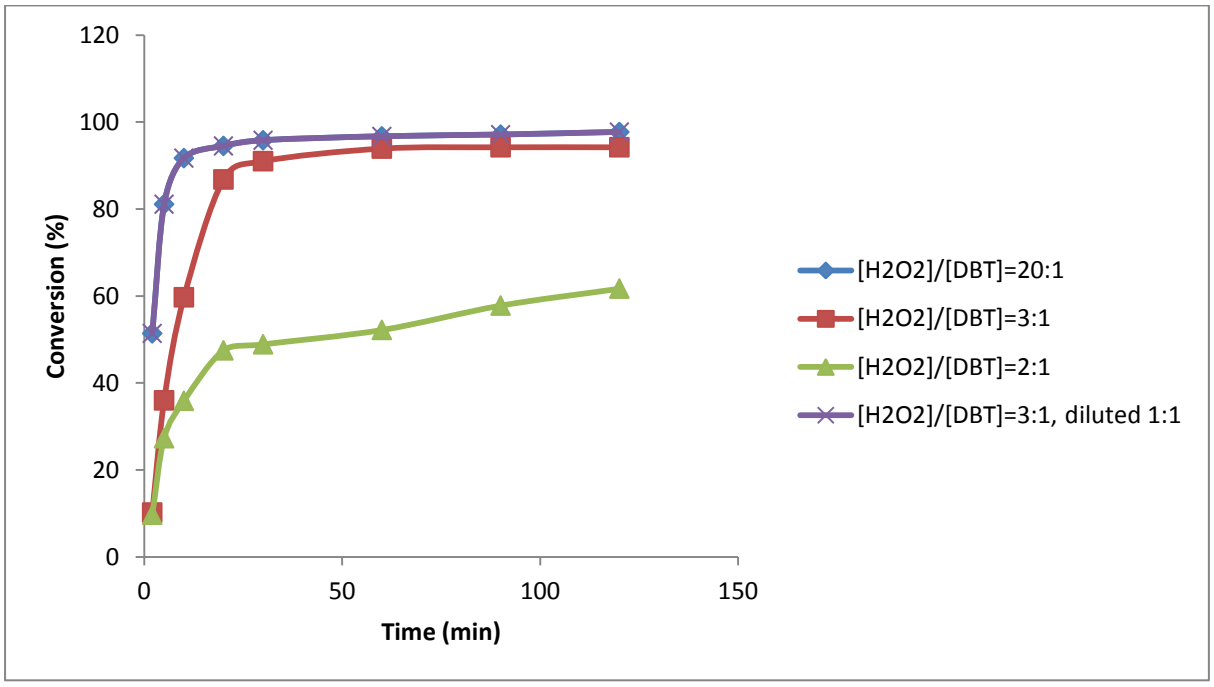

Fig. 4.9 Effect of $[H_2O_2]/[DBT]$ ratio on DBT conversion ($H_3PW_{12}O_{40}$, 60 ^oC, toluene (10 mL), DBT (0.50 mmol, 1 wt%), aqueous 30% H_2O_2 (0.15 mL); molar ratios: BzPN/POM = 4:1, DBT/POM = 90:1, DBT/H_2O_2 = 1:3).

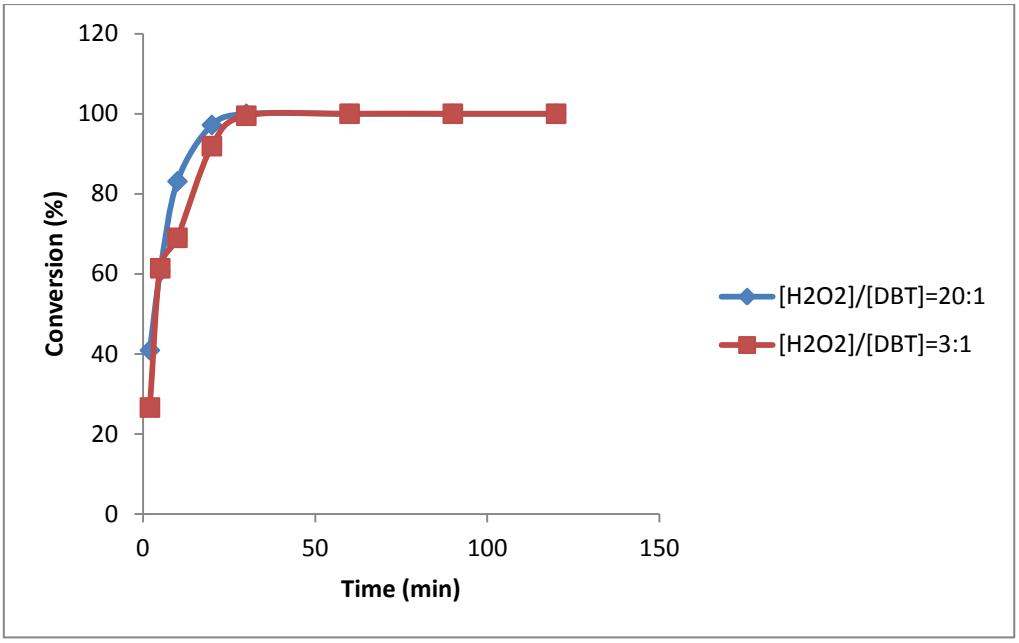

Fig. 4.10 Effect of $[H_2O_2]$/[DBT] ratio on DBT conversion ($H_3PMo_{12}O_{40}$, 60 ^oC, toluene (10 mL), DBT (0.50 mmol, 1 wt%), aqueous 30% H_2O_2 (0.15 mL); molar ratios: BzPN/POM = 4:1, DBT/POM = 90:1, DBT/H_2O_2= 1:3).

In this DBT oxidative desulfurization system, there was a serious competitive reaction in the decomposition of hydrogen peroxide. According to the stoichiometric reaction, the oxidation of 1 mol of DBT to DBT sulfone consumed 2 mol of hydrogen peroxide. In this experiment, 10 mL of model oil containing DBT (0.5 mmol), with a sulfur content of 500 ppm, 1 mmol hydrogen peroxide was sufficient on the basis of the stoichiometric reaction. Titration using standardised permanganate solution before and after the reaction was used to ensure there was no decomposition observed.

4.1.6 Effect of [RPN]/[POM] ratio

The molar ratio of RPN to POM was found to be an important factor influencing desulfurization efficiency. Sulfur removal with BzPN/PW = 2:1 was 80% at 60 ^oC (Table 4.5). When the molar ratio increased from 4 to 10, the conversion reached 100% in 30 min at 60 ^oC (Fig. 4.11).

Table 4.5 Effect of [RPN]/[POM] ratio on oxidation of DBT by H_2O_2 in toluene-H_2O two-phase system in the presence of BzPN-bound POM catalysts.

POM	RPN/POM (mol/mol)	Temp. (^oC)	Conv. (%)	H_2O_2 efficiency (%)
PW	4:1	60	96.9	>99
PMo	4:1	60	100	>99
PW	10:1	60	100	>99
PW	6:1	60	100	>99
PW	2:1	60	80.5	>99

Toluene (10 mL), DBT (0.50 mmol, 1 wt%), aqueous 30% H_2O_2 (0.15 mL); molar ratios: DBT/POM = 90:1, DBT/H_2O_2:3:1, 0.5 h reaction time. DBT sulfone was the only reaction product observed.

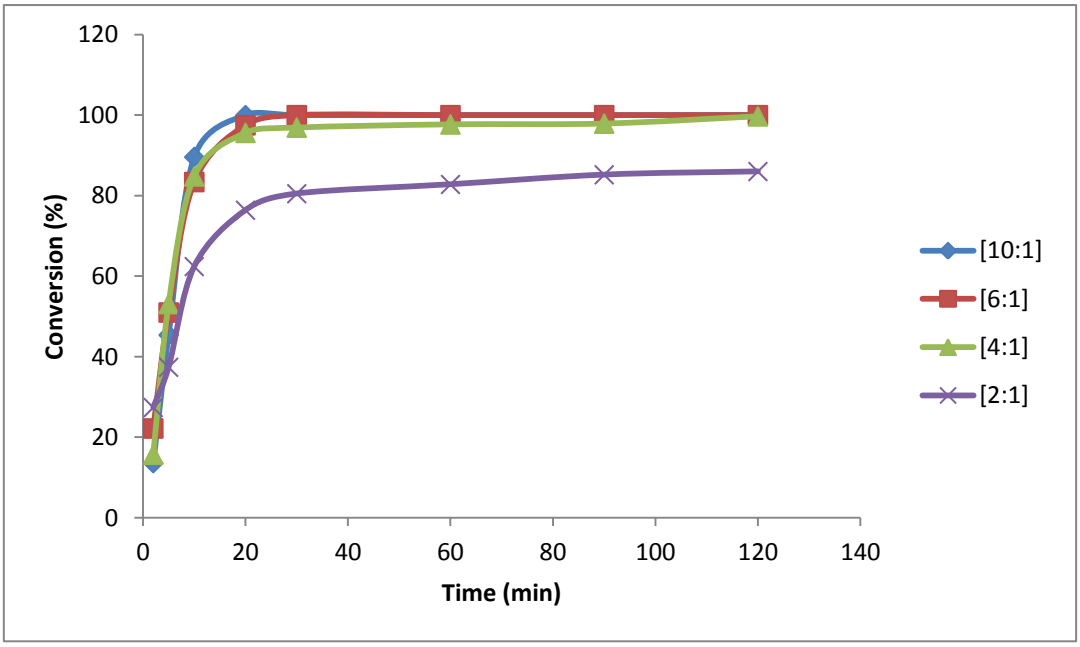

Fig. 4.11 Effect of [BzPN]/[POM] ratio on DBT conversion ($H_3PW_{12}O_{40}$, 60 ^oC, toluene (10 mL), DBT (0.50 mmol, 1 wt%), aqueous 30% H_2O_2 (0.15 mL); molar ratios: DBT/POM = 90:1, DBT/H_2O_2 =1:3).

4.1.7 Effect of [DBT]/[POM]

The effect of DBT/POM molar ratio on DBT oxidation was studied at molar ratios from 50:1 to 300:1 at 60 ^{o}C. The removal of sulfur compounds decreased at higher ratios from 100% to 41% as indicated in Table 4.6 and Fig. 4.12.

Table 4.6 Effect of [DBT]/[POM] ratio on oxidation of DBT by H_2O_2 in toluene-H_2O two-phase system in the presence of RPN-bound POM catalysts.

POM	DBT/POM (mol/mol)	Temp. (^{o}C)	Conv. (%)	H_2O_2 efficiency (%)
PW	90:1	60	96.9	>99
PMo	90:1	60	100	>99
PW	300:1	60	41.5	>99
PW	200:1	60	64.4	>99
PW	50:1	60	100	>99

Toluene (10 mL), DBT (0.50 mmol, 1 wt%), aqueous 30% H_2O_2 (0.15 mL); molar ratios: [BzPN]/[POM] = 4:1, DBT/H_2O_2:3:1, 0.5 h reaction time. DBT sulfone was the only reaction product observed.

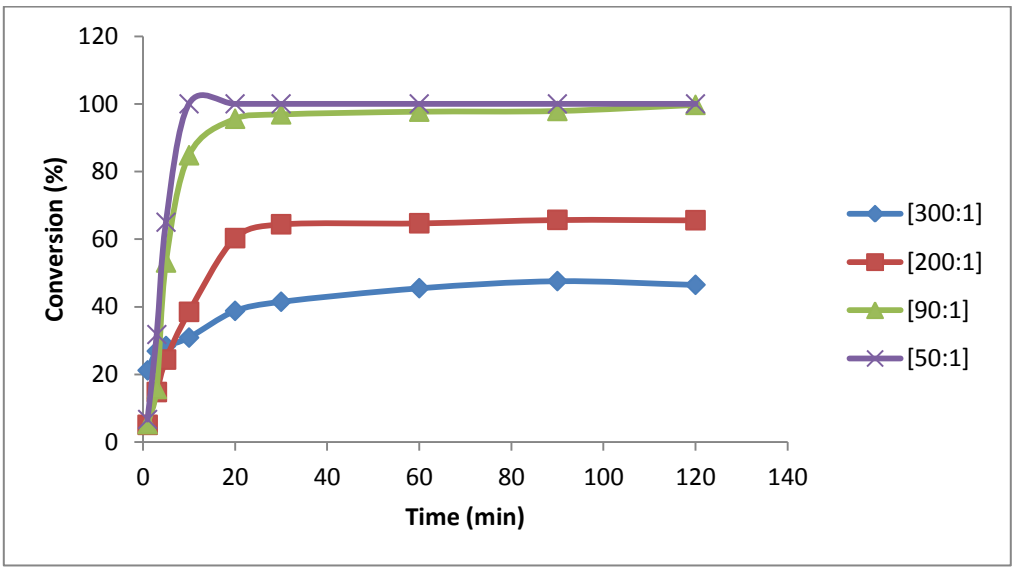

Fig. 4.12 Effect of [DBT]/[POM] ratio on DBT conversion ($H_3PW_{12}O_{40}$, 60 ^{o}C, toluene (10 mL), DBT (0.50 mmol, 1 wt%), aqueous 30% H_2O_2 (0.15 mL); molar ratios: BzPN/POM = 4:1, DBT/H_2O_2 = 1:3).

4.1.8 Effect of solvent

Different types of solvent were studied in the oxidation of DBT. The results are shown in Table 4.7. As can be seen, the oxidative activity in toluene was slightly better than in 1,2-dichloroethane, while in octane no reaction was observed. The conversion of DBT reached 100% in the desulfurization system with toluene and 1,2-DCE as shown in Fig. 4.13.

Table 4.7 Effect of solvent on oxidation of DBT by H_2O_2 in toluene-H_2O two-phase system in the presence of BzPN-bound POM catalysts.

POM	Solvent	Temp. (^oC)	Conv. (%)	H_2O_2 efficiency (%)
PW	Toluene	60	96.9	>99
PMo	Toluene	60	100	>99
PW	1,2-DCE	60	97.5	>99
PW	Octane	60	0	>99

Solvent (10 mL), DBT (0.50 mmol, 1 wt%), aqueous 30% H_2O_2 (0.15 mL); molar ratios: [BzPN]/[POM] = 4:1, DBT/H_2O_2 = 3:1, [POM]/[DBT] = 90:1, 0.5 h reaction time. DBT sulfone was the only reaction product observed.

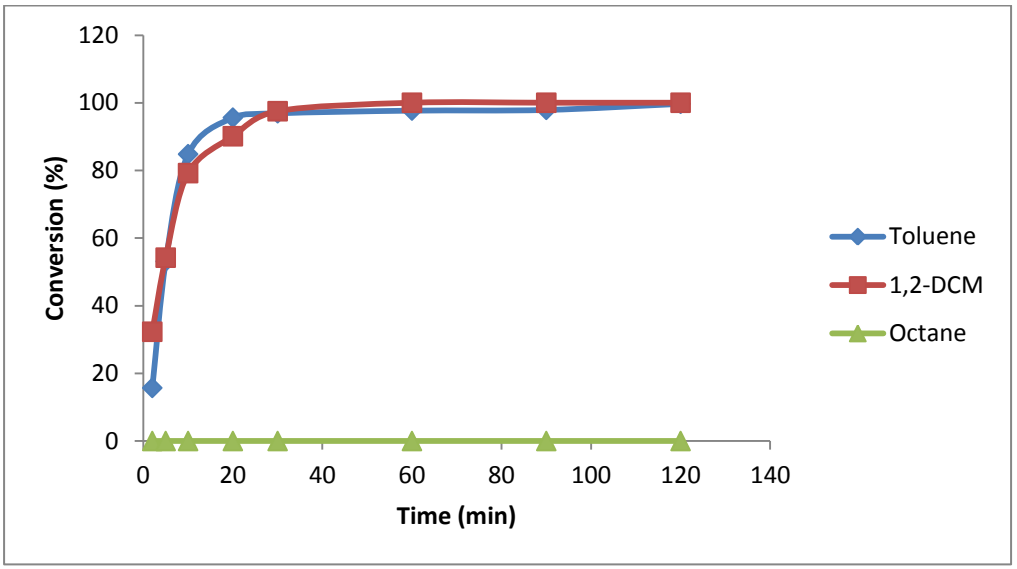

Fig. 4.13 Effect of solvent on DBT conversion ($H_3PW_{12}O_{40}$, 60 ^oC, solvent (10 mL), DBT (0.50 mmol, 1 wt%), aqueous 30% H_2O_2 (0.15 mL); molar ratios: BzPN/POM = 4:1, DBT/H_2O_2 = 1:3, POM/DBT = 90:1).

4.1.9 Effect of stirring speed

At sufficiently high stirring speeds the mechanical energy of stirring is a significant source of reaction rate increase. Additionally, stirring speed may increase the transfer of oxygen from the water phase to the organic phase by peroxo species by providing a larger interface between the two systems. As indicated in Fig. 4.14, there is a significant decrease in conversion from 77% to 27% after 30 min at 60 ^{o}C as the stirring speed is decreased from 500 rpm to 200 rpm.

Table 4.8 Effect of stirring speed on oxidation of DBT by H_2O_2 in toluene-H_2O two-phase system in the presence of BzPN-bound POM catalysts.

Stirring speed (rpm)	**DBT/H_2O_2 (mol/mol)**	**Temp. (^{o}C)**	**Conv. (%)**	**H_2O_2 efficiency (%)**
200	1:3	60	26.9	>99
400	1:3	60	48.1	>99
500	1:3	60	77.0	>99
700	1:3	60	90.8	>99
900	1:3	60	96.8	>99
1000	1:3	60	100	>99

Toluene (10 mL), DBT (0.50 mmol, 1 wt%), aqueous 30% H_2O_2 (0.15 mL); molar ratios: DBT/POM = 90:1, BzPN/POM = 4:1, 0.5 h reaction time. DBT sulfone was the only reaction product observed.

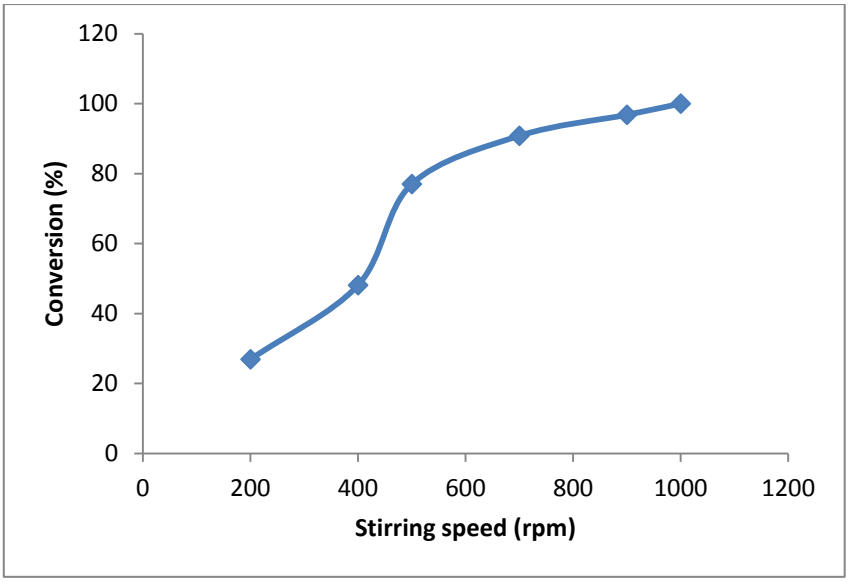

Fig. 4.14 Effect of stirring speed on DBT conversion (60 ^{o}C, toluene (10 mL), DBT (0.50 mmol, 1 wt%), aqueous 30% H_2O_2 (0.15 mL); molar ratios: BzPN/POM= 4:1, DBT/POM = 90:1, DBT/H_2O_2 = 1:3).

4.1.10 Effect of reaction procedure

The order in which the reaction is set up and reactants are added to the system is also an important factor that can affect the conversion. In reaction with hexylphosphazene and dihexylphosphazene using our first oxidation procedure with addition the POM last (Sect. 2.4.1.1), an induction period of 5-10 min was observed (Fig. 4.15 and Fig. 4.16). It was suggested that this was caused by relatively slow formation of active peroxo species. To overcome this problem, we applied another procedure allowing enough time for the peroxo species to form before reaction started. In the second procedure (Sect. 2.4.1.2) all the required components except the substrate were added to the reactor and stirred at reaction temperature for 5 min then the substrate was added to start the reaction off. As can be seen from Fig. 4.15 and 4.16, the second procedure completely eliminated induction period in these reactions.

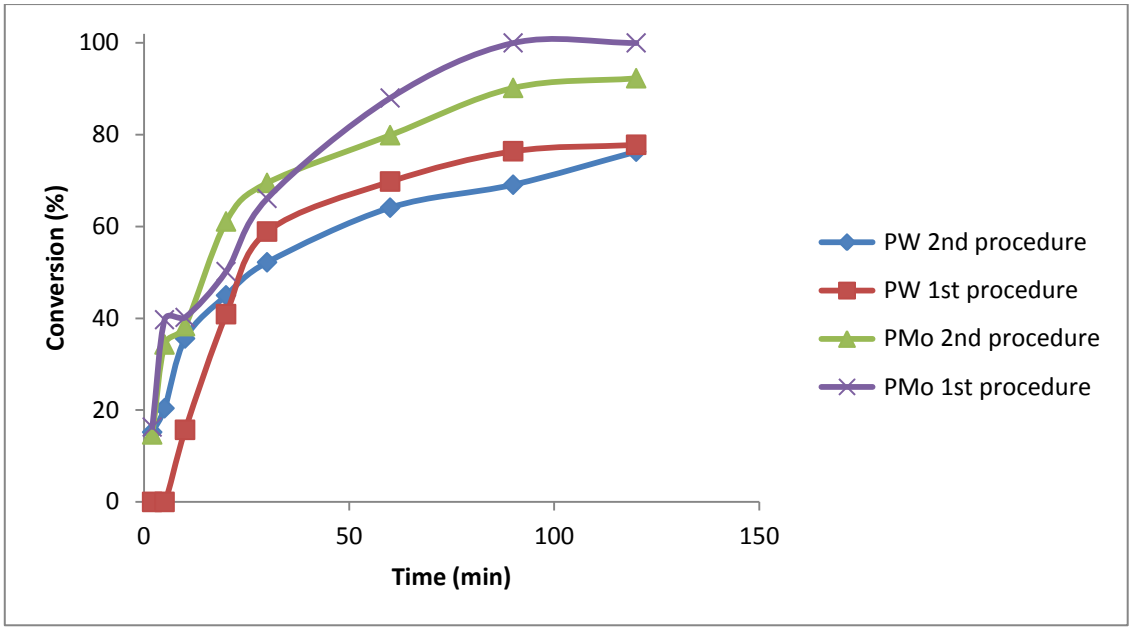

Fig. 4.15 Effect of reaction procedure on DBT conversion (40 ^{o}C, toluene (10 mL), DBT (0.50 mmol, 1 wt%), aqueous 30% H_2O_2 (0.15 mL); molar ratios: HexPN/POM = 4:1, DBT/PW = 90:1, DBT/H_2O_2 = 1:3).

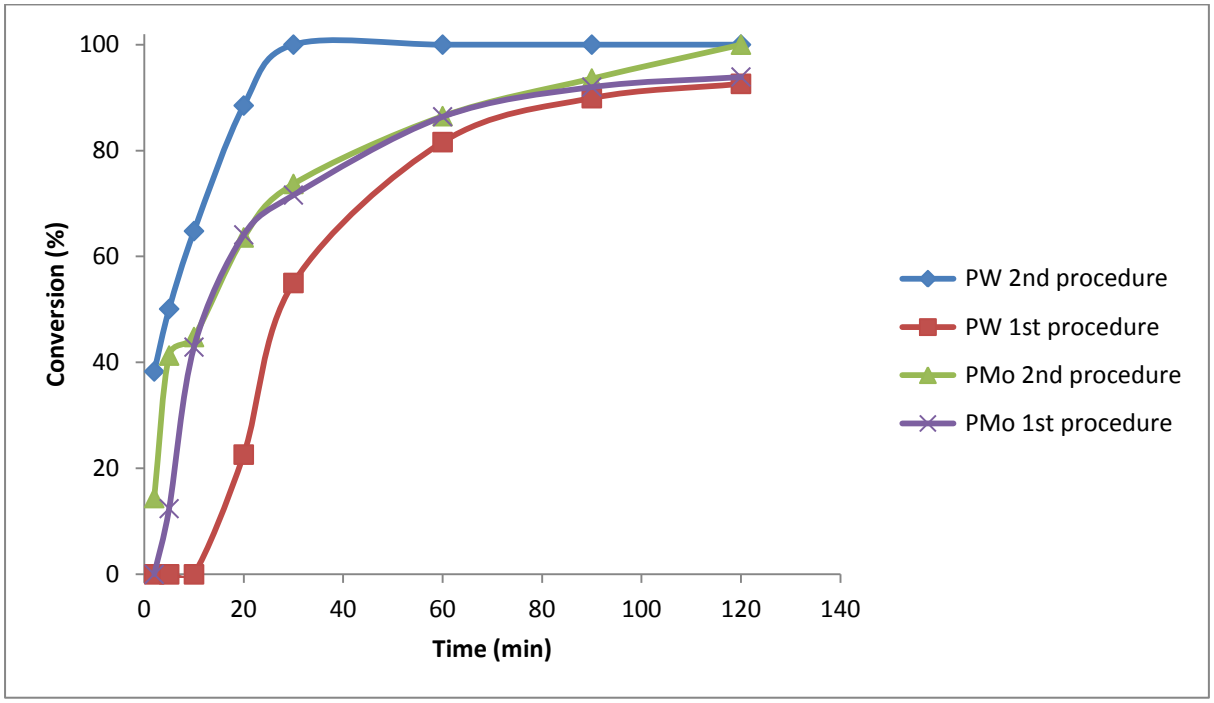

Fig. 4.16 Effect of reaction procedure on DBT conversion (40 ^{o}C, toluene (10 mL), DBT (0.50 mmol, 1 wt%), aqueous 30% H_2O_2 (0.15 mL); molar ratios: DiHexPN/POM = 4:1, DBT/PW = 90:1, DBT/H_2O_2 = 1:3).

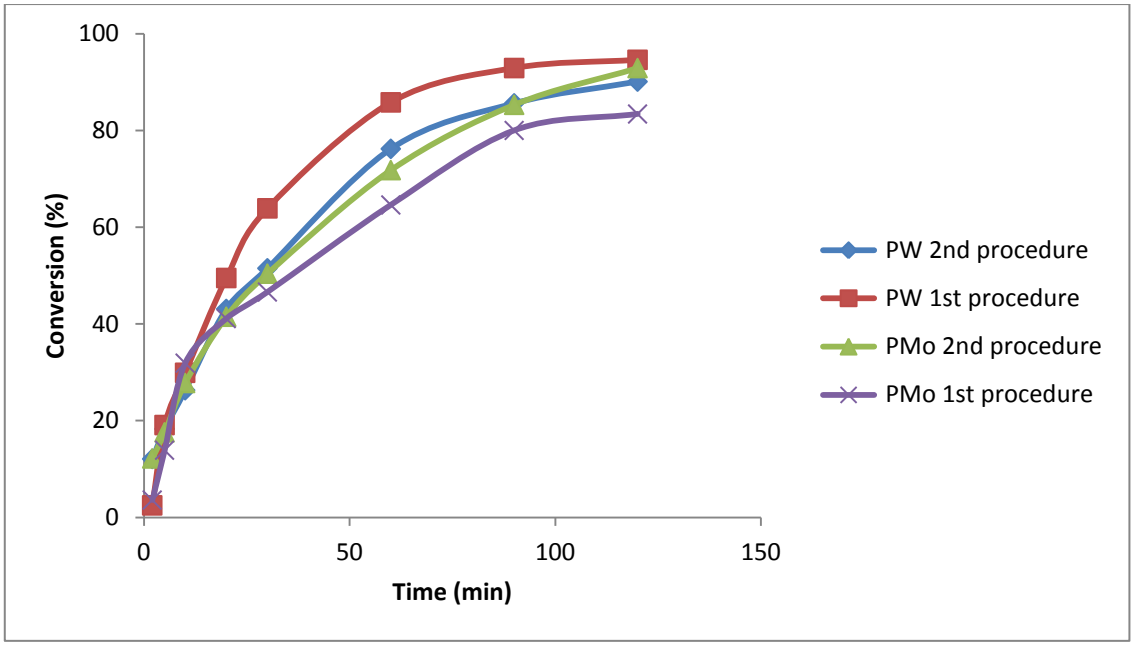

Fig. 4.17 Effect of reaction procedure on DBT conversion (25 ^{o}C, toluene (10 mL), DBT (0.50 mmol, 1 wt%), aqueous 30% H_2O_2 (0.15 mL); molar ratios: BzPN/POM = 4:1, DBT/POM = 90:1, DBT/H_2O_2 = 1:20).

The effect of the procedure was also evident in reaction with other RPN. DBT conversion after 2 min for PMo and PW in the presence of BzPN was 13% using the second procedure, while only 3% using the first procedure at same conditions, namely 25 ^{o}C, DBT/POM = 90:1, DBT/H_2O_2 = 1:20 and BzPN/POM = 4:1 (Fig. 4.17).

Using iBuPN instead of BzPN as a phase transfer agent, conversion reached around 25% with both PMo and PW after 2 min using the second procedure in comparison to the first procedure which only gave 17% conversion with both POMs after the same length of time (Fig. 4.18). The difference in conversion between the two procedures is believed to be a direct result of the 5 min stirring time used at the beginning of the second procedure. This stirring time allows active peroxo species to form before the reaction is started making more peroxo species available for DBT oxidation once the reaction has begun.

Using iPrPN as a phase transfer agent, no significant difference was seen in conversion between either of the procedures using either PMo or PW as the catalyst (Fig. 4.19). This implies that the efficiency of reactions with iPrPN as a phase transfer agent is not affected by the reaction procedure.

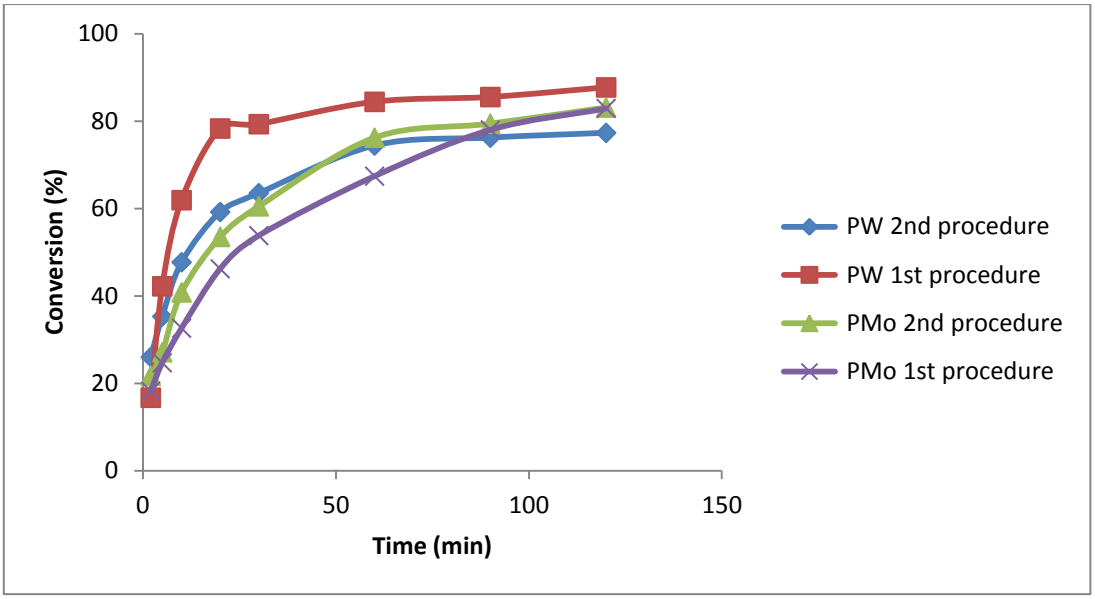

Fig. 4.18 Effect reaction procedure on DBT conversion (40 ^{o}C, toluene (10 mL), DBT (0.50 mmol, 1 wt%), aqueous 30% H_2O_2 (0.15 mL); molar ratios: iBuPN/POM = 4:1, DBT/POM = 90:1, DBT/H_2O_2 = 1:20).

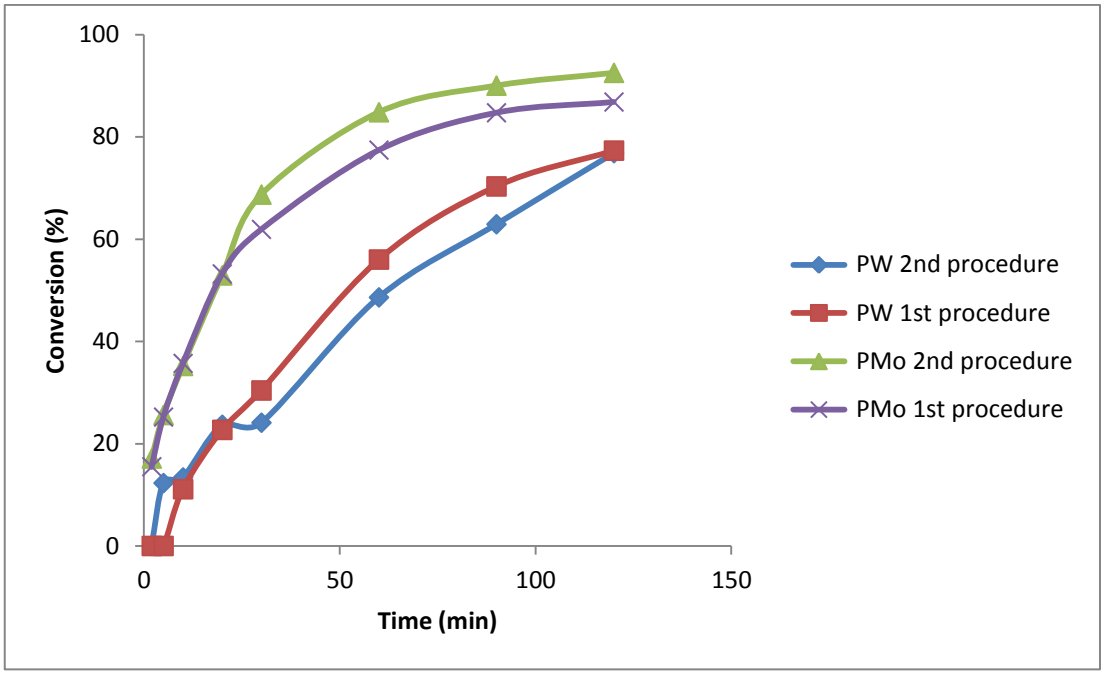

Fig. 4.19 Effect reaction procedure on DBT conversion (40 ^{o}C, toluene (10 mL), DBT (0.50 mmol, 1 wt%), aqueous 30% H_2O_2 (0.15 mL); molar ratios: iBuPN/POM = 4:1, DBT/POM = 90:1, DBT/H_2O_2 = 1:20).

4.2 Reaction order in DBT and apparent activation energy

With a 20-fold excess of H_2O_2 over DBT, the oxidation of DBT in the presence PW–BzPN was found to be first order in DBT. Fig. 4.20 shows the first-order plot for this reaction.

The reaction with PW and PMo had an apparent activation energy of 38.3 and 37.4 kJ/mol, respectively, in the temperature range of 25-60 ^{o}C. The Arrhenius plot for the reaction with PMo is shown in Fig. 4.21.

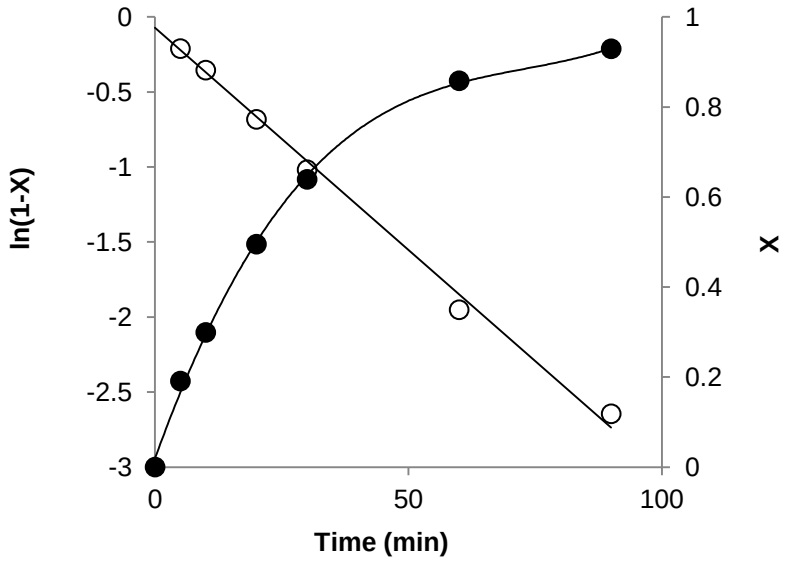

Fig. 4.20 Time course of oxidation of DBT by H_2O_2 in PhMe-H_2O two-phase system in the presence of PW–BzPN: DBT conversion (*X*, solid circles) and first-order plot –ln(1-*X*) = *kt* (open circles) (25 ^{o}C, 0.50 mmol DBT, [DBT]/[POM] = 90:1, [H_2O_2]/[DBT] = 20:1, [BzPN]/[POM] = 3.4:1).

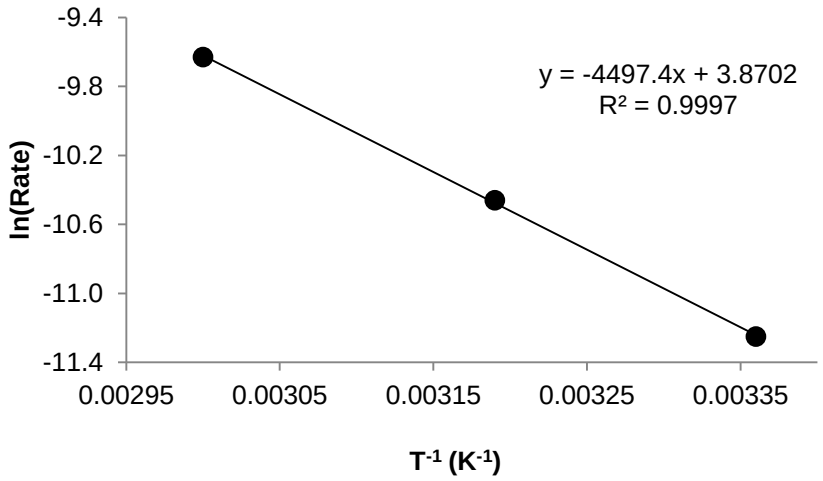

Fig. 4.21 Arrhenius plot of ln(Rate) (in mol/min) vs. inverse temperature for oxidation of DBT by H_2O_2 in PhMe-H_2O two-phase system in the presence of PMo–BzPN (25-60 ^oC, 0.50 mmol DBT, [DBT]/[POM]=90:1, [H_2O_2]/[DBT] = 3:1, [BzPN]/[POM] = 4:1).

4.3 Catalyst reuse

4.3.1 First catalyst reuse method

The following procedure was employed for the recovery of BzPN-POM catalyst in the oxidation of DBT. After the first reaction cycle had run to completion, new portions of DBT (0.50 mmol) and H_2O_2 (30%, 0.15 ml) were added to the reaction mixture to start a new cycle. Changes in catalytic activity are shown in Table. 4.9 and Fig. 4.22. Once the conversion had reached 89.8% (after 60 min), the third cycle was started. However, the DBT conversion decreased markedly to 0.7%, which meant that the catalyst was no longer active.

Table 4.9 Catalyst reuse in oxidation of DBT by H_2O_2 in toluene–H_2O two-phase system in the presence of PW–BzRN catalyst.

Run	**Time (min)**	**Conversion (%)**
1st	20	80.2
2nd	60	89.8
3rd	60	0.7

Toluene (10 mL), DBT (0.50 mmol, 1 wt%), aqueous 30% H_2O_2; molar ratios: [DBT]/[POM] = 90:1, [DBT]/[H_2O_2] = 1:3, [RPN]/ [POM] = 4:1; at 60 ^oC.

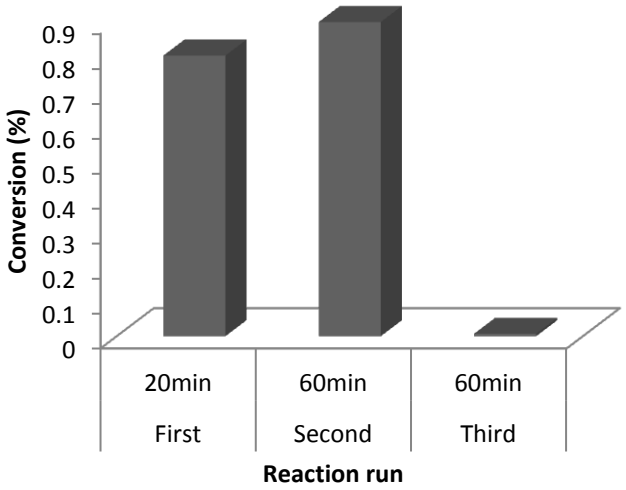

Fig. 4.22 Catalyst reuse in oxidation of DBT by H_2O_2 in toluene–H_2O two-phase system in the presence of PW–BzRN catalyst.

PMo exhibited a longer life time and higher conversion at 60 ^oC compared to PW. Table 4.10 and Fig. 4.23 show that, under the same conditions, DBT conversion was 91.5% while with PW it was only 0.7% after 60 min in the third run. In fact, it was found that PMo can be used up to five times with a major decrease in activity at 60 ^oC.

Table 4.10 Catalyst reuse in oxidation of DBT by H_2O_2 in toluene–H_2O two-phase system in the presence of PMo–BzRN catalyst.

Run	**Time** (min)	**Conversion %**
1st	20	88.5
2nd	40	100
3rd	40	91.5
4th	40	79.6
5th	40	59.5

Toluene (10 mL), DBT (0.50 mmol, 1 wt%), aqueous 30% H_2O_2; molar ratios: [DBT]/[POM] = 90:1, [DBT]/[H_2O_2] = 1:3, [RPN]/ [POM] = 4:1; at 60 ^oC.

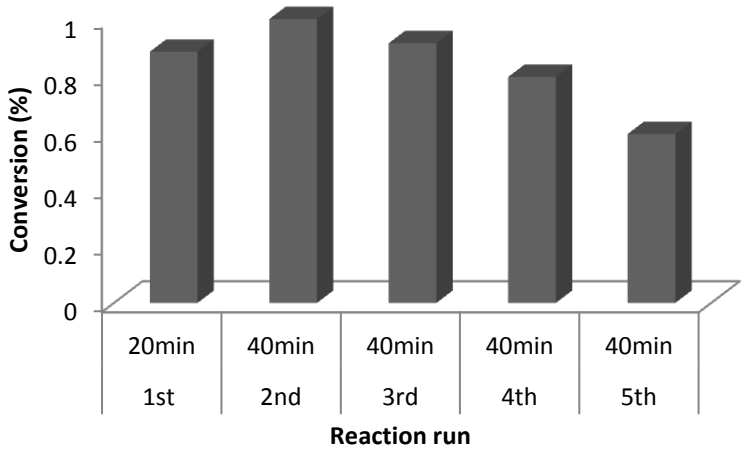

Fig. 4.23 Catalyst reuse in oxidation of DBT by H_2O_2 in toluene–H_2O two-phase system in the presence of PMo–BzRN catalyst at 60 ^oC.

4.3.2 Second catalyst reuse method

In the second method for the reuse of POM-BzPN catalysts, once the first cycle was complete toluene was evaporated off using pump evaporator and a new portion of toluene, internal standard, DBT (0.5 mmol) and H_2O_2 (30%, 0.15 ml) were added to the reaction mixture and new cycle was run. Changes in catalytic activity are shown in Table 4.11 and Fig. 4.24. This procedure allowed for satisfactory catalyst reuse, with a slow decline in activity which was probably due to catalyst degredation.

Table 4.11 Catalyst reuse in oxidation of DBT by H_2O_2 in toluene–H_2O two-phase system in the presence of PMo–BzRN catalyst**.**

Run	**Time** (min)	**Conversion (%)**
1^{st}	60	100
2^{nd}	80	86.0
3^{rd}	90	84.6
4^{th}	90	72.7

Toluene (10 mL), DBT (0.50 mmol, 1 wt%), aqueous 30% H_2O_2; molar ratios: [DBT]/[POM] = 90:1, [DBT]/[H_2O_2] = 1:3, [RPN]/ [POM] = 4:1; at 60 ^oC.

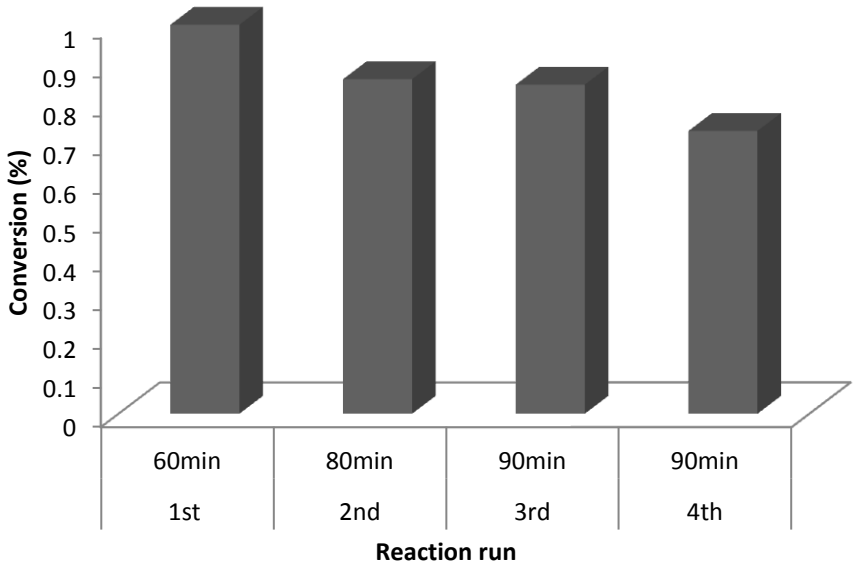

Fig. 4.24 Catalyst reuse in oxidation of DBT by H_2O_2 in toluene–H_2O two-phase system in the presence of PMo–BzRN catalysts at 40 ^oC.

4.4 Reaction mechanism

A plausible mechanism for the biphasic oxidation of DBT can be proposed as shown in Fig. 4.25. An active peroxo polyoxometalate is formed in aqueous phase by interacting the Keggin heteropoly anion with hydrogen peroxide [33]. With the phase transfer agent, RPN, the peroxo polyoxometlate is almost fully transferred into organic phase because RPN is soluble in organic solvent [33]. The reaction takes place in the organic phase via the oxygen atom transfer from peroxo polyoxometalate to the sulfur-organic substrate [33]. Then, the peroxo polyoxometalate is regenerated at the interface by interaction with H_2O_2.

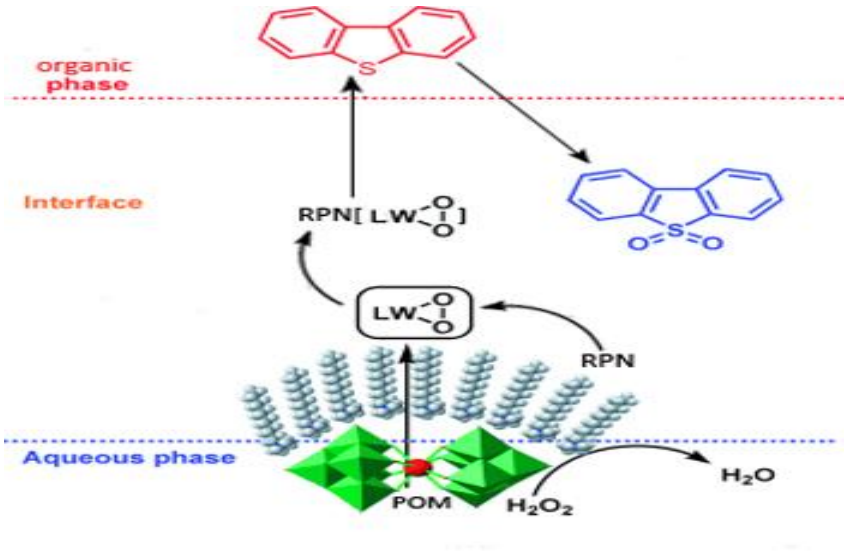

Fig. 4.25 Mechanism for the biphasic oxidation of DBT in the presence of RPN-POM catalyst.

4.5 Conclusion

In conclusion, we have demonstrated that novel POM–phosphazene salt aggregates possess high efficiency as amphiphilic catalysts for environmentally benign oxidations with H_2O_2 in biphasic systems. These catalysts self-assemble in situ simply by mixing commercial Keggin POMs and readily available phosphazenes. The phosphazene ligands provide large arrays of hydrogen bonding sites enabling the effective encapsulation of polyanions.

References

1. Y. Hu, Q. He, Z. Zhang, N. Ding, B. Hu, Chem. Commun. **47** (2011) 12194.
2. I. Babich, J. Moulijn, Fuel **82** (2003) 607.
3. D. Huang, Y. Wang, L. Yang, G. Luo, Ind. Eng. Chem. Res. **45** (2006) 1880.
4. H. Mei, B. Mei, T. Yen, Fuel **82** (2003) 405.
5. A. Hernandez, F. Yang, G. Qi, R. Yang, Appl. Catal. B **56** (2005) 111.
6. X. Ma, S. Velu, J. Kim, C. Song, Appl. Catal. B **56** (2005) 137.
7. L. Verduzco, E. Garcia, R. Quintana, V. Pena, F. Guevara, Catal. Today **98**, 2004, 289.
8. C. Song, X. Ma, Appl. Catal. B **41** (2003) 207.
9. W. Trakarnpruk, K. Rujiraworawut, Fuel **90** (2009) 411.
10. O. Bortolini, S. Campestrini, F. Furia, G. Modena, J. Org. Chem. **52** (1987) 5093.
11. P. Moreau, V. Hulea, S. Gomez, D. Brunel, F. Di Renzo, Appl. Catal. A **155** (1997) 253.
12. D. Wang, E. W. Qian, H. Amano, K. Okata, A. Ishihara, T. Kabe, Appl. Catal. A **253** (2003) 91.
13. S. Murata, K. Murata, K. Kidena, M. Nomura, Energ. Fuels **18** (2004) 116.
14. A. Anisov, E. Fedorova, A. Lesnugin, V. Senyavin, L. Aslanov, V. Rybakov, A. Tarakonova, Catal. Today **78** (2003) 319.
15. L. Caero, E. Hernandez, F. Pedraza, F. Murrieta, Catal. Today **107** (2005) 564.
16. F. Collins, A. Lucy, C. Sharp, J. Mol. Catal. A: Chem. **117** (1997) 397.
17. D.E. Katsoulis, Chem. Rev. **98** (1998) 359.
18. M. Te, C. Fairbridge, Z. Ring, Appl. Catal. A **219 (**2001) 267.
19. H. Lu, J. Gao, Z. Jiang, F. Jing, Y. Yang, G. Wang, C. Li, J. Catal. **239** (2006) 369.
20. C. Komintarachat, W. Trakarnpruk, Chem. Res. **45** (2006) 1853.
21. F. Zannikos, E. Lois, S. Stournas, Fuel Proc. Technol. **42** (1995) 35.
22. M. Craven, R. Yahya, E. Kozhevnikova, R. Boomishankar, C. Robertson, A.Steiner, I. Kozhevnikov, Chem. Commun. **49** (2013) 349.
23. Polyphosphazenes: A World Insight, ed. M. Gleria, R. Dejaeger, Nova Science Publishers, New York, 2004.
24. H. R. Allcock, Chem. Rev. **72** (1972) 315.

25. J. F. Bickley, R. Bonar-Law, G. T. Lawson, P. I. Richards, F. Rivals, A. Steiner, S. Zacchini, Dalton Trans. (2003) 1235.
26. H. R. Allcock, T. J. Fuller, K. Matsumura, Inorg. Chem. **21** (1982) 515.
27. A. Steiner, in Polyphosphazenes for Biomedical Applications, ed. A. K. Adrianov, Wiley, New Jersey, 2009.
28. H. R. Allcock, E. C. Bissell, E. T. Shawl, Inorg. Chem. **12** (1973) 2963.
29. Z. Jiang, H. Lu, Y. Zhang and C. Li, Chin. J. Catal. **32** (2011) 707.
30. B. Y. Zhang, Z. X. Jiang, J. Li, Y. N. Zhang, F. Lin, Y. Liu, C. Li, J. Catal. **287** (2012) 5.
31. H. S. Gao, C. Guo, J. M. Xing, H. Z. Liu, Sep. Sci. Technol. **47** (2012) 325.
32. J. H. Xu, S. Zhao, W. Chen, M. Wang, Y. F. Song, Chem. Eur. J. **18** (2012) 4775.
33. Y. Dong, Y. Nie, Q. Zhou, Chem. Eng. Technol. **36** (2013) 435
34. I. V. Kozhevnikov, Catalysis by Polyoxometalates, Wiley, Chichester, 2002.

Chapter 5. Polyisobutylene oligomer-bound polyoxometalates as catalysts for oxidative desulfurization

Polyisobutylene (PIB) oligomer-bound amines render Keggin polyoxometalates (POM) heptane soluble, making them efficient and recyclable catalysts for environmentally benign biphasic oxidations with hydrogen peroxide. This is illustrated using it on oxidative desulfurization reaction that can be efficiently carried out in a heptane-water two-phase system occurring through facile phase transfer of POM by the amine terminated PIB oligomer [14].

Polyoxometalates (POMs), comprising O-sharing MOx polyhedral (most often M = Mo^{VI} and W^{VI}), have found applications in various disciplines, of which catalysis is by far the most important [1-7]. This includes large-scale industrial processes such as the oxidation of methacrolein to methacrylic acid, the hydration of alkenes to alcohols and the synthesis of ethyl acetate by direct addition of acetic acid to ethylene [3].

It has been extensively documented that POMs, especially those comprising Keggin type polyanions $[XM_{12}O_{40}]^{m-}$ {X = P^{V} (m = 3) and Si^{IV} (m = 4)}, serve as precursors of highly efficient catalysts for environmentally benign biphasic oxidations with hydrogen peroxide. We look at reactions of significant practical importance oxidative desulfurization [8-10]. It is catalyzed by POMs in homogeneous or two-phase systems and is the subject of much current interest. There is compelling evidence that Keggin polyanions are transformed by excess H_2O_2 in solution to form peroxo polyoxometalate species, e.g. $\{PO_4[WO(O_2)_2]_4\}^{3-}$, which have been suggested to be the active intermediates in oxidations with H_2O_2 [11-13]. Biphasic oxidations in a water–organic system are particularly attractive, as such systems facilitate product/catalyst separation. These reactions typically involve phase transfer catalysis with peroxo polyanion transport through the water-organic interface and require an efficient agent to move the peroxo polyanions from the aqueous phase into the organic phase.

Commonly, POM aggregates containing quaternary ammonium cations with C_8–C_{18} alkyl groups as phase-transfer agents are used to facilitate organic phase solubility of the POM oxidant. Recently, we have reported cyclophosphazenes are also effective peroxo POM carriers between the phases [14]. However, while we and others have had some success, more efficient biphasic oxidation processes using the POM/H_2O_2 system could address specific challenges which include improving catalyst activity and recyclability in alkane-water two-phase systems. This is particularly important for reactions such as the POM-catalyzed oxidative desulfurization with aqueous hydrogen peroxide as the "green" oxidant, which has been developed as a promising method for deep desulfurization of transportation fuel [10]. Here we show that the activity and recyclability of POM catalyst in such reactions may be improved by using functionalized alkene oligomers with much longer-chain alkyl groups as organic solvent supports as compared to the conventional phase-transfer agents.

Terminally functionalized polyisobutylene (PIB) derivatives readily soluble in nonpolar solvents like heptane have been demonstrated to have the potential to improve the recovery and recycling of homogeneous catalysts [15-21]. These derivatives can be synthesized by functionalization of vinyl terminated PIB oligomers with a molecular weight, *Mn*, of 1000-2300 Da, which are commercially available [22,23]. We now report on the use of amine terminated PIB oligomer as a highly efficient hydrocarbon solubilizing agent for Keggin POM catalysts in oxidative desulfurization and alkene epoxidation with hydrogen peroxide in a heptane-water two-phase system.

5.1 Biphasic oxidation of dibenzothiophene with hydrogen peroxide catalysed by polyisobutylene oligomer-bound polyoxometalates

Oxidation of dibenzothiophene (DBT) could be carried out in a two-phase system containing heptane as an organic solvent and aqueous H_2O_2 at 25-60 ^oC in a 50-mL glass reactor equipped with a magnetic stirrer, a reflux condenser and a heat circulator (see chap 2).

The reactions were monitored by taking aliquots from the organic phase and submitting them to GC analysis to determine substrate conversion and product yield. After reaction, the amount of remaining H_2O_2 was determined by titration with $KMnO_4$ for the efficiency of

hydrogen peroxide use to be estimated. Diethylamine terminated PIB_{1000} (PIB_{1000}-$CH_2N(CH_2CH_3)_2$) and its quaternary salt (PIB_{1000}-$CH_2N(CH_2CH_3)_2CH_3^+I^-$) were synthesized from commercially available PIB_{1000} by a sequence using ozonolysis, a haloform reaction, amidation, reduction, and alkylation with CH_3I (Chap 1) [9].

The oxidation of DBT (Eqn. 5.1) is typically employed as a model reaction for catalyst testing in oxidative desulfurization [8-10]. We found that PIB oligomer-bound Keggin POMs are highly active and easily recyclable catalysts for DBT oxidation with H_2O_2 in a heptane-water biphasic system, yielding DBT sulfone as the sole product. The two catalyst components can simply be added separately to the reaction mixture to form the active catalyst *in situ* (Eqn. 5.2-5.3). The PIB amine support was introduced as a 0.5 M heptane solution of diethylamine terminated PIB. The POM was an off-the-shelf heteropoly acid hydrate $H_3PW_{12}O_{40}$, $H_3PMo_{12}O_{40}$ or $H_4SiW_{12}O_{40}$, containing roughly 20 H_2O molecules per Keggin unit, here after abbreviated as PW, PMo and SiW.

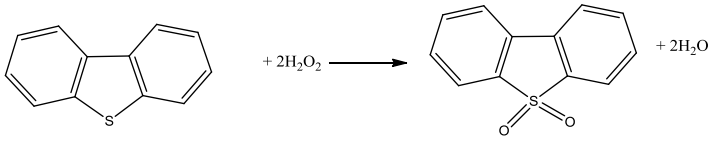

(5.1)

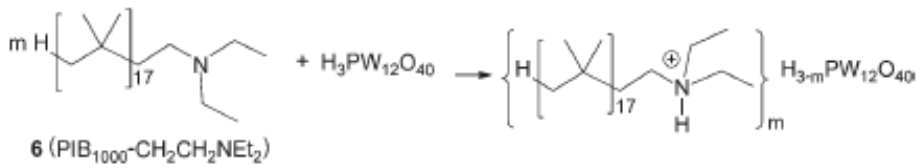

6 (PIB_{1000}-$CH_2CH_2NEt_2$)

(5.2)

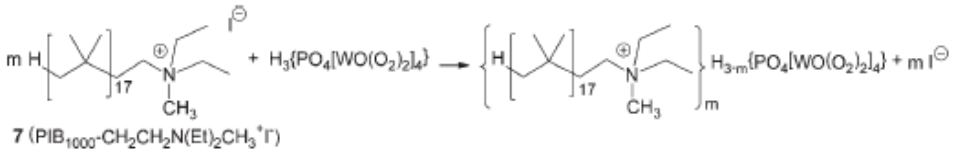

7 (PIB_{1000}-$CH_2CH_2N(Et)_2CH_3^+I^-$)

(5.3)

Representative results for DBT oxidations at 25-60 ^oC are shown in Fig. 5.1. As expected, the catalyst activity increased with the PIB/POM molar ratio (fig. 5.2), levelling off at a ratio of 4:1 – 6:1 (entries 1- 4). What is remarkable though, and different from the conventional C_8-

C_{18} quaternary ammonium surfactants, is that the catalyst was quite active already at a 1:1 PIB/POM molar ratio, giving 70% DBT conversion in 0.5 h (entry 1) and 100% in 1 h. This can be explained by the higher phase-transfer efficiency of the PIB surfactant due to its much longer hydrocarbon chain involving ca. 70 carbon atoms in total. Amongst the POMs tested, PW exhibited the highest activity followed by PMo (entries 3, 7). With PW, the conversion of DBT reached 100% in 0.5 h at 60 ^{o}C and a PIB/PW molar ratio of 6:1. In contrast, SiW showed no activity at all within 0.5 h reaction time, with a slow conversion rate after 1 h induction period (Fig. 5.1). This is in agreement with the well-known stability of SiW to degradation in solution and its resistance to form peroxo species [3]. It is important to note that practically no decomposition of H_2O_2 to molecular oxygen took place in the PIB–POM reaction system, giving >99% efficiency of H_2O_2 utilization.

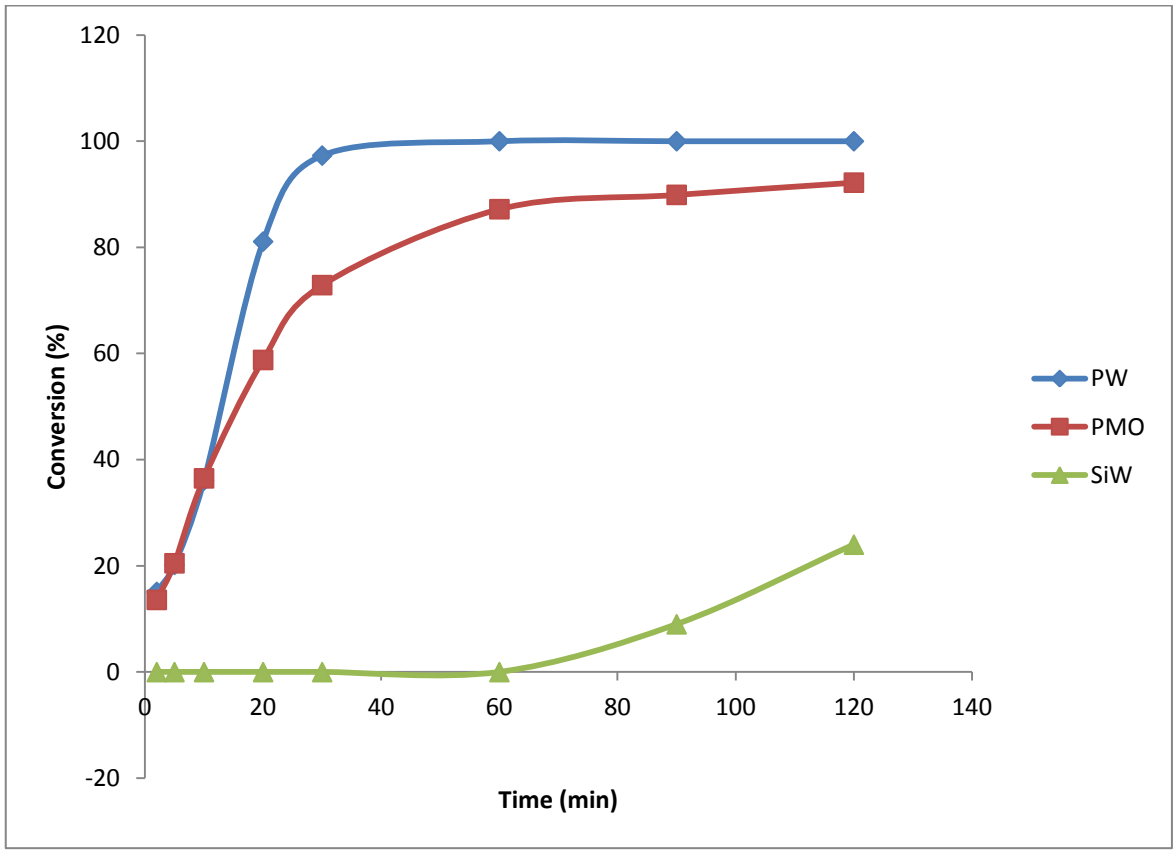

Fig. 5.1 Effect of POM on DBT conversion (60 °C, heptane (10 mL), DBT (0.50 mmol, 1 wt%), aqueous 30% H_2O_2 (0.15 mL); molar ratios: PIB/POM = 4 : 1, DBT/POM = 90 : 1, DBT/H_2O_2 = 1 : 3).

Table 5.1 Oxidation of DBT by H_2O_2 in Heptane–H_2O two-phase system in the presence of POM–PIB catalysts[a].

Entry	**POM**	**PIB/POM (mol mol^{-1})**	**Temp. (°C)**	**Conv. (%)**	**H_2O_2 efficiency (%)**
1	PW	1:1	60	70	>99
2	PW	2:1	60	96	>99
3	PW	4:1	60	97	>99
4	PW	6:1	60	100	>99
5	PW	4:1	40	49	>99
6	PW	4:1	25	30	>99
7	PMo	4:1	60	73	>99
8	SiW	4:1	60	0	>99

[a] Heptane (10 mL), DBT (0.50 mmol, 1 wt%), aqueous 30% H_2O_2 (0.15 ml); molar ratios: [DBT]/[POM] = 90 : 1, [DBT]/[H_2O_2] = 1 : 3, [PIB]/[POM] = 4 : 1; 30 min time. DBT sulfone was the only reaction product.

In addition to diethylamine terminated PIB oligomer, PIB_{1000}–$CH_2CH_2NEt_2$ we also tested the corresponding quaternary salt PIB_{1000}–$CH_2CH_2N(Me)Et_2^+I^-$. The latter was found to be less efficient compared to PIB_{1000}–$CH_2CH_2NEt_2$ producing only 30% DBT conversion at 60 °C with a PIB/PW ratio of 4 : 1 in 0.5 h. This is not unexpected if the ion exchange in Eqn (5.3) is less favourable than the acid base reaction in Eqn (5.2).

It should be pointed out that DBT sulfone is insoluble in heptane and precipitated during the reaction as a white powder. It can be quantitatively extracted from heptane– water mixture, together with water, by acetonitrile or dimethylformamide, which are immiscible with heptanes [9,10]. On the other hand, the PIB–POM catalyst is essentially insoluble in these solvents, which allowed for easy catalyst recycling.

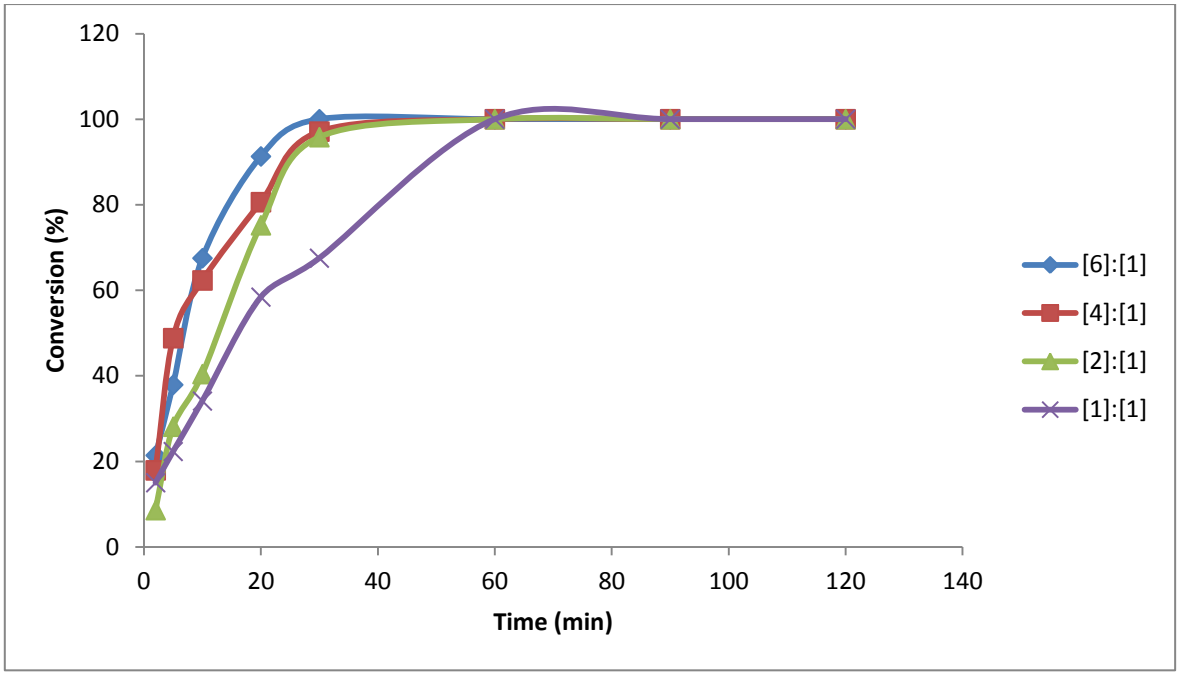

Fig. 5.2 Effect of [PIB]/[POM] conversion ($H_3PW_{12}O_{40}$, 60 °C, heptane (10 mL), DBT (0.50 mmol, 1 wt%), aqueous 30% H_2O_2 (0.15 mL); molar ratios: DBT/POM = 90 : 1, DBT/H_2O_2 = 1 : 3).

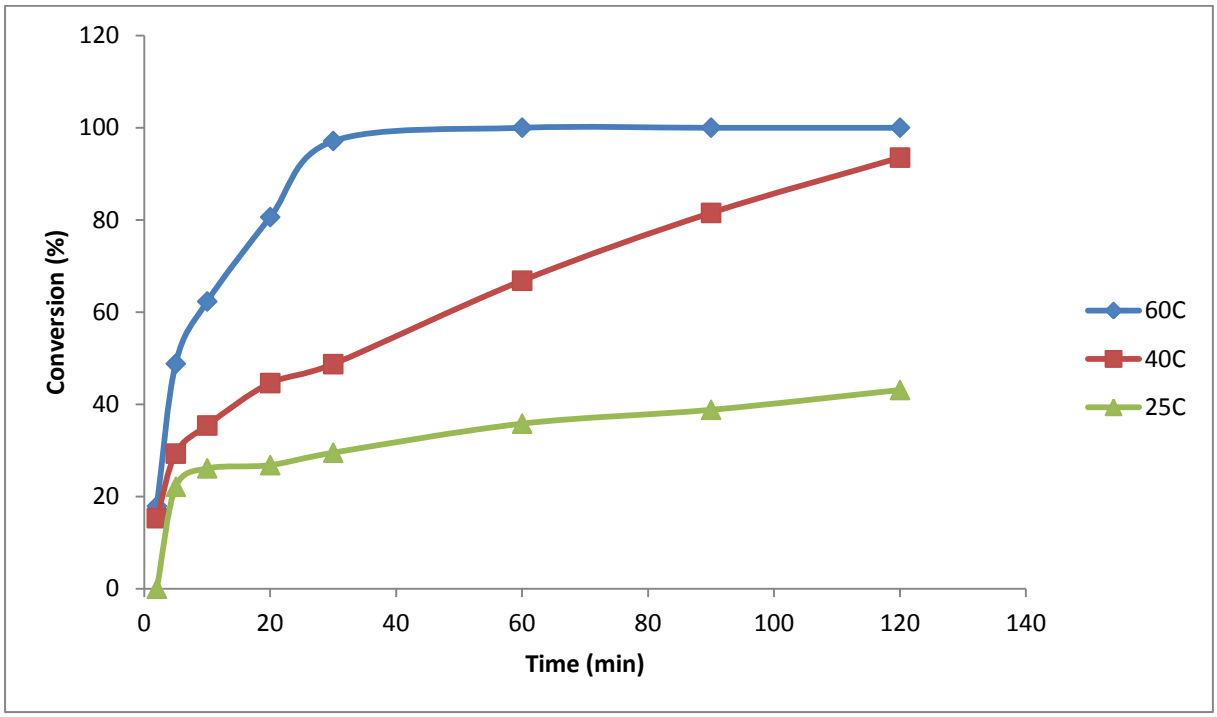

Fig. 5.3 Effect temperature on DBT conversion ($H_3PW_{12}O_{40}$, 60 °C, heptane (10 mL), DBT (0.50 mmol, 1 wt%), aqueous 30% H_2O_2 (0.15 mL); molar ratios: PIB/POM = 4 : 1, DBT/POM = 90 : 1, DBT/H_2O_2 = 1 : 3).

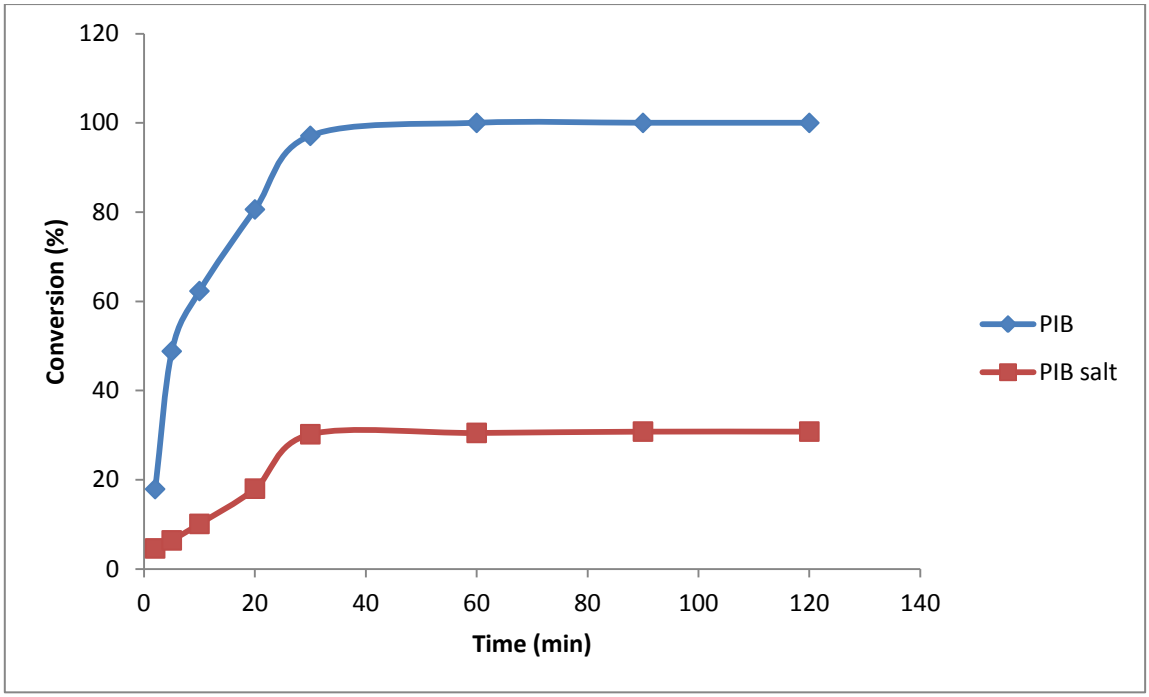

Fig. 5.4 Effect nature of PIB on DBT conversion ($H_3PW_{12}O_{40}$, 60 °C, heptane (10 mL), DBT (0.50 mmol, 1 wt%), aqueous 30% H_2O_2 (0.15 mL); molar ratios: PIB/POM = 4 : 1, DBT/POM = 90 : 1, DBT/H_2O_2 = 1 : 3).

5.2 Catalyst reuse

The phase behaviour and catalyst recycling using extraction with acetonitrile is illustrated in Fig. 5.5. Excellent recyclability of the PIB–PW catalyst is demonstrated in Fig. 5.6. The catalyst was recovered and reused five times without any loss of activity.

The catalytic performance of PIB–POM compares well with the best results reported so far. Jiang et al. [9]. Used amphiphilic decatungstate $[(CH_3)_3NC_{16}H_{33}]_4W_{10}O_{32}$ as the catalyst under similar conditions and observed similar DBT conversions (99.6%), but without giving the H_2O_2 efficiency. Similar results have also been reported for the $[(C_{18}H_{37})_2N(CH_3)_2]_3[PW_{12}O_{40}]$ catalyst [10]. These catalysts, however, have to be pre-synthesized via quite a laborious procedure, which is not required for the PIB–POM system [9].

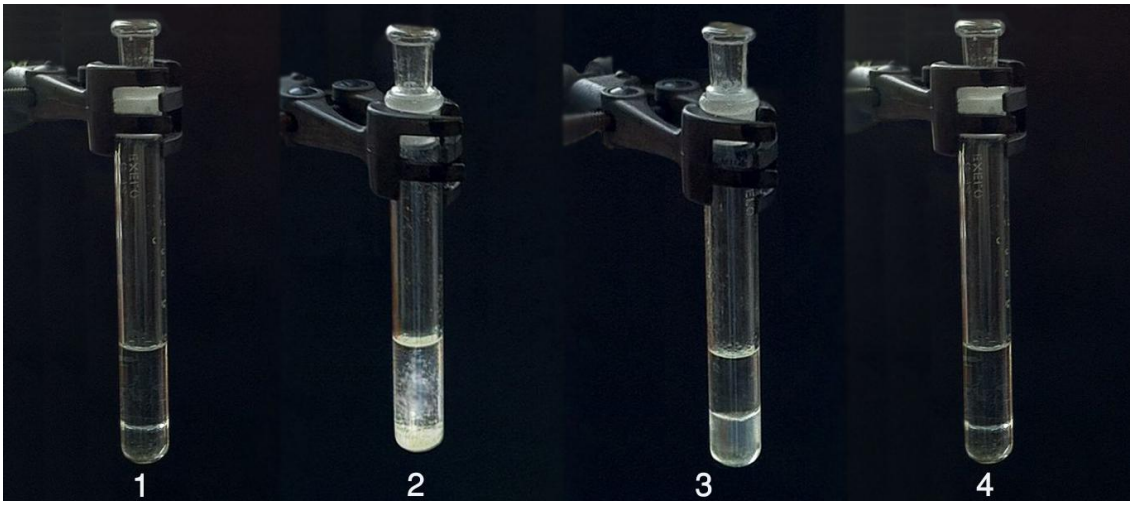

Fig. 5.5 Catalyst recycling and phase behaviour in DBT oxidation in heptane–water two-phase system catalysed by PIB–PW (for better presentation, the amount of aqueous phase was increased five-fold): (1) initial reaction system with heptane phase (top) and aqueous H_2O_2 phase (bottom); (2) the system after the first reaction run was complete, showing DBT sulfone (white precipitate); (3) the system after second extraction with acetonitrile – heptane phase (top) and acetonitrile phase (bottom); (4) the system ready for second run with fresh amounts of DBT and aqueous H_2O_2 added.

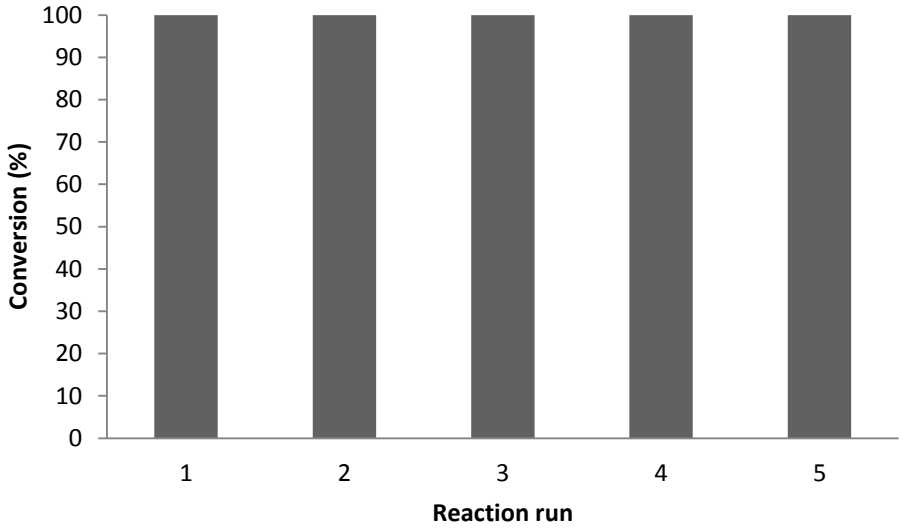

Fig. 5.6 Catalyst reuse in DBT oxidation (PIB–PW catalyst, 60 °C, 0.5 h, heptane (10 mL), DBT (0.50 mmol, 1 wt%), aqueous 30% H_2O_2 (0.15 mL); molar ratios: PIB/PW = 4 : 1, DBT/POM = 90 : 1, DBT/H_2O_2 = 1 : 3). After each run, DBT sulfone was extracted by MeCN and fresh DBT and 30% H_2O_2 were added.

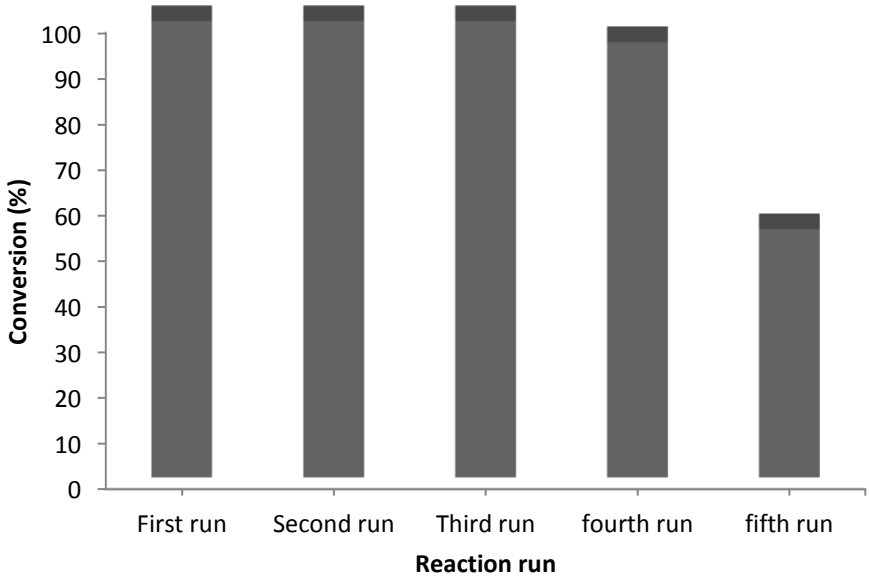

Fig. 5.7 Catalyst reuse in DBT oxidation (PIB–PW catalyst, 60 °C, 20 min, heptane (10 mL), DBT (0.50 mmol, 1 wt%), aqueous 30% H_2O_2 (0.15 mL); molar ratios: PIB/PW = 4 : 1, DBT/POM = 90 : 1, DBT/H_2O_2 = 1 : 3). After each run, DBT sulfone was extracted by MeCN and fresh DBT and 30% H_2O_2 were added.

Fig. 5.7 shows catalysts reuse in DBT oxidation for a shorter reaction time of 20 min (cf. Fig. 5.6 with the reaction time of 30 min). Full catalyst reuse was observed in first three runs, with activity decline in the following forth and fifth runs. This may be explained by partial catalyst degradation.

Finally, it is interesting to compare the performance of PIB and RPN in the POM-catalysed oxidation of DBT in two-phase system. Fig. 5.8 shows some representative results. As can be seen, these two catalyst systems are quite similar as regards their activity. However, the PIB-POM catalyst has the advantage of better catalyst recovery and reuse in comparison to the RPN-POM catalyst.

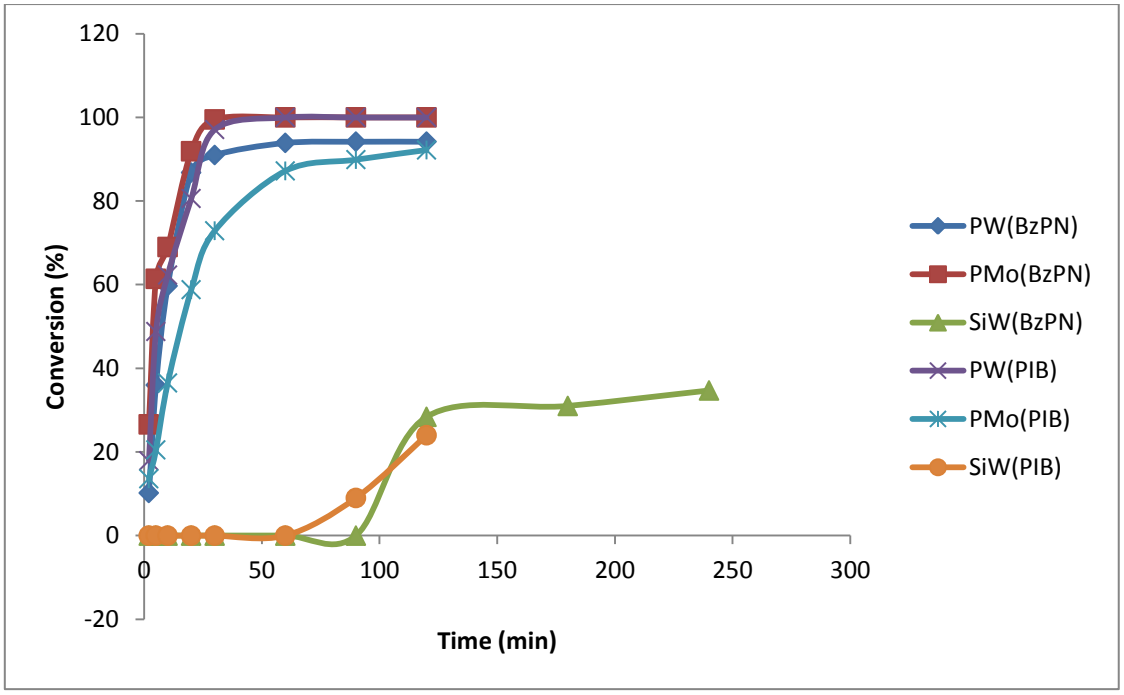

Fig. 5.8 Effect of PIB and BzPN on DBT conversion (60 °C, heptane (10 mL), DBT (0.50 mmol, 1 wt%), aqueous 30% H_2O_2 (0.15 mL); molar ratios: PIB/POM = 4 : 1, BzPN/POM = 4 : 1, DBT/POM = 90 : 1, DBT/H_2O_2 = 1 : 3).

5.3 Conclusion

In conclusion, we have demonstrated that the PIB oligomerbound Keggin polyoxometalates are efficient and recyclable catalysts for environmentally benign biphasic oxidations with hydrogen peroxide, including the oxidation of DBT to DBT sulfone, in a heptane–water two phase system. These catalysts self-assemble in situ by mixing commercial Keggin POMs and amine terminated PIB oligomer. The oxidation reactions occur through facile phase transfer of peroxo POM intermediates into the heptane phase facilitated by the amine terminated heptane phase selectively soluble PIB oligomer.

References

1. M. T. Pope, Heteropoly and Isopoly Oxometalates, Springer, Berlin, 1983.
2. C. L. Hill, C. M. Prosser-McCartha, Coord. Chem. Rev. **143** (1995) 407.
3. I. V. Kozhevnikov, Catalysis by Polyoxometalates, Wiley, Chichester, 2002.
4. T. Okuhara, N. Mizuno, M. Misono, Adv. Catal. **41** (1996) 113.
5. R. Neumann, Prog. Inorg. Chem. **47** (1998) 317.
6. Special issue on polyoxometalates. C. L. Hill, Chem. Rev. **98** (1998) 1.
7. I. V. Kozhevnikov, J. Mol. Catal. A: Chem. **305** (2009) 104.
8. F. M. Collins, A. R. Lucy, C. Sharp, J. Mol. Catal. A: Chem. 117 (1997) 397.
9. X. Jiang, H. Li, W. Zhu, L. He, H. Shu, J. Lu, Fuel **88** (2009) 431.
10. Z. Jiang, H. Lü, Y. Zhang and C. Li, Chin. J. Catal. **32** (2011) 707.
11. C. Venturello, E. Alneri, M. Ricci, J. Org. Chem. **48** (1983) 3831.
12. Y. Ishii, K. Yamawaki, T. Ura, H. Yamada, T. Yoshida, M. Ogawa, J. Org. Chem. **53** (1988) 3587.
13. K. Kamata, K. Yonehara, Y. Sumida, K. Yamaguchi, S. Hikichi and N. Mizuno, Science **300** (2003) 964.
14. M. Craven, R. Yahya, E. Kozhevnikova, R. Boomishankar, C. M. Robertson, A. Steiner, I. Kozhevnikov, Chem. Commun. **49** (2013) 349.
15. D. E. Bergbreiter, ACS Macro Lett. **3** (2014) 260.
16. M. Al-Hashimi, C. Hongfa, B. George, H. S. Bazzi, D. E. Bergbreiter, J. Polym. Sci., Part A: Polym. Chem. **50** (2012) 3954.
17. N. Priyadarshani, Y. Liang, J. Suriboot, H. S. Bazzi, D. E. Bergbreiter, ACS Macro Lett. **2** (2013) 571.
18. D. E. Bergbreiter, D. Ortiz-Acosta, Tetrahedron Lett. **49** (2008) 5608.
19. D. E. Bergbreiter, J. Tian, Tetrahedron Lett. **48** (2007) 4499.
20. N. Priyadarshani, J. Suriboot, D. E. Bergbreiter, Green Chem. **15** (2013)1361.
21. Y. Yang, M. L. Harrell, D. E. Bergbreiter, Angew. Chem., Int. Ed. **53** (2014) 8087
22. J. Li, S. Sung, J. Tian, D. E. Bergbreiter, Tetrahedron **51** (2005) 12081.
23. http://www.performancechemicals.basf.com/ev/internet/polyisobutene/en/content/EV3/polyisobutene/glissopal (accessed August 26, 2014).

Chapter 6. General conclusions

Sulfur present in crude oil not only poisons the catalysts used in oil refining industries, it also causes a series of environmental problems among which acid rain is the typical one [1]. Therefore, removal of sulfur from oil products has attracted growing attention in the past few decades [1, 2].

Hydrodesulfurization (HDS) technology has become very efficient to remove mercaptans, sulfides and disulfides [1, 2]. However, operation at high temperature and high hydrogen pressure creates many problems, including high investment, high operating cost and reduction of the length of the catalyst life [3,4,5]. Besides, HDS has some inherent problems in the treatment of aromatic sulfur compounds, such as dibenzothiophene (DBT) and their methylated derivatives [6,7].

Oxidative desulfurization (ODS) is considered to be one of the most promising processes to reduce refractory sulfur-containing compounds (dibenzothiophene and its alkylated derivatives) [8]. The oxidising agents for ODS are H_2O_2 [8, 9], peracids [8,10], t-BuOOH [8, 11] and O_2 or O_3 [8,12]. The reaction can be carried out in non-acidic media in the presence of catalytic amounts of transition metal, e.g. Mo, W or V on several supports [8,13,14]. Phosphotungstic acid can catalyse the oxidation of dibenzothiophene with H_2O_2 in the presence of a phase transfer agent or without a phase transfer agent in oil/acetic acid biphasic system [8,15,16].

Polyoxometalates are a valuable class of inorganic compounds because of their tunable size and charge and the inclusion of a variety of transition metals [8,17]. Different polyoxometalate catalyst precursors with a phase transfer agent were reported for oxidative desulfurization of dibenzothiophene with H_2O_2 [8,18]. It was reported that a $[(C_{18}H_{37})_2N(CH_3)_2]_3[PW_{12}O_{40}]$ catalyst, assembled in an emulsion in diesel, could selectively oxidise DBT and its derivativatives into their corresponding sulfones using H_2O_2 [8,19].

It has been extensively documented that POMs, especially those comprising Keggin type polyanions $[XM_{12}O_{40}]^{m-}$ {X = P^V (m = 3) and Si^{IV} (m = 4)}, serve as precursors of highly

efficient catalysts for environmentally benign biphasic oxidations with hydrogen peroxide. Oxidative desulfurization catalysed by POM using aqueous H_2O_2 as a "green" oxidant in a two-phase system has been developed as a promising method for deep desulfurization of transportation fuel.

Biphasic oxidations in a water–organic system are particularly attractive, as such systems facilitate product/catalyst separation. These reactions typically involve phase-transfer catalysis with peroxo polyanion transport through the water-organic interface and require an efficient agent to move the peroxo polyanions from the aqueous phase into the organic phase. The primary objective of this project was to investigate hexa-alkyl(amino)cyclotriphosphazenes as novel phase transfer agents for biphasic oxidation of benzothiophenes to sulphones catalysed by Keggin type POMs. In particular, we focused on the oxidation of dibenzothiophene (DBT) which is typically employed as a model reaction for catalyst testing. We also aimed to gain insight into phase behaviour of POM-phosphazene catalysts and reaction mechanism.

Terminally functionalized polyisobutylene (PIB) derivatives readily soluble in nonpolar solvents like heptane have been demonstrated to have the potential to improve the recovery and recycling of homogeneous catalysts. In this work, in collaboration with Prof. D. E. Bergbreiter group (Texas A&M University, USA), we investigated the use of amine terminated PIB oligomer as a solubilizing agent for Keggin POM catalysts in oxidative desulfurization with hydrogen peroxide in a heptane-water two-phase system. It was demonstrated that the PIB oligomer-bound Keggin polyoxometalates are efficient and recyclable catalysts for environmentally benign biphasic oxidation of benzothiophene derivatives with hydrogen peroxide to the corresponding sulfones.

Oxidative desulfurization catalyzed by tungsten POMs using 30% H_2O_2 as a ''green'' oxidant has been developed as a promising method for deep desulfurization of transportation fuel [20, 21]. We found that POM–RPN aggregates are highly active catalysts for DBT oxidation with H_2O_2 in a biphasic system, e.g. toluene–water, yielding DBT sulfone as the sole product. The POM–RPN aggregates can be introduced in the reaction system as pre-synthesized compounds or, if preferred, POM and RPN components can simply be added separately to form the active catalyst in situ [20]. Catalyst activity was found to increase with the size of the R group in line with increasing phase-transfer efficiency of RPN: iPr < iBu < Bz. The

activity also increased with the [BzPN]/[POM] molar ratio, levelling off at a ratio of 6 : 1. Unexpectedly, PMo exhibited a higher activity than PW whereas SiW showed no activity at all. The latter is in agreement with the well-known stability of SiW to degradation in solution and its resistance to form peroxo species. It is important to note that practically no decomposition of H_2O_2 to molecular oxygen took place in this system, giving >99% efficiency for H_2O_2 utilization [20,22].

Moreover, the catalyst could be recovered and reused without loss of activity. This compares well with the best results reported so far. Jiang et al. [23] have used amphiphilic decatungstate $[(CH_3)_3NC_{16}H_{33}]_4W_{10}O_{32}$ as the catalyst under similar conditions and observed similar DBT conversions (99.6%), but without giving the H_2O_2 efficiency. Similar results have also been reported for the $[(C_{18}H_{37})_2N(CH_3)_2]_3[PW_{12}O_{40}]$ catalyst [24]. These catalysts, however, have to be pre-synthesized via a cumbersome procedure [23], which is not required for the POM–RPN system. The other advantage of our system is that molybdenum based systems can be used instead of tungsten, which reduces the catalyst weight by 25–30%.

We also found that PIB oligomer-bound Keggin POMs are highly active and easily recyclable catalysts for DBT oxidation with H_2O_2 in a heptane–water biphasic system, yielding DBT sulfone as the sole product [25]. As expected, the catalyst activity increased with the PIB/POM molar ratio, levelling off at a ratio of 4 : 1-6 : 1. What is remarkable though, and different from the conventional C8–C18 quaternary ammonium surfactants, is that the catalyst was quite active already at a 1 : 1 PIB/POM molar ratio, giving 70% DBT conversion in 0.5 h and 100% in 1 h [25].

Amongst the POMs tested, PW exhibited the highest activity followed by PMo. With PW, the conversion of DBT reached 100% in 0.5 h at 60 °C and a PIB/PW molar ratio of 6 : 1. In contrast, SiW showed no activity at all within 0.5 h reaction time, with a slow conversion rate after 1 h induction period. This is in agreement with the well-known stability of SiW to degradation in solution and its resistance to form peroxo species. It is important to note that practically no decomposition of H_2O_2 to molecular oxygen took place in the PIB–POM reaction system, giving >99% efficiency of H_2O_2 utilization [25].

In conclusion, we have synthesized and structurally characterised novel POM–phosphazene salt aggregates and demonstrated their high efficiency as amphiphilic catalysts for

environmentally benign oxidations with H_2O_2 in biphasic systems. These catalysts self-assemble in situ simply by mixing commercial Keggin POMs and readily available phosphazenes. Studies on the oxidation of other sulfur compounds using this catalyst are underway.

We have also demonstrated that the PIB oligomer-bound Keggin polyoxometalates are efficient and recyclable catalysts for environmentally benign biphasic oxidations with hydrogen peroxide, including the oxidation of DBT to DBT sulfone and, in a heptane–water two-phase system. The oxidation reactions occur through facile phase transfer of peroxo POM intermediates into the heptane phase facilitated by the amine terminated heptane phase selectively soluble PIB oligomer.

Future work could provive further optimisation of the RPN-POM catalyst system. In particular, it is interesting to study a wider range of phosphazenes as phase transfer agents, especially those with longer-chain alkyl substituents, which are expected to be more efficient phase transfer agents in alkane-water two-phase systems required for the oxidative desulfurization of diesel fuel. Other types of polyoxometalates are also of interest in this context. Especially interesting are lacunary silicotungstates, which have been demonstrated recently to be highly active catalysts for alkene epoxidation with hydrogen peroxide (N. Mizuno et al.). Finally, more detailed kinetic and mechanistic studies complemented by thorough multinuclear NMR characterisation of POM species would help to further optimise these catalyst systems.

References

1. Y. Hu, Q. He, Z. Zhang, N. Ding, B. Hu, Chem. Commun. **47** (2011) 12194.
2. I. Babich, J. Moulijn, Fuel **82** (2003) 607.
3. D. Huang, Y. Wang, L. Yang, G. Luo, Ind. Eng. Chem. Res. **45** (2006)1880.
4. H. Mei, B. Mei, T. Yen, Fuel **82** (2003) 405.
5. A. Hernandez, F. Yang, G. Qi, R. Yang, Appl. Catal. B **56** (2005) 111.
6. X. Ma, S. Velu, J. Kim, C. Song, Appl. Catal. B **56** (2005) 137.
7. L. Verduzco, E. Garcia, R. Quintana, V. Pena, F. Guevara, Catal. Today **98** (2004) 289.
8. C. Song, X. Ma, Appl. Catal. B **41** (2003) 207.
9. W. Trakarnpruk, K. Rujiraworawut, Fuel **90** (2009) 411.
10. O. Bortolini, S. Campestrini, F. Furia, G. Modena, J. Org. Chem. **52** (1987) 5093.
11. P. Moreau, V. Hulea, S. Gomez, D. Brunel, F. Di Renzo, Appl. Catal. A **155** (1997) 253.
12. D. Wang, E.W. Qian, H. Amano, K. Okata, A. Ishihara, T. Kabe, Appl. Catal. A **253** (2003) 91.
13. S. Murata, K. Murata, K. Kidena, M. Nomura, Energ. Fuels **18** (2004) 116.
14. A. Anisov, E. Fedorova, A. Lesnugin, V. Senyavin, L. Aslanov, V. Rybakov, A. Tarakonova, Catal. Today **78** (2003) 319.
15. L. Caero, E. Hernandez, F. Pedraza, F. Murrieta, Catal.Today **107** (2005) 564.
16. F. Collins, A. Lucy, C. Sharp, J. Mol. Catal. A Chem. **117** (1997) 397.
17. D.E. Katsoulis, Chem. Rev. **98** (1998) 359.
18. M. Te, C. Fairbridge, Z. Ring, Appl. Catal. A, **219** (2001) 67.
19. H. Lu, J. Gao, Z. Jiang, F. Jing, Y. Yang, G. Wang, C. Li, J. Catal. **239** (2006) 369.
20. M. Craven, R. Yahya, E. Kozhevnikova, R. Boomishankar, C. Robertson, A. Steiner, I. Kozhevnikov, Chem. Commun. **49** (2013) 349.
21. Z. Jiang, H. Lu, Y. Zhang, C. Li, Chin. J. Catal. **32** (2011) 707.
22. I. V. Kozhevnikov, Catalysis by Polyoxometalates, Wiley, Chichester, 2002.
23. X. Jiang, H. Li, W. Zhu, L. He, H. Shu, J. Lu, Fuel **88** (2009) 431.
24. Z. Jiang, H. Lu, Y. Zhang, C. Li, Chin. J. Catal. **32** (2011) 707.
25. R. Yahya, M. Craven, E. F. Kozhevnikova, A. Steiner, P. Samunual, I. V. Kozhevnikov, D. E. Bergbreiter, Catal. Sci. Technol. **5** (2015) 818.